STUDY OF DRAG REDUCING POLYMERS AND MECHANISMS OF THEIR INTRAVASCULAR EFFECT

by

Joie Nicole Marhefka

BChE, Villanova University, 2000

Submitted to the Graduate Faculty of

The School of Engineering in partial fulfillment

of the requirements for the degree of

Doctor of Philosophy

University of Pittsburgh

2007

UNIVERSITY OF PITTSBURGH

SCHOOL OF ENGINEERING

This dissertation was presented

by

Joie Nicole Marhefka

It was defended on

March 19, 2007

and approved by

James F. Antaki, Ph.D.
Professor, Departments of Biomedical Engineering & Computer Science, Carnegie Mellon University; Professor, Departments of Bioengineering & Surgery, University of Pittsburgh

Harvey S. Borovetz, Ph.D.
Professor & Chair, Department of Bioengineering; Robert L. Hardesty Professor, Department of Surgery; Professor, Department of Chemical & Petroleum Engineering

Toby M. Chapman, Ph.D.
Associate Professor, Department of Chemistry

Richard R. Koepsel, Ph.D.
Research Associate Professor, Department of Chemical & Petroleum Engineering

Marina V. Kameneva, Ph.D.
Dissertation Director
Research Professor, Departments of Bioengineering & Surgery

STUDY OF DRAG REDUCING POLYMERS AND MECHANISMS OF THEIR INTRAVASCULAR EFFECT

Joie Nicole Marhefka, PhD

University of Pittsburgh, 2007

Blood-soluble drag reducing polymers (DRPs) have been shown to produce considerable beneficial effects on blood circulation, including an increase in tissue perfusion and tissue oxygenation and a decrease in vascular resistance, when injected in blood at minute concentrations in animal models of normal and especially pathological circulation. DRPs have potential applications in treating tissue hypoperfusion caused by cardiovascular disease, stroke, peripheral vascular disease, diabetes, and other illnesses. To help to translate this novel therapy from the lab bench to the clinic, standard tests need to be developed for characterization and efficacy testing of candidate polymers. Furthermore, elucidation of the mechanisms of the observed DRP effects on blood circulation is extremely important for their future medical applications. Finally, effective, biocompatible and stable polymers which can be easily produced in large quantities must be identified.

In this work a sequence of tests was developed to characterize and assess efficacy of DRPs for possible use in treating circulatory disorders. This research study also provided a better understanding of mechanical degradation of DRPs, especially in the presence of blood cells or particles. It was discovered that an increase in particle concentration led to an increase in degradation rate, and that rigid particles caused an even higher degradation rate than deformable red blood cells (RBCs).

Microfluidic studies in models of microvessels showed that DRPs prevented RBC movement from the walls of microchannels toward the center and lessened plasma skimming at bifurcations, delivering more RBCs to smaller branches and thus to capillaries. *In vivo*, this may lead to a reduction of the near-wall plasma layer, which would facilitate gas transport, increase local wall shear stress and promote vasodilation decreasing vascular resistance in microvessels.

Three polymers, including an aloe vera derived polysaccharide (AVP), poly(N-vinyl formamide), and hyaluronic acid (HA), were evaluated and characterized as new drag reducers for potential clinical use and found to be very effective. HA and AVP were found to be the most resistant to mechanical degradation of the tested polymers. Finally, relaxation time and gyration radius were found to be the polymer's physical properties which best predicted their drag reducing effectiveness.

TABLE OF CONTENTS

LIST OF TABLES

LIST OF FIGURES

NOMENCLATURE

δ	Plasma layer size
ΔP	Pressure drop
λ	Friction factor
μ	Dynamic viscosity
ν	Kinematic viscosity
ρ	Density
AVP	Aloe vera-derived DRP
D	Diameter
DR	Drag reduction
DR(0)	Initial drag reduction
DR(t)	Drag reduction at a given time t
DRP	Drag reducing polymer
FCD	Functional capillary density
FDA	Food and Drug Administration
F-L	Fåhraeus-Lindquist
GPC	Gel permeation chromatography
HA	Hyaluronic acid
Ht	Hematocrit
ID	Tube inner diameter
IV	Intrinsic viscosity

k	Rate constant for DRP degradation
l, L	Tube length
l_e	Entrance length
M_n	Number average molecular weight
MW	Molecular weight
M_w	Weight average molecular weight
M_z	Z average molecular weight
NVF	N-vinylformamide
PAM	Polyacrylamide
PBS	Phosphate buffered saline
PEO	Poly(ethylene oxide)
PEO-200	Poly(ethylene oxide) molecular weight 200 kDa
PEO-600	Poly(ethylene oxide) molecular weight 600 kDa
PEO-1000	Poly(ethylene oxide) molecular weight 1000 kDa
PEO-2000	Poly(ethylene oxide) molecular weight 2000 kDa
PEO-3500	Poly(ethylene oxide) molecular weight 3500 kDa
PEO-4500	Poly(ethylene oxide) molecular weight 4500 kDa
PEO-5000	Poly(ethylene oxide) molecular weight 5000 kDa
PDI	Polydispersity index
PDMS	Poly(dimethyl siloxane)
PNVF	Poly(N-vinylformamide)
Q	Flow rate
r	Tube radius

RBC	Red blood cell
Re	Reynolds number
R_g	Radius of gyration
R_h	Hydrodynamic radius
t	Time
τ_w	Wall shear stress
v	Velocity
Wi	Weissenberg number

PREFACE

I would like to thank my advisor, Dr. Marina Kameneva, for giving me the opportunity and resources necessary to complete this research, and for all of time she has spent teaching me both the theory and applications of rheology and how to become a better researcher. I truly appreciate all of her guidance and patience throughout the years. I would also like to thank my co-advisor, Dr. Toby Chapman, for all of his help with the chemistry aspects of my research. I am grateful for all he has taught me, both about chemistry and about life. I would like to thank Drs. James Antaki, Harvey Borovetz, and Richard Koepsel for agreeing to be members of my committee. The time, expertise, and advice they provided were invaluable in completing this work.

I would like to acknowledge Rui Zhao for her help with all of the microfluidic and imaging experiments, and for her patience throughout the process. I am also indebted to Dr. Sachin Velankar for his help with microchannel experiments and for the valuable discussions on rheology and microfluidics.

Thanks to all of the members, past and present, of the Hemodynamics, Hemorheology, and Artificial Blood Research Laboratory for their assistance in completing the experiments included in this dissertation, especially Dorian Arnold, Elaine Blyskun, Chenara Johnson, and Jude Menie. My lab mates and officemates have definitely made the work days more fun, and for this I am grateful. Special thanks are due to Stephanie Shaulis and Phil Marascalco for all of their

help with research, data analysis, and proofreading, as well as for their moral support and friendship.

I couldn't have done this without the support of all of my wonderful friends, especially those I have made during my grad school years. Thanks to Tiffany Sellaro and Susan Moore for being great friends and for being there for me, rain or shine, over the last seven years. Thanks to Jill Slaboda for helping to keep me sane while writing this dissertation, and of course for her friendship.

To my family, for their constant love and support, I am forever grateful. I couldn't have done it without you. My sister Juli has always been a great friend, thanks for always being there for me and putting up with me. Thanks to Uncle Michael for being supportive throughout my grad school days and always. My parents have always encouraged me to work hard and to follow my dreams. Without their endless support, I wouldn't be where I am today. I appreciate all of the advice and constant encouragement that my Mom has given me, throughout grad school and my entire life. My Dad taught me to never give up. This is something I will always remember. Thank you all for everything!

Finally, I would like to acknowledge the Pittsburgh Foundation, Lifecore Biomedical, the Commonwealth of Pennsylvania and the PA Department of Health, the Pittsburgh Tissue Engineering Initiative and the National Tissue Engineering Center, and the University of Pittsburgh Provost's Development Fund for providing the financial resources necessary to complete this work.

1.0 INTRODUCTION

Treatment of tissue hypoperfusion is extremely important for millions of patients suffering from cardiovascular disease, stroke, peripheral vascular disease, diabetes, and other illnesses. Standard therapies available today for treatment of tissue hypoperfusion include administration of vasopressive agents to enhance pressure and administration of inotropic agents to enhance myocardial contractility and cardiac output [1]. More advanced treatments of cardiovascular diseases are being developed using tissue engineering and regenerative medicine methods. In spite of significant progress in treatments of cardiovascular diseases and some decline in mortality due to these diseases, they are still major causes of death in the United States and other developed countries. The costs associated with treatment of these diseases and related disabilities are enormous. Thus, development of novel methods of enhancement of impaired microcirculation, which is the major cause of tissue hypoperfusion, is essential. The objective of this study was to develop special blood-soluble drag reducing polymers (DRPs) as a novel concept for improving inadequate microcirculation. Intravascular flow enhancement by DRP additives to blood has been demonstrated *in vivo* in experimental animals [1-14]. The remarkable ability of DRP additives to reduce/prevent the mortality of animals subjected to hemorrhagic shock and acute hypoxia and to significantly improve microcirculation in animal models of diabetes and myocardial infarction makes these polymers desirable candidates for new therapies for treatment of insufficient blood circulation of any origin.

DRPs are soluble polymers which reduce resistance to turbulent flow in a pipe when added to flowing fluid at nanomolar concentrations [15]. Polymer drag reduction is a physical phenomenon that was discovered about 60 years ago and is still not completely understood. Blood-soluble DRPs have been shown to produce significant beneficial effects on animal blood circulation, including an increase in tissue perfusion and tissue oxygenation and a decrease in vascular resistance, when intravenously injected at minute concentrations (1 – 10 μg/ml). These polymers have been successfully applied in animal models of various pathologies including hemorrhagic shock, atherosclerosis, and diabetes [1-4, 6, 8, 9, 12, 14, 16, 17]. It was shown that the polymers did not affect blood viscosity and did not have a direct effect on the vessel tone. Several hypotheses regarding the mechanisms underlying the observed beneficial hemodynamic effects of DRPs were proposed in the past. It was first suggested that the DRPs may enhance fluidity of the blood by reducing resistance to turbulent flow in the vascular system, which may exist due to some pathological states. [18]. However, the DRP effect was seen in normal animals in which turbulent blood flow is not present. *In vitro* studies regarding DRP effects on flow separation in models of bifurcating vessels demonstrated that under flow conditions corresponding to realistic vascular hemodynamics (1≤ Reynolds number (Re) ≤ 800), DRPs reduced the size of the flow separation and delayed the development of vortices at bifurcations [19, 20]. *In vivo*, this phenomenon would reduce pressure loss in arterial vessels and thus increase precapillary pressure, thereby increasing the density of functional capillaries (tissue perfusion). However, the exact mechanisms underlying the DRP intravascular phenomenon remain incompletely understood. Several DRPs, including polyethylene oxides, polyacrylamides, and certain polysaccharides have been identified and applied in various *in vivo* models of circulation. These polymers are chemically dissimilar, but all possess drag reducing properties as

demonstrated in *in vitro* tests. Thus, the mechanisms underlying the demonstrated beneficial hemodynamic effects of DRPs are most likely based on the fluid dynamic and/or viscoelastic properties of the DRPs versus the actual chemistry of these polymers [1].

Several DRPs have been shown to be effective *in vivo* including high molecular weight polyethylene oxide (PEO) [1, 3, 12, 14], polyacrylamide (PAM) [2, 4, 8, 9], and certain polysaccharides [1, 6, 17]. However, none of the tested DRPs were found, in their present form, to be ideal for biomedical applications. PEO was very effective *in vivo*, but rapidly mechanically degraded when exposed to turbulent flow and other high stress conditions. PAM was also shown to be effective *in vivo* and was relatively resistant to mechanical degradation. However, it was not a good DRP candidate for biomedical applications because of its reported toxicity [9, 12]. High molecular weight polysaccharides were also shown to be very effective *in vivo* [1, 6, 17] and resistant to mechanical degradation [21-23]. Additionally, polysaccharides as a class are generally non-toxic [24, 25]. However, currently there is no method for their production in large amounts. Therefore, it is essential to develop new DRPs for potential clinical use and to develop a set of tests to characterize these new DRPs and assess their properties required for the successful use *in vivo*.

This project aimed to develop a biocompatible DRP suitable for biomedical applications, to make a significant step toward understanding the mechanisms of the intravascular DRP phenomenon, and to find physicochemical characteristics of DRPs necessary for *in vivo* efficiency. An ideal DRP preparation for biomedical applications, which is effective, biocompatible, mechanically stable, well defined, and reproducible during preparation, must be developed, and the mechanism responsible for the intravascular DRP effect must be identified in

order to translate this novel technology from the lab bench to the clinic. This development of DRPs for bioengineering applications was accomplished through the following **specific aims**:

1) Develop a set of hydrodynamic, rheological, and molecular tests to characterize blood soluble drag reducing polymers

To achieve this specific aim, a hydrodynamic system was developed for standardized testing of polymer drag reducing efficiency in saline or in blood, molecular properties of the DRPs were characterized using gel permeation chromatography (GPC), viscoelastic properties of DRPs were characterized using rheological methods, and the mechanical degradation of DRPs due to exposure to shear stress was characterized at a wide range of pipe flow conditions (Reynolds numbers). The developed series of tests was applied to a well-known DRP, PEO, and then to characterize and test new DRPs described in Specific Aim 3.

2) Determine potential mechanisms of the intravascular effects of drag reducing polymers using *in vitro* microscale methods

In order for DRPs to be applied in the medical field, it is important to have an understanding of the mechanism for their effects on hemodynamics. Therefore, an *in vitro* microscale method of testing the rheological efficacy of DRPs and of studying their mechanism was developed. Microchannel systems were fabricated, microfluidic studies of the DRP effects on flow of blood or suspensions of red blood cells (RBCs) were performed, and the data were fit to a model of RBC concentration distribution across the microchannel.

3) Develop and test new drag reducing polymers

Several DRPs, including high molecular weight PEOs, PAMs, and plant-derived polysaccharides were applied and found to be effective in blood circulation in previous *in vivo* studies. However, the search continues for new DRPs, which are biocompatible, mechanically

stable, well defined, and reproducible, for clinical use. Therefore, three novel blood soluble DRPs were characterized and tested for potential biomedical applications including a DRP derived from the aloe vera plant, poly(N-vinylformamide), and hyaluronic acid. Mechanical degradation behavior of the polymers was compared. Correlations were determined between physicochemical and rheological properties of these polymers and their drag reducing efficiency. The physical and molecular properties which best predict a polymer's effectiveness in microflow systems and thus likely *in vivo* were also determined.

2.0 BACKGROUND

2.1 DRAG REDUCING POLYMERS

Various types of additives, including solid particles such as sands and fibers, colloidal systems like surfactants and soaps, and many soluble polymers both synthetic and natural, have been shown to reduce friction and, therefore, enhance fluid flow [26]. The class of soluble polymers, so called drag reducing polymers (DRPs), has been proven to be the most effective of the drag reducers. It was discovered several decades ago that the addition of minute concentrations of some special soluble polymers could significantly decrease resistance to flow without affecting viscosity or density of the fluid [15]. This phenomenon, known as the Toms effect, occurs in developed turbulent flow with DRPs that exhibit certain physicochemical properties. Figure 2-1 shows the effect of DRPs, which cause a reduction in pressure gradient at a constant flow rate or an increase in flow at a constant pressure, on turbulent pipe flow when added to flowing water at the concentration of 10 μg/ml. Many organic and water-soluble long-chain polymers were found to have drag reducing properties. Small concentrations of these DRPs can reduce friction by up to 80% [26]. To possess drag reducing activity a polymer must have a high molecular weight ($MW>10^6$ Da) and at least a fairly linear structure [26]. At the same molecular weight, a linear polymer will be a more effective drag-reducer than a branched polymer [26]. Highly branched polymers, such as high molecular weight dextran, have no drag reducing ability. It is important

for the polymer to be in a good solvent that will extend the polymer coil and increase flexibility of the polymer chain. A poor solvent will cause a polymer to become rigid, inhibiting its drag reducing activity [26]. The polymer's drag reducing efficiency is best defined by degree of polymerization, which describes the number of monomer units and therefore chain length. The number of backbone chain links is important in determining a DRP's efficacy [27]. Therefore, if two polymers have the same molecular weight, the one with the lower molecular weight monomer will be the better drag-reducer [27].

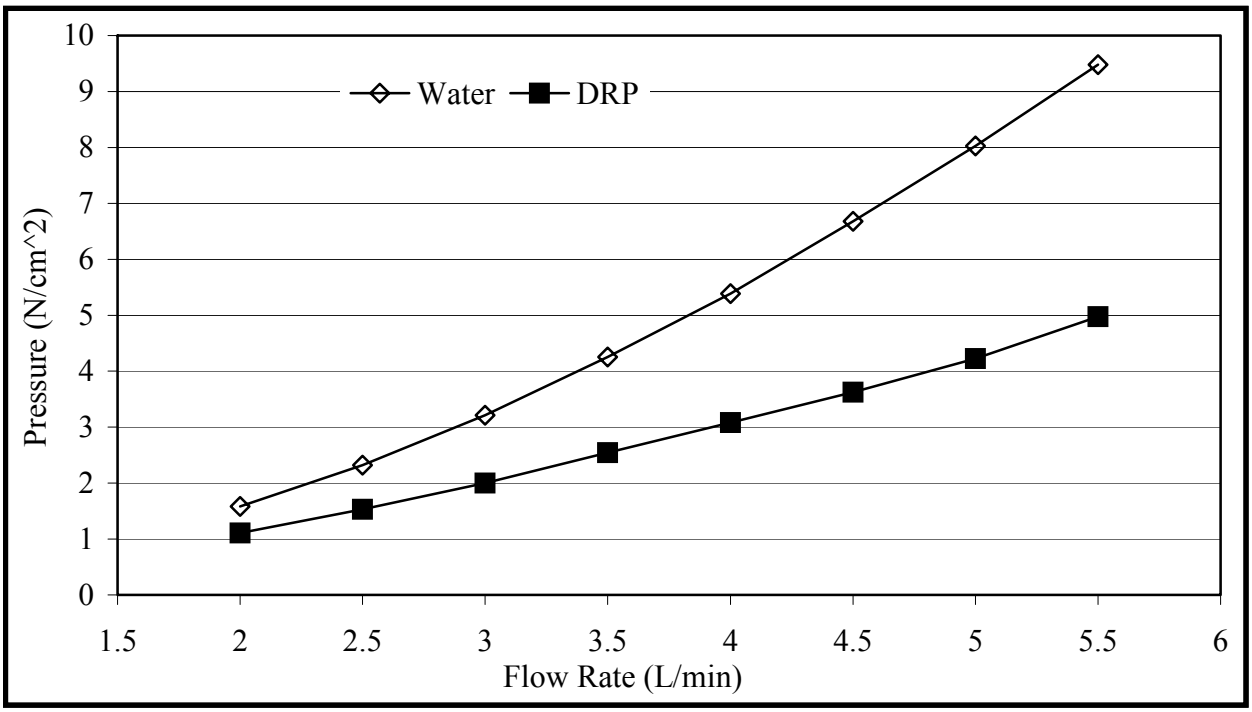

Figure 2-1. Effect of DRPs on turbulent flow in a pipe.

Kulicke [26] reviewed the properties required for an effective DRP in detail by analyzing primary, secondary, tertiary, and quaternary structure. He found, that average absolute molecular weight, which is represented by the weight average (M_w) or number average (M_n) molecular

weight and describes the primary structure, must be greater than 10^6 Da. In general, the high molecular weight tail of the distribution determines the polymer's effectiveness as a drag-reducer. Polymers that are more flexible, and therefore occupy a larger volume by forming a solvent filled coil, are more effective DRPs [26]. Polyelectrolytes, which have a larger hydrodynamic volume in distilled water than in salt solutions, exhibit better drag reducing efficiency with decreasing concentrations of salt [26]. Ionic groups, arranged with a certain structural orientation of charges, can also enhance a DRP's activity [26]. It was found by Kinnier [28] that, to obtain the same drag reduction with polymers of different molecular weights, equal hydrodynamic volumes of the polymers are required.

The DRPs do not have any effect on pipe laminar flow characteristics and do not change fluid viscosity at the effective concentrations. It was found, however, that DRP additives reduced hydrodynamic resistance in systems with nonturbulent (disturbed laminar) flow, such as pulsating flow in straight and spiral pipes or Couette flow with Taylor vortices at low Reynolds numbers [29, 30]. The class of DRPs includes organic polymers such as polymethylmethacrylate, polyisobutylene and polystyrene as well as several water soluble polymers. Well-known, effective, water soluble DRPs include synthetic polymers such as PEO, PAM, poly(acrylic acid), and natural polymers such as guar gum, xanthan, carboxymethylcellulose, DNA, hyaluronic acid, a polysaccharide from the okra plant [17], several algae [31], fish slimes [32, 33], and several bacterial polysaccharides [32]. More recently, a new DRP was discovered in the inner matter of the aloe vera leaves [34], which was later successfully applied in an animal model of a lethal hemorrhagic shock as an additive to a resuscitation fluid [1]. The Toms phenomenon has been investigated and used for various industrial and engineering applications including crude oil transport through pipelines, firefighting, and reducing drag on ships and submarines [35-37].

After several decades of intensive studies, several theories have been proposed, but the exact mechanism of the Toms phenomenon is still unknown.

2.2 INTRAVASCULAR EFFECTS OF DRPS

While DRPs have been studied and applied in numerous industrial and engineering uses, their application in the biomedical area is not well known. It has been shown, however, that the same polymers that reduce resistance to turbulent flow also produce remarkable effects on blood circulation *in vivo*. Blood soluble DRPs, when injected in the vascular system at nanomolar concentrations, increase blood flow, tissue perfusion, and tissue oxygenation and reduce vascular resistance with no direct effect on blood viscosity or blood vessel tone [12, 16, 38]. Figure 2-2 shows a typical record of the effect that a single intravenous injection of DRP, given to a normal animal, has on tissue perfusion and mean arterial blood pressure [39]. DRPs caused both an increase in tissue perfusion (top curve) and a slight decrease in the mean arterial pressure (bottom curve), which indicated that the microvascular resistance was decreased. In animal models of various pathological conditions, blood soluble DRPs have been applied and were found to produce beneficial effects on the vascular system including a significant increase (up to 50%) in linear blood velocity in capillaries and in number of functioning capillaries in diabetic rats [3] and a delay in the development of atherosclerosis in animals kept on atherogenic diet and chronically injected with minute concentrations of DRPs [2, 4, 9, 13]. Most recently it was shown that the DRPs, when used as a component of a resuscitation fluid, were able to significantly improve tissue perfusion and oxygenation and to reduce/prevent lethality in animals subjected to severe hemorrhagic shock [1, 6].

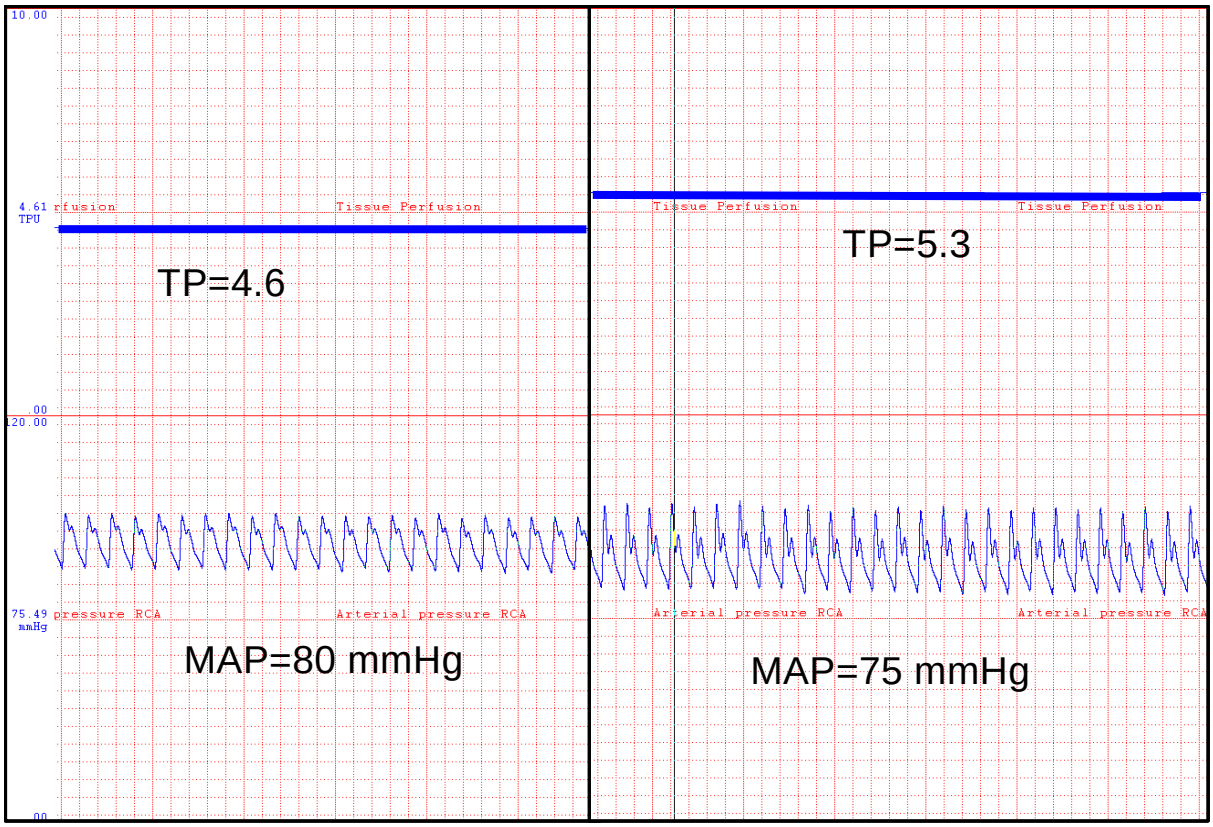

Figure 2-2. Effect of a single injection of DRP (PNVF) injected in a normal animal at the concentration of 4 μg/ml in blood.

2.3 DRPS IN TREATMENT OF HEMORRHAGIC SHOCK

Traumatic injury is the leading cause of death among Americans under 44 years of age [40], and hemorrhage and hemorrhagic shock are major causes of these deaths. Currently, treatment of hemorrhagic shock is based on hemorrhage control and volume expansion, including intravenous infusion of large volumes of crystalloid and/or colloid solutions as well as blood products. While these therapies are effective in restoring fluid volume, they do not adequately address the problem of impaired microvascular circulation caused by hemorrhagic shock [6]. Blood soluble

DRPs present a potential novel therapy for hemorrhagic shock which specifically addresses microcirculatory complications.

In a recent study, the effects of DRPs on blood circulation were tested in anesthetized rats exposed to acute hemorrhagic shock [1]. The animals were acutely resuscitated either with a 2.5% dextran solution (Control) or with the same solution containing a 5 μg/ml concentration of one of two blood soluble DRPs: high molecular weight (MW=3,500 kDa) polyethylene oxide (PEO-3500) or a DRP extracted from aloe vera (AVP). An additional group of animals was resuscitated with a 75 μg/ml concentration of polyethylene oxide with a molecular weight of 200 kDa (PEO-200), which possesses no drag reducing ability. The animals were observed for two hours following the initiation of fluid resuscitation or until they expired. It was found that infusion of the DRP solutions significantly improved tissue perfusion, tissue oxygenation, and two-hour survival rate. The survival rate increased from 19% in the Control group and 14% in the PEO-200 group to 100% in the AVP and PEO-3500 groups. Furthermore, the Control and PEO-200 animals that survived required a three times larger volume of infused fluid to maintain their blood pressure than the AVP and PEO-3500 animals. This study demonstrated that blood soluble DRPs, when injected at very low concentrations (as low as 5 μg/ml) in animals in hemorrhagic shock, rapidly increased blood pressure and restored microcirculatory flow, resulting in increased oxygen delivery to tissues and a significant decrease in lethality.

In another study, Macias et al. showed that resuscitation with a small volume of DRP solution significantly prolonged survival and reduced mortality in a rat model of lethal, volume controlled hemorrhagic shock [6]. It was found that infusion of 7 ml/kg of a 50 μg/ml solution of AVP increased mean arterial blood pressure and whole body oxygen consumption (VCO_2) and delayed death compared to animals resuscitated with the same volume of normal saline.

Moreover, McClosky et al. showed that pretreatment of rats with DRPs (PEO-1000, 25 μg/ml in blood) injected prior to exposing them to hemorrhagic shock preserved tissue perfusion and oxygenation during hemorrhagic shock and prevented development of liver tissue hypoxia [7].

While these *in vivo* studies have shown that DRPs improve outcomes following severe hemorrhage, the mechanism of their action in the vascular system is not yet known. One hypothesis is based on the fact that, in small vessels (diameter less than 0.5 mm) at physiological conditions, RBCs migrate toward the center of the vessel leaving a cell-free plasma layer near the vessel wall [41]. It was hypothesized that the DRPs cause a redistribution of red blood cells across the vessel, reducing the size of the cell free plasma layer and attenuating the plasma skimming effect at vessel bifurcations [1]. The relocation of RBCs to the near wall space causes an increase in apparent viscosity near the walls of the microvessels. Tsai and Intaglietta showed that an increase in plasma viscosity during extreme hemodilution helped to maintain animal functional capillary density (FCD), which was proven to be a major factor of survival in hemorrhagic shock [42]. In this study, the high viscosity solution allowed for wall shear stress dependent mechanisms to maintain optimal microvascular function even at extremely low hematocrit. Kameneva et al. hypothesized that DRPs might maintain this microvascular function in a similar manner by redistributing RBCs and thus increasing near wall viscosity [1].

2.4 DRP DEGRADATION

While DRPs have shown promise as a potential therapy for many pathological states including acute enhancement of microcirculation in diabetic animals and treatment of hemorrhagic shock, these polymers show a tendency to mechanically degrade over time when exposed to high stress

conditions. This could present a potential obstacle to clinical use of DRPs to treat chronic conditions such as microcirculatory impairment caused by diabetes or atherosclerosis if the drag reducing effect is diminished too quickly for practical use. Therefore, the degradation behavior of these polymers must be investigated in detail. For clinical use, it is important to know how quickly the polymer will degrade in order to determine how often the treatment would need to be given. It is also necessary to select DRPs which would degrade sufficiently slowly for chronic administration to be practical since DRP preparations have to be delivered via intravenous injections.

DRP degradation has been intensively studied for decades [21, 22, 39, 43-51]. Degradation experiments have been performed in single pass turbulent flow systems [22, 45] and in a rotating disk apparatus [47]. However, the effects of red blood cells (RBCs) or similar size particles on dynamics of this process have not yet been identified. DRP mechanical degradation can be defined as the chemical process by which the activation energy for the scission of a polymer chain is provided by mechanical stresses on the polymer [46]. Mechanical degradation of DRPs can also be defined as the loss of a polymer's drag reduction effectiveness which is not regained after mechanical stress is abolished [52]. High molecular weight PEOs were demonstrated to be the most effective drag-reducers among commonly used DRPs [22]. At the same time, it was shown that this class of DRPs quickly mechanically degrade in turbulent pipe flow causing the drag reducing effect to diminish over a short exposure time [45]. Polyacrylamides were shown to degrade more slowly than PEOs [22, 45]. Certain high molecular weight polysaccharides were found to be good drag reducers that are much more resistant to mechanical degradation than PEOs [21-23]. The degradation of DRPs in solutions is likely caused by chain scission. However, some studies have shown the drag reducing ability of

partially hydrolyzed PAM degrades in turbulent flow with little change in MW suggesting that degradation occurs at least in part due to the breakup of molecular aggregates [49, 51].

It was shown that the effective biological half life of one DRP, polyacrylamide (Separan AP-30), was about 35 hours in rats [53]. Mechanical degradation is likely responsible, at least in part, for this loss of polymer effectiveness over time.

2.5 MECHANISMS OF INTRAVASCULAR DRP EFFECTS

Elucidation of the mechanism(s) underlying intravascular effects of DRPs would have both academic and practical significance and is essential for the future applications of DRPs. Since there is little turbulent flow in the vascular system (excluding the aorta) the mechanism responsible for the intravascular DRP effect is likely different than that of the Toms effect. Several hypotheses have been proposed for the intravascular DRP phenomenon.

The initial hypothesis was that DRPs acted in the vascular system by reducing resistance in regions where turbulent flow may occur and enhancing fluidity of the blood [18]. However, there is no turbulence in blood circulation in small animals, and DRPs reduce vascular resistance in these animals, therefore the mechanism of the intravascular DRP effect is likely not based on turbulent drag reduction.

Several *in vitro* studies have shown that DRPs reduce the size and delay development of vortices and recirculation zones at vessel bifurcations under physiologically relevant flow conditions [19, 20], therefore reducing resistance to flow. In *in vitro* studies of laminar flow in either a bifurcated glass channel or an elastic tube containing a stenosis, DRPs were shown to

reduce the tendency of eddies to form. Tube diameters in these studies ranged from 3-12 mm, and experiments were performed at Reynolds numbers ranging from 1 – 800.

Another hypothesis [1] behind the increase in tissue oxygenation caused by the DRPs was that DRPs could increase plasma mixing efficiency in capillaries, thereby facilitating oxygen transport. This hypothesis, which is yet to be proven, was based on the previously published results of experiments which demonstrated that very viscous liquids containing a small amount of DRP could be efficiently mixed in a curved channel (d = 3 mm) at very low Reynolds numbers ($Re<<1$) which are similar to the conditions in the capillaries, and at relatively high Weissenberg numbers ($Wi>1$) at which an elastic instability of flow occurred [54].

A new hypothesis proposed by Kameneva et al. [1], which was further tested in these studies, deals with the Fåhraeus Effect and the Fåhraeus-Lindquist Effect [41, 55, 56]. The Fåhraeus Effect states that, in small vessels (diameter less than 0.5 mm) at physiological conditions, RBCs migrate toward the center of the vessel leaving a cell-free plasma layer near the vessel wall [56]. The velocity of the RBCs in the core region is therefore higher than the mean blood velocity, and the ratio of hematocrit in the tube to feed hematocrit decreases with a decrease in tube size [56]. This leads to a reduction in apparent viscosity, and thus flow resistance, in small tubes compared to that in larger tubes (Fåhraeus-Lindquist Effect) and a decrease in apparent blood viscosity with decrease in tube diameter [56]. The observed decrease in apparent viscosity is likely caused by the Fåhraeus effect, which states that hematocrit is lower in smaller vessels, or by the rheological effects of uneven distribution of RBCs across the vessel [56]. These phenomena produce a plasma skimming effect at bifurcations, where, due to the migration of RBCs to the center of the vessel, a lower concentration of RBCs relative to that in the parent branch enters the daughter branch at a bifurcation. This leads to a reduced hematocrit

in smaller vessel branches and, thus, in capillaries. While the original work of Fåhraeus and Lindquist [41, 55, 56] states that this effect occurs in vessels with diameters < 0.3 mm, there is discrepancy in the literature about the diameter where this effect becomes apparent. This exact vessel diameter has yet to be quantitatively determined [57]. It has previously been shown that the Fåhraeus Effect is more prominent at lower hematocrit for a given vessel diameter [56]. The near wall plasma layer in arterioles presents a barrier to oxygen diffusion to tissues. While under normal conditions this plasma skimming is not detrimental for circulation and oxygen transport, in certain pathological states, such as hemorrhagic shock, it might hinder the ability of the RBCs to transport oxygen to the tissues. It has been shown *in vitro* that the addition of a minute concentration of DRPs to red blood cells (RBCs) flowing in a straight microchannel significantly reduces the size of the near-wall cell free plasma layer [1, 58] as shown in Figure 2-3. *In vivo* this may result in enhancement of oxygen transport to the tissue. In addition, this would attenuate the plasma skimming effect and increase intracapillary hematocrit. This decrease in plasma layer size would also lead to an increase in wall shear stress in the small vessels. The resulting increase in wall shear stress would cause the endothelial cells to release endothelial-derived relaxing factor comprised of nitric oxide leading to vasodilation and ultimately to a decrease in systemic vascular resistance [59]. Average microvascular hematocrit has been shown to increase when tissue perfusion is increased, and this change has been attributed to vasodilation of the arterioles [57].

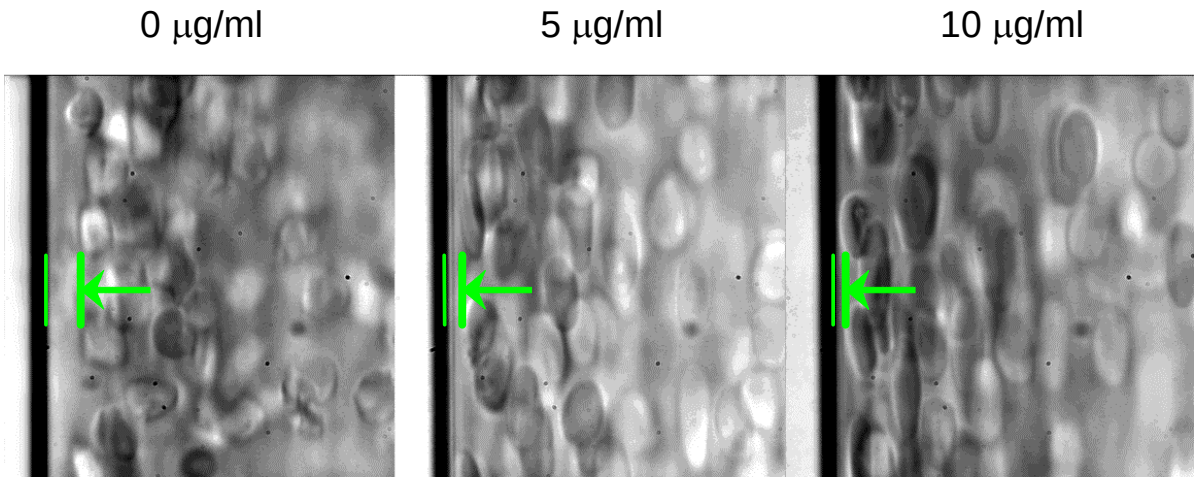

Figure 2-3. The size of the near wall plasma layer in a 100 micron channel decreases with an increase in DRP concentration (57).

Neither the Fåhraeus Effect nor the drag reducing polymer effect is completely understood. These two phenomena have nothing in common, but may come together in the vascular system to produce interesting effects which have significant potential applications in microfluidic technology and in medicine.

2.6 BLOOD-SOLUBLE DRAG REDUCING POLYMERS FOR POTENTIAL BIOMEDICAL APPLICATIONS

Several DRPs, including PEO, PAM, and certain polysaccharides [1-14, 16, 17, 38] have been applied and have shown beneficial effects in animal models. High molecular weight PEOs, PAMs, and plant-derived polysaccharides are the most effective water soluble DRPs. The polymers significantly reduce resistance to turbulent pipe flow and were found to produce

beneficial effects on blood circulation. PEO, however, mechanically degrades when exposed to turbulent flow or other high shear stress conditions even for relatively short exposure times [45]. PAMs, on the other hand, are much more resistant to mechanical degradation, but their apparent toxicity presents problems for potential biomedical use [9, 12]. Plant-derived DRPs are highly resistant to mechanical degradation [22-24] and many polysaccharides are non-toxic [24, 25]. However, they are not well characterized and often difficult to manufacture in industrial quantities. Therefore, the search continues for a DRP which produces beneficial effects on blood flow, and is well characterized, biocompatible, resistant to mechanical degradation and easy to manufacture.

Three candidates for DRP that could meet these requirements are a natural polymer derived from the aloe vera plant (AVP), high molecular weight poly(N-vinylformamide) (PNVF), which is synthesized from a non-toxic isomer of acrylamide, and hyaluronic acid, a polysaccharide produced in the cellular plasma of vertebrates as well as by certain bacteria.

2.6.1 Aloe vera derived DRP

High molecular weight polysaccharides, such as a polymer extracted from okra and characterized as a rhamnogalactogalacturonan, have been shown to be effective drag reducing polymers which produced beneficial hemodynamic effects in a rodent model [17]. It was first discovered by Gowda [60, 61] that high molecular weight polysaccharides could be isolated from aloe plants via alcohol extraction. An aloe based polysaccharide would be an attractive DRP for biomedical applications since toxicological studies have shown that Acemannan, a product extracted from the aloe leaf gel, has minimal systemic toxicity when injected intraperitoneally or intravenously [24]. Recently, it was discovered that a polymer extracted from the aloe vera plant mucilage was

also a very effective drag-reducer [1, 34, 62]. The aloe vera leaf consists of three major components: clear sheets comprised of cell walls and membranes, microparticles comprised of degenerated cellular organelles, and a viscous liquid gel comprised of the liquid components of mesophyll cells. The DRP is extracted from the viscous gel portion of the aloe with ethanol. It is known that the ethanol insoluble portion of the gel is > 50% carbohydrate [63]. A mannan component has been identified in this portion of all aloe species studied, although differences in molecular weight, degree of acetylation, and mannose-glucose ratio have been observed [60, 63]. In one study, the polysaccharides found in the aloe vera gel have been characterized as at least four different partially acetylated linear glucomannans which contain 1-4 glycosidic linkages [64]. In another study, the polysaccharides in aloe vera were shown to be composed of β-(1,4)-linked acetylated polymannans containing O-acetyl groups with a mannose monomer to acetyl ratio of approximately 1:1 [24]. A structure for the major component of aloe vera gel was proposed by Chow et al. [60] based on data from chromatography, carbohydrate compositional analysis, linkage analysis and NMR. This structure consists of a linear β-1,4-linked mannose backbone with β-1,4-linked glucose substituting for mannose approximately every 30 residues. Mannose residues are acetylated at O2, O3 or O6 and sidechains are single galactose residues α-1,6-linked to the mannoses residues in the backbone. This proposed structure is shown in Figure 2-4. However, the structure of the active drag reducing component of the aloe vera DRP remains unknown.

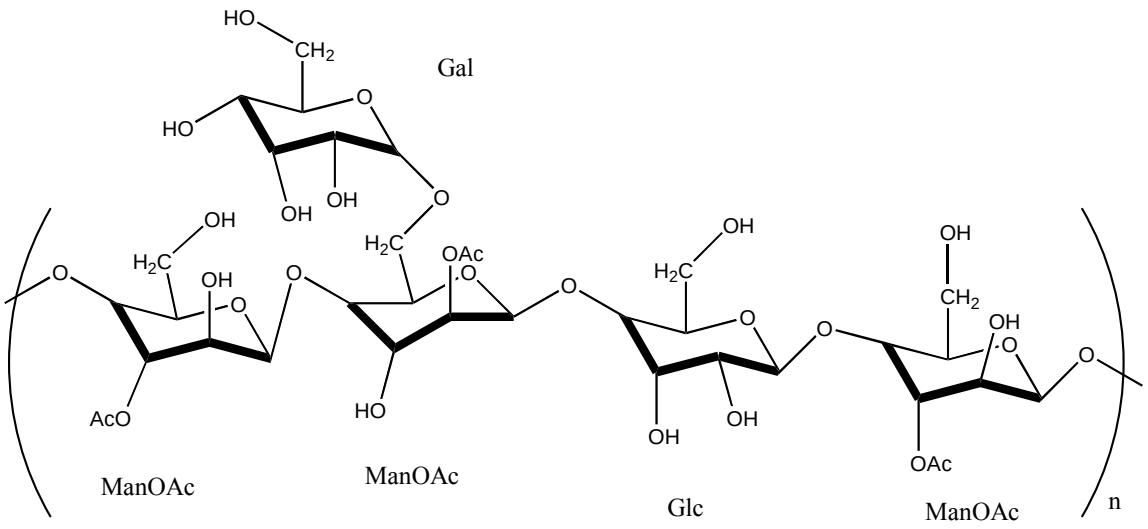

Figure 2-4. Proposed structure of the major component of aloe vera gel [60]

2.6.2 Poly(N-vinylformamide)

Water-soluble PNVF has been known for the past 40 years but has become more common in the last decade due to the development of improved processes for synthesis and purification of the N-vinylformamide (NVF) monomer as well as the growing uses for PNVF and its derivatives in industrial applications [65]. The polymer has been considered as a replacement for toxic acrylamide polymers for industrial use [66]. Applications for PNVF and its hydrolysis products include water treatment, papermaking, production of textiles, personal care items, adhesives and coatings, and use in oil field industry and as a rheology modifier [67]. PNVF, shown in Figure 2-5, is synthesized from the NVF monomer, which is a highly reactive isomer of acrylamide with low toxicity [67]. It was shown that very high molecular weight PNVF ($6.7x10^6$ Da) could be synthesized using an inverse emulsion technique [68]. Due to its similarities with PAM, a well-known very effective DRP, its ease of polymerization [68], and its high solubility in water [67],

high molecular weight PNVF could be a good candidate for a DRP. The low toxicity of the NVF monomer [67] provides motivation for testing PNVF as a potential DRP for biomedical use. Although hydrolysis products of PNVF, including poly(vinyl amine), have been tested and shown to be effective DRPs [69], the drag reducing ability of PNVF was never tested before.

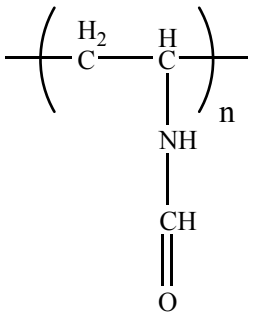

Figure 2-5. Structure of PNVF

2.6.3 Hyaluronic Acid

Hyaluronic acid (HA), also referred to as hyaluronan since it primarily exists in its polyanion form and not as the free acid form, is a linear, unbranched, negatively charged polysaccharide with a molecular weight ranging from 10^5 to 10^7 Da. It is comprised of alternating units of D-glucuronic acid and N-acetyl-D-glucosamine. The structure of HA is shown in Figure 2-6. It is synthesized in the cellular plasma and found in all tissues and body fluids of vertebrates and also in certain bacteria. HA was first discovered by Meyer and Palmer in 1934 [70]. Its medical applications include wound care, medical device coating, orthopedic and ophthalmic applications, and use as a drug-delivery vehicle [71]. One of the most successful applications of HA in the medical field is in treating osteoarthritis [70]. HA was previously shown to have drag reducing ability [72], and its current FDA approval for certain biomedical applications [73] makes it an ideal candidate to be applied for enhancement of blood circulation.

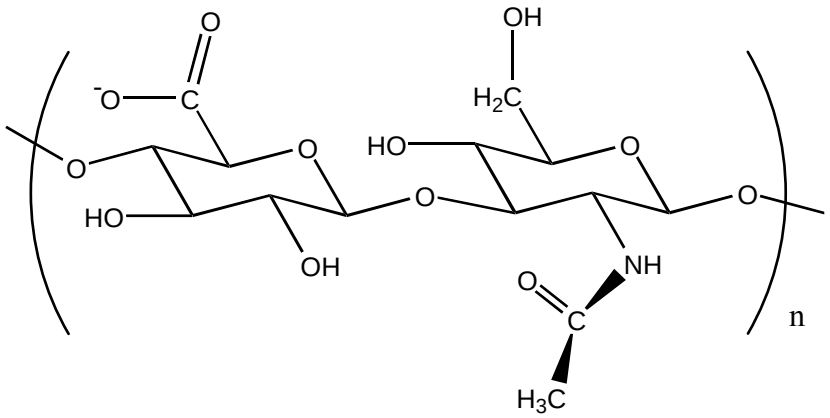

Figure 2-6. Structure of hyaluronic acid

3.0 HYDRODYNAMIC, RHEOLOGICAL, AND MOLECULAR TESTS TO CHARACTERIZE BLOOD SOLUBLE DRAG REDUCING POLYMERS

In order to help to choose DRPs for potential clinical use, a standard set of tests was developed for their characterization and evaluation of efficacy. It has previously been shown that polymers which are effective at reducing resistance to turbulent flow *in vitro* are most effective in improving hemodynamics *in vivo.* It is also known that high molecular weight, linear structure, and non-Newtonian behavior of concentrated solution are characteristics of effective DRPs [26]. Therefore, methods were developed to evaluate these properties and predict a polymer's likelihood to be a good DRP for biomedical use. Microscale methods were also developed as a next step in the prediction of whether a DRP would be effective in improving blood flow *in vivo*. These methods involve the study of RBC flow in microchannels and will be discussed in detail in Specific Aim 2. In addition, it is important to ensure that the DRPs maintain their activity in the presence of flowing RBCs. Test methods were also developed to assess mechanical degradation of these polymers in order to compare relative stability of DRPs and potentially gauge how long the DRPs could be effective in the body. Since PEO is known to be one of the most effective of the commonly used DRPs [22] and is commercially available at several molecular weights, and dextran is known to be a high molecular weight polymer which has no drag reducing properties, PEOs and dextran were used to assess the reliability of the tests developed in this specific aim. Several PEOs, PEO-5000 (MW = 5000 kDa, Aldrich Chemical), PEO-4500 (MW = 4500 kDa,

Polyox WSR-301, Dow Chemical), PEO-2000 (MW = 2000 kDa, Aldrich Chemical), PEO-1000 (MW = 1000 kDa, Aldrich Chemical), PEO-600 (MW = 600 kDa, Aldrich Chemical), and PEO-200 (MW = 200 kDa, Aldrich Chemical), were used for these studies.

3.1 METHODS

3.1.1 Polymer drag reduction in turbulent flow

The Toms effect is known to occur only in developed turbulent flow. Therefore the first test system to identify candidate polymers was developed with the capacity to run at sufficiently high Reynolds numbers. This recirculating flow system for testing the turbulent flow drag reducing ability of polymers consists of a centrifugal pump (BioMedicus, Inc.), a flow meter and clamp-on flow probe (Transonic Systems, Inc.), a pressure transducer (PCB Piezotronics, Inc.), a smooth glass resistive tube with known dimensions (either 0.44 cm ID, 91.5 cm length or 0.56 cm ID, 120 cm length), and a one liter open fluid reservoir connected with 3/8 inch Tygon tubing (Cole-Parmer). A schematic of the system is shown in Figure 3-1. Flow rates and system geometry were chosen based on criteria necessary for the assessment of the drag reducing phenomenon. Entrance length, l_e, calculated using

$$l_e = 4.4 \cdot \mathrm{Re}^{\frac{1}{6}} \cdot d \qquad (1)$$

where d = tube diameter and Re = tube Reynolds number, is ~10% of the tube length [74]. DRP was added to circulating saline to give concentrations ranging from 1 to 500 μg/ml in solution. Saline was chosen as a testing vehicle (vs. water) since the ultimate goal of this study was to

bring DRPs to the animal test point and since some of DRPs have significantly different physicochemical properties when dissolved in saline vs. water. Pressures and flow rates were recorded before and after DRP addition. The *in vitro* flow experiments were performed at room temperature. Drag reduction at a constant flow rate was calculated using

$$DR = \frac{\Delta P_p - \Delta P_0}{\Delta P_0} \cdot 100 \quad (2)$$

where DR = drag reduction (%), ΔP_P = pressure drop for polymer solution, and ΔP_0 = pressure drop for saline alone. This formula, which represents a simple percent error, was chosen to quantify drag reduction since it is the most commonly used metric in DRP literature. This generally accepted definition of drag reduction was provided by Savins in the 1960s [26, 32]. Reynolds number (Re) was calculated using the formula [74]

$$\mathrm{Re} = \frac{4 \cdot Q}{\pi \cdot d \cdot \nu}, \quad (3)$$

where Q = volumetric flow rate, d = tube diameter and ν = kinematic viscosity. A dimensionless friction factor, λ, was calculated for the DRP solutions and compared to that of saline alone using [74]

$$\lambda = \frac{d^5 \cdot \pi^2 \cdot \Delta P}{8 \cdot l \cdot \rho \cdot Q^2}, \quad (4)$$

which is derived from the Darcy-Weisbach equation, where λ = friction coefficient, ρ = density of the fluid, and P = the pressure drop along the tube length, *l*. Blasius friction factor for turbulent flow was also calculated using the Equation 5 [74],

$$\lambda = \frac{0.316}{\mathrm{Re}^{0.25}} \quad (5)$$

and used for comparison to the experimental data.

Drag reducing effectiveness of several PEOs, PEO-5000, PEO-4500 PEO-2000, PEO-1000, PEO-600, and PEO-200, was determined. Results for experimental data are presented as mean friction factor ± standard deviation. Mean friction factors were compared using one-way ANOVA followed by unpaired, two-sample Student's *t*-tests assuming unequal variances.

Although blood flow in the body is not turbulent and the mechanism of the DRPs in the circulatory system most likely differs from that in turbulent flow, previous studies have shown that the DRPs that provide the highest drag reduction in turbulent flow also have the greatest beneficial effects on blood circulation. On the other hand, polymers which do not produce drag reduction are not effective *in vivo.* Therefore, the DRPs which give the best drag reducing ability were determined using the turbulent flow test system, and these DRPs were used to perform microchannel studies in order to evaluate their effectiveness in more physiologically relevant conditions and elucidate the mechanism responsible for the intravascular DRP phenomenon as well as to perform *in vivo* tests.

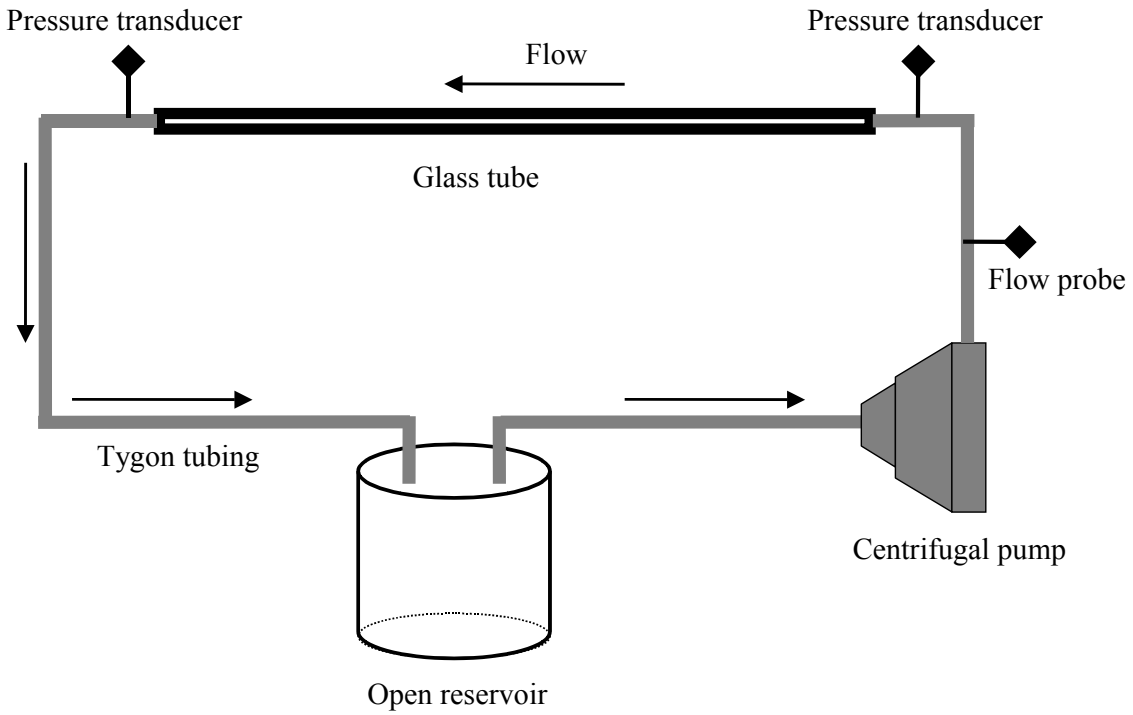

Figure 3-1. Schematic for turbulent flow system used to test DRP efficacy

3.1.2 Polymer drag reduction in turbulent flow of blood

The efficacy DRPs in turbulent blood flow was tested using the circulating system described in 3.1.1 with blood replacing saline as the test fluid. This allowed for the assessment of the DRPs performance in the presence of RBCs, which is important since DRPs injected intravenously contact blood cells *in vivo*. It was therefore important to ensure that RBCs were not detrimental to the DRPs' activity.

Bovine blood obtained from a local slaughterhouse and diluted to the desired hematocrit of 20% with saline was used for these tests. The drag reducing efficiency of two DRPs, PEO-4500 and an aloe based DRP (AVP), was studied at concentrations ranging from 10 to 100 μg/ml

using the methods described in 3.1.1. Reynolds numbers for these studies of turbulent blood flow ranged from 5,000 to 10,000. Results are presented as average drag reduction ± standard deviation at each tested flow rate (Reynolds number).

3.1.3 Gel Permeation Chromatography (GPC)

Molecular characteristics, including high molecular weight and linear structure are important in determining a DRP's potential drag reducing efficiency. Number average and weight average molecular weights (M_n and M_w), intrinsic viscosity (IV), radius of gyration (R_g), hydrodynamic radius (R_h), and polydispersity index (PDI) were measured using a Viscotek Triple Detector Array gel permeation chromatography (GPC) system (Viscotek, Houston, TX).

M_n is defined as the summation of the mole fraction of each species multiplied by its molecular weight and is sensitive toward molecules of relatively low molecular weight ($<10^4$ to $5x10^5$). It can be determined through methods such as end group analysis, membrane osmometry, and vapor pressure osmometry. M_w is defined as the summation of the weight fraction of each species multiplied by its molecular weight. It is more sensitive to molecules of average molecular weight ($5x10^5$ to 10^7). It can be calculated by light scattering and ultracentrifugation. PDI is defined as M_w/M_n and describes the MW distribution of a polymer [75]. Another average molecular weight, z average (M_z), is a higher order molecular weight which is sensitive to molecules of high molecular weight. IV, defined as specific viscosity divided by concentration and extrapolated to zero concentration, is used to describe the hydrodynamic size of a particular polymer. Its units are volume per mass (dl/g), and it is proportional to the hydrodynamic volume of one gram of polymer. R_h can be calculated from the hydrodynamic volume of the polymer molecule, determined from intrinsic viscosity. R_h calculation assumes the molecule to be

spherical in shape. R_g calculation, on the other hand, takes into account the fact that most polymers are actually random coils, not hard spheres as assumed in R_h calculations. R_g is determined through light scattering and viscometry.

Separation was performed on a methacrylate-based column with an exclusion limit of $5x10^7$ Da. The system combines a refractive index detector, a right angle laser light scattering detector, and a differential viscometer in order to determine average MWs (M_n and M_w), IV, R_g, R_h, and molecular weight distribution in a single experiment. Column and detector temperatures were maintained at 30ºC and the mobile phase was 0.1 M $NaNO_3$ with 0.01% NaN_3. The system was calibrated using a PEO standard with a molecular weight of 22 kDa and a narrow molecular weight distribution (PDI ~ 1.0). Results are presented as mean ± standard deviation.

3.1.4 Rheological Characterization

Rheological parameters such as viscosity, elasticity, and relaxation time also can be analyzed in order to fully characterize DRPs since these polymers are known to have high viscosity and elasticity in relatively concentrated solutions. These DRP solutions are also known to exhibit non-Newtonian flow behavior. A non-Newtonian fluid is defined as a fluid in which viscosity depends on shear strain rate. Due to the non-Newtonian nature of concentrated DRP solutions, it is advantageous to measure rheological properties over a wide range of shear rates. This was accomplished using a Brookfield cone and plate rotational rheometer (Middleboro, MA) as well as a Vilastic 3 viscoelasticity analyzer (Austin, TX). The Vilastic 3 employs controlled oscillatory flow in a cylindrical tube to measure the major rheological parameters including viscosity, elasticity, and relaxation time.

Viscosity is defined as a measure of resistance of a material to flow, and elasticity can be defined as the ability of a material to return to its original state following deformation caused by applied stress. Relaxation time is the time necessary for a system to forget the configuration it had prior to a perturbation [76].

Mean values of each rheological parameter ± standard deviation were plotted as a function of shear rate. Rheological parameters were measured in solutions with a concentration of 2.5 mg/ml in saline. Asymptotic viscosity of DRP solutions at a concentration of 100 μg/ml was measured using a capillary viscometer (Cannon Manning). At this concentration, the DRP solutions behave as Newtonian fluids, and therefore measurement of asymptotic viscosity is sufficient for rheological characterization.

3.1.5 DRP Degradation Studies

DRPs, especially PEO, were shown to produce strong beneficial effects on blood circulation with a considerable potential for clinical applications, but quickly mechanically degrade when exposed to turbulent flow or other relatively high shear stress conditions even for relatively short exposure times [45]. For practical use, it is important to understand the degradation behavior of the DRPs. Although there is almost no turbulent flow in the body, degradation studies were performed in turbulent flow since it provides the shear stresses necessary to compare degradation of different DRPs in a relatively short time period and allowed for measurement of polymer degradation via decline of their drag reducing ability. The circulating flow system described in 3.1.1 was also used to study mechanical degradation of DRPs in turbulent flow. A decrease in a polymer's ability to reduce resistance to flow, signified by a decrease in flow rate at fixed wall shear stress, indicated mechanical degradation of the polymer. Turbulent flow degradation

studies also allowed for comparison with literature since most previous studies were performed in turbulent flow. Wall shear stress in the resistive tube was held constant at 45 N/m^2 throughout the degradation experiments. While shear stresses in the arteries of a healthy human range from 1 to 10 N/m^2 [77], arteries with stenosis can have shear stresses greater than 10 N/m^2 [78], and shear stress in artificial heart valves and blood pumps can reach greater than 100 N/m^2 [78]. Reynolds numbers (based on the diameter of the glass tube) ranged from 10,000 – 27,000. Baseline pressure and flow rate were recorded before polymer addition, and DRP was added to the system at a concentration of 0.1, 0.25, or 0.5 mg/ml. Pressure and flow were monitored throughout a five-hour period or until the DRP ceased to produce any effect. Drag reduction at constant wall shear stress (and therefore constant pressure drop) was calculated for each time point using

$$DR = \frac{Q_P - Q_0}{Q_0} \times 100 \qquad (6)$$

where Q_P = flow rate of polymer solution and Q_0 = flow rate of saline alone. Results are presented as mean drag reduction ± standard deviation. The degradation behavior of several PEOs including PEO-4500, PEO-2000, PEO-1000, PAM (Praestol 2510, Stockhausen, Inc.), PNVF, and HA was studied.

GPC, as described in 3.1.3 was used to monitor MW (M_n, M_w, M_z), IV, R_g, and PDI during exposure to flow. M_z is the z average molecular weight, which is sensitive to molecules in the high end of the MW distribution. Polymer chain scission was signified by a decrease in average MW and/or a shift in the MW distribution. The effects of exposure to flow, and therefore mechanical degradation, on PDI were carefully examined. Chain scission and break up of aggregates have both been shown to contribute to DRP degradation [49, 51]. A significant

change in MW and MW distribution with loss in drag reducing ability would show that the primary cause is chain scission. No significant change in MW distribution would occur if the major factor is break up of aggregates.

Additionally, the degradation of DRPs in the presence of RBCs or rigid particles was investigated. This study was motivated by the fact that no previously published work was found on the effect of the presence of particles in DRP solutions on degradation of DRPs. Moreover, because DRPs only affect hemodynamics when they are injected intravenously, it is an important consideration for potential clinical use. Bovine blood was obtained from a local slaughterhouse and centrifuged for 15 minutes at 3600 rpm to remove plasma and buffy coat which consisted of platelets and white blood cells. The RBCs were resuspended in saline at a concentration of 5, 10, or 20%. A rigid particle suspension was prepared by adding glass particles (Potters Industries Inc., one to one mixture of 110P8 and 60P18 with mean diameters of 11 and 18 μm and densities of 1.1 g/cm^3 and 0.6 g/cm^3 respectively) to saline at a concentration of either 1 or 5% by volume. The degradation behavior of two DRPs, PEO-4500 and AVP, was investigated in the presence of RBCs, and that of PEO-4500 was also tested in the presence of rigid particles. Additionally, PEO-4500 degradation was tested in a 15% glycerol solution, prepared as a viscosity analog for the 20% RBC suspension. The viscosity of the 20% RBC suspension was measured to be ~ 1.8 cP using a capillary viscometer (Cannon Manning) at a shear rate of ~ 600 s^{-1}. Therefore, a 15% glycerol solution (~1.7 cP) was prepared as an equiviscous analog for the 20% RBC suspension to determine whether the effects of particles on degradation were due to the particles themselves or to the increase in viscosity.

In order to quantitatively compare the degradation behavior between two DRPs or between DRPs in the presence or absence of particles, the mechanical degradation behavior of

DRPs in the turbulent flow system, both in saline solution and in the presence of RBCs or rigid particles, was examined by fitting it to a previously developed single relaxation decay model [44, 46] as

$$\frac{DR(t)}{DR(0)} = \exp(-k * t) \qquad (7)$$

where t is exposure time of the polymer to flow, DR(0) and DR(t) are drag reduction at time 0 and t respectively, and k, while not a true rate constant, is a property that quantifies rate of loss of drag reducing activity.

3.2 RESULTS

A comprehensive set of hydrodynamic, rheological, and molecular tests for the characterization and evaluation of blood soluble drag reducing polymers, which have potential for clinical use, was developed. The tests were performed on various PEOs, which ranged in molecular weight from 2 x 10^5 – 5 x 10^6 Da in order to show that the these tests could be effectively used to characterize new DRPs. The tests were also performed on high MW dextran (Aldrich, MW claimed by manufacturer = 2,000 – 40,000 kDa), which is known to be highly branched and therefore not a drag reducer, as a negative control.

3.2.1 Polymer drag reduction in turbulent flow

The drag reducing properties of PEOs and a high MW dextran were characterized using the turbulent flow system described in section 3.1.1. It was found that drag reduction (DR) produced

by PEOs increased with an increase in MW, and that, as expected, dextran exhibited no DR. Friction factor for saline agreed well with values calculated using the Blasius equation, whereas the friction factors for PEOs with MW above 1000 kDa were much lower than the those calculated using the Blasius equation. All of the tested PEOs, with the exception of PEO-200, produced a statistically significant reduction in friction compared to saline (control) over the entire range of studied Reynolds numbers ($p < 0.01$). Figure 3-2 shows dimensionless friction factor vs. Re for PEO when added to the circulating system at 100 μg/ml, and Table 3-1 shows the average DR produced by each polymer.

These tests were used in this project to characterize and evaluate the potential of new DRPs to be effective in blood circulation. Results of these studies are discussed in Section 5.

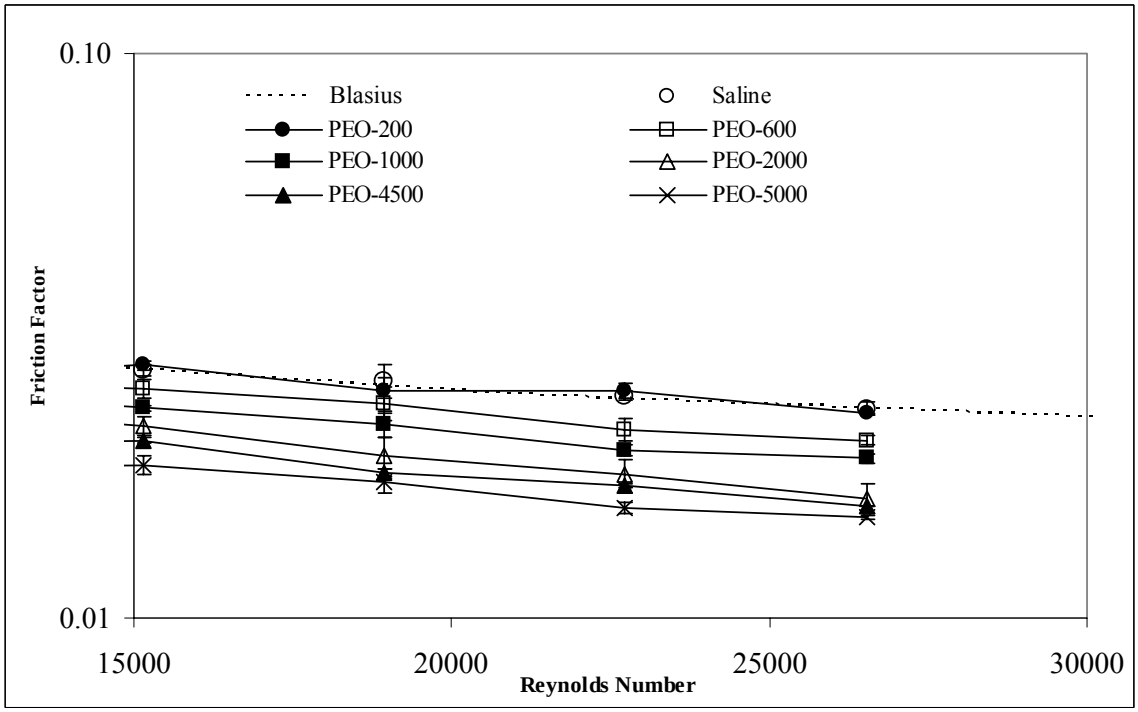

Figure 3-2. Friction factor vs. Re for several PEOs tested in a turbulent flow circulating system at 100 μg/ml. The drag reducing ability of PEO increased with an increase in MW of the PEO

Table 3-1. Average drag reduction produced by various PEOs at a Reynolds number of 23,000

MW (Da)	Drag Reduction at 100 μg/ml (%)
200K	0
600K	15
1000K	22
2000K	29
4500K	34
5000K	38
Dextran 2-40million	0

3.2.2 Polymer drag reduction in turbulent flow of blood

The efficacy of DRPs in turbulent blood flow was investigated using the flow system described in 3.1.1. Bovine blood obtained from a slaughterhouse and diluted with saline to a hematocrit of 20% was used for this study. Two DRPs, PEO-4500 and aloe derived DRP (AVP), were tested, and both were found to be able to significantly reduce flow resistance in blood. Figure 3-3 shows the drag reduction produced by these polymers in turbulent blood flow [79]. As one can see, aloe-based DRP has much higher drag-reducing efficiency than PEO-4500 when compared at the same concentrations. Since the viscosity of blood was significantly higher than that of water, the Reynolds numbers obtained in the blood loop were lower than those in the saline loop and, therefore, the drag reducing effect in blood was not as strong as that in saline. It is known that drag reducing ability increases with increased Reynolds number [27].

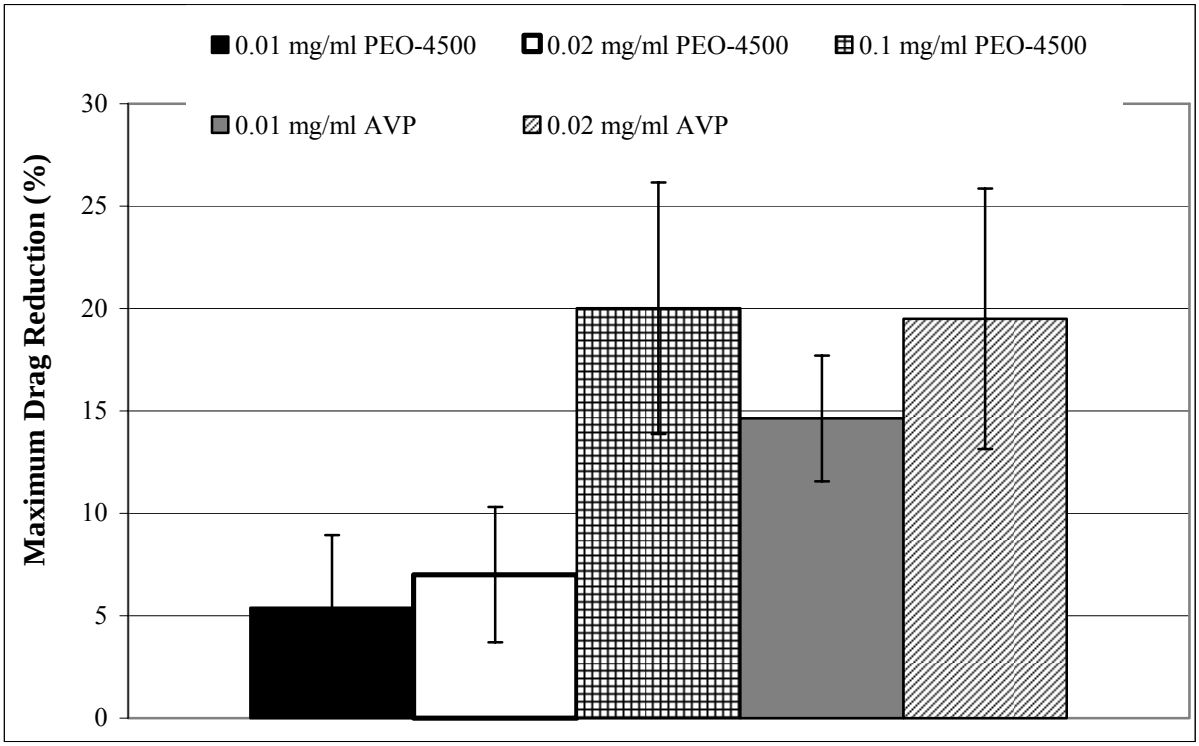

Figure 3-3. Maximum drag reduction in turbulent flow of blood produced by PEO-4500 and AVP at various concentrations.

3.2.3 GPC

Molecular characteristics, including M_n, M_w, IV, R_g, R_h, and PDI were determined for several different PEOs and for high MW dextran. Results, obtained by GPC and presented as mean ± standard deviation, are shown in Table 3-2.

Table 3-2. Molecular characteristics of PEO and dextran obtained using GPC.

	M_n	M_w	IV	R_g	R_h	PDI
	(Da)	(Da)	(dl/g)	(nm)	(nm)	
PEO-200	$4.0x10^4 \pm .3x10^4$	$2.0x10^5 \pm .02x10^5$	1.6 ± .01	20.0 ± .1	15.4 ± .1	5.1 ± .3
PEO-600	$2.1x10^5 \pm .2x10^5$	$9.5x10^5 \pm .3x10^5$	5.0 ± .06	50.3 ± 1.2	38.7 ± .6	4.5 ± .3
PEO-1000	$5.1x10^5 \pm 1.0x10^5$	$1.5x10^6 \pm .2x10^6$	6.8 ± .4	65.3 ± 4.0	50.7 ± 2.9	3.0 ± .3
PEO-2000	$5.3x10^5 \pm 1.5x10^5$	$1.9x10^6 \pm .8x10^6$	8.6 ± .4	77.7 ± 1.5	60.0 ± 1.0	3.1 ± .2
PEO-4500	$2.8\ x10^6 \pm .6x10^6$	$4.4x10^6 \pm .2x10^6$	13.0 ± .5	120.1 ± 3.6	92.1 ± 3.1	1.7 ± .4
PEO-5000	$2.0x10^6 \pm .4x10^6$	$3.0x10^6 \pm .3x10^6$	12.7 ± .7	107.3 ± 5.5	82.3 ± 4.5	1.6 ± .2
Dextran	$6.8x10^6 \pm .3x10^6$	$1.4x10^7 \pm .09x10^7$	0.9 ± .06	73.2 ± 1.5	56.3 ± .6	2.0 ± .1

3.2.4 Rheological Characterization

Concentrated PEO solutions with MW above 1 x 10^6 Da exhibited non-Newtonian behavior, a well-known property of DRPs. Viscosity vs. shear rate curves for these solutions at a concentration of 2.5 mg/ml, determined using a cone and plate viscometer, are shown in Figure 3-4. Viscosity, elasticity, and relaxation time vs. shear rate curves for the PEO solutions with MW 1 x 10^6 Da and greater are shown in Figures 3-5, 3-6, and 3-7. Elasticity and relaxation time are negligible for the lower MW PEOs and are therefore shown only for the two tested PEOs with the highest MW (PEO-4500 and PEO-2000). PEOs with MW below 1 x 10^6 Da, however, behaved as Newtonian fluids. PEO-200 and PEO-600 had viscosities of 1.4 and 1.8 cP at 2.5 mg/ml, respectively. Asymptotic viscosities at a concentration of 0.1 mg/ml were measured using a capillary viscometer at 22°C ± 1°C and are shown in Table 3-3. At low concentrations, the DRPs behave as Newtonian fluids where viscosity is independent of shear rate. Therefore it is valid to use asymptotic viscosity in characterizing these polymer solutions.

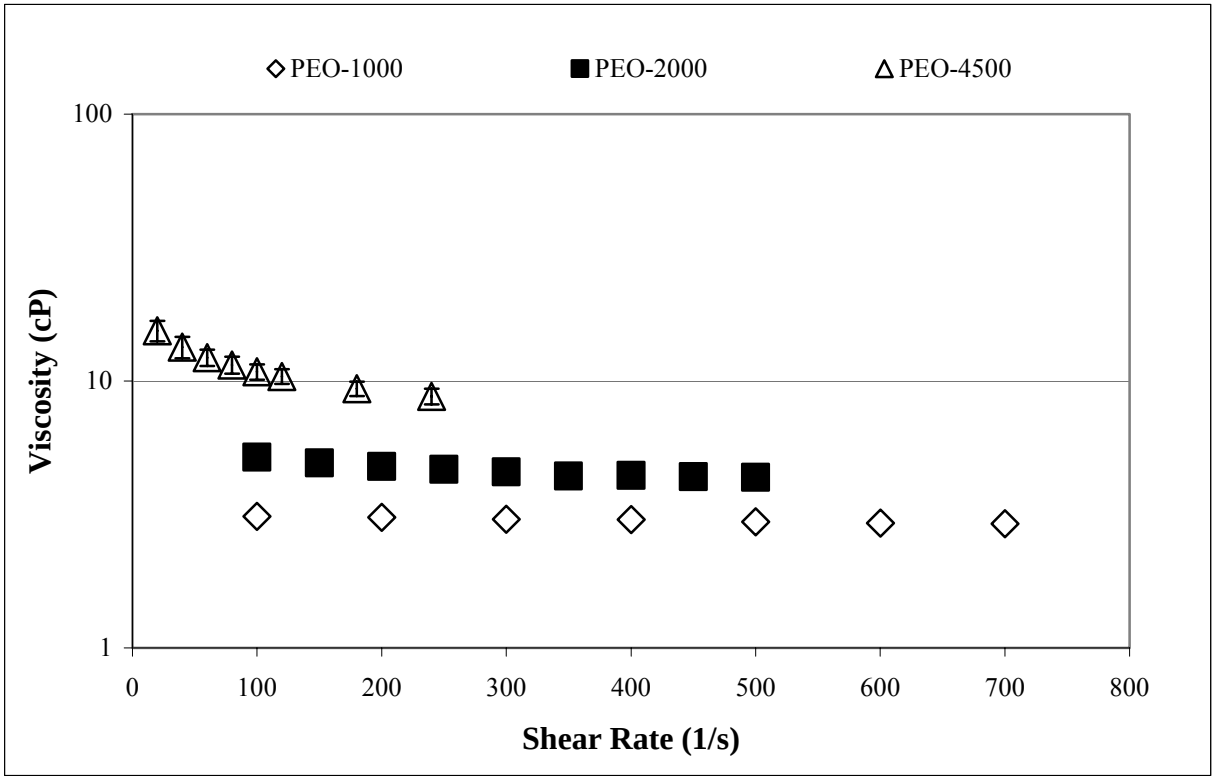

Figure 3-4. Viscosity data for PEOs at 2.5 mg/ml measured using a Brookfield cone and plate rheometer

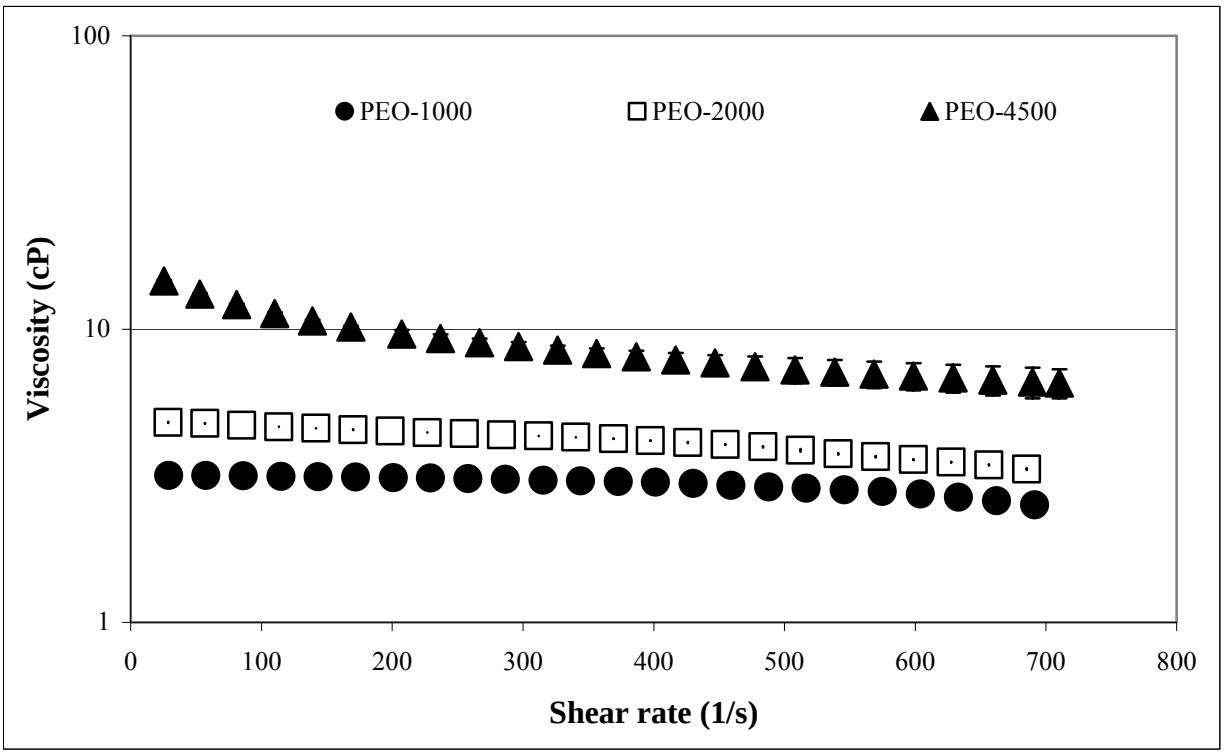

Figure 3-5. Viscosity data for PEOs at 2.5 mg/ml obtained using a viscoelastometer (Vilastic)

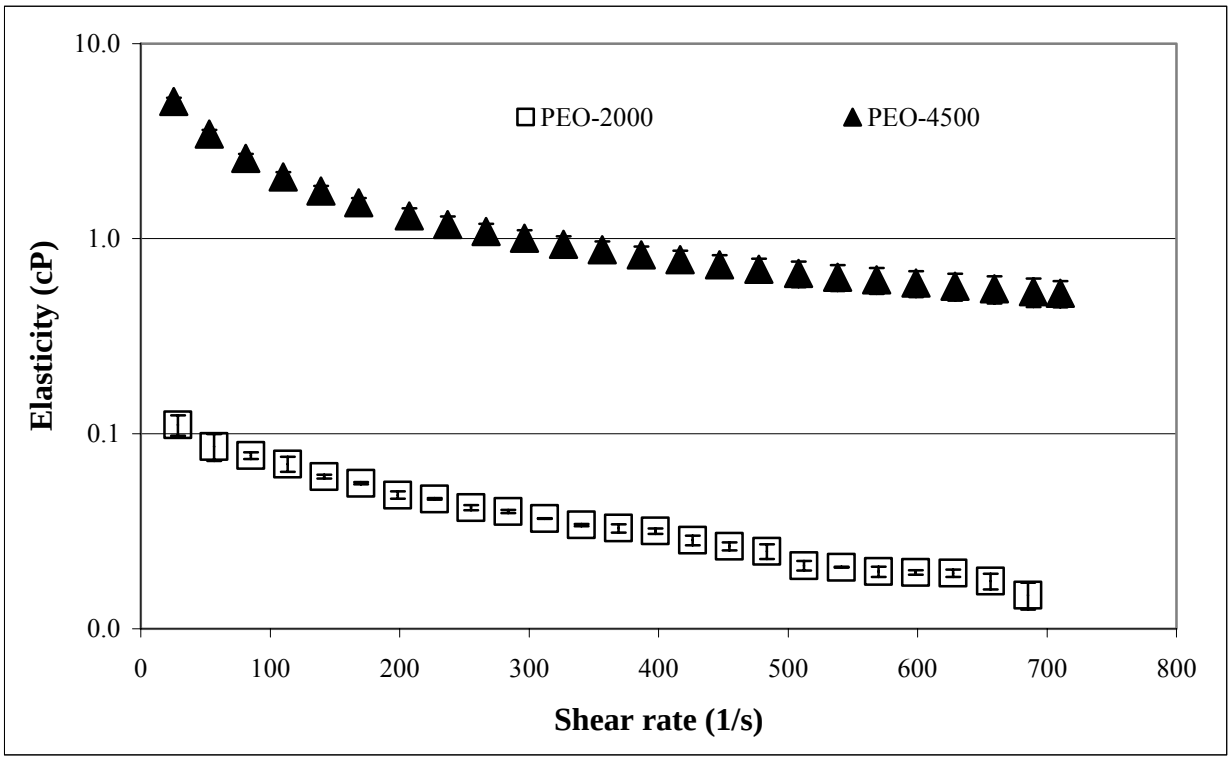

Figure 3-6. Elasticity data for PEOs at 2.5 mg/ml obtained using a viscoelastometer (Vilastic)

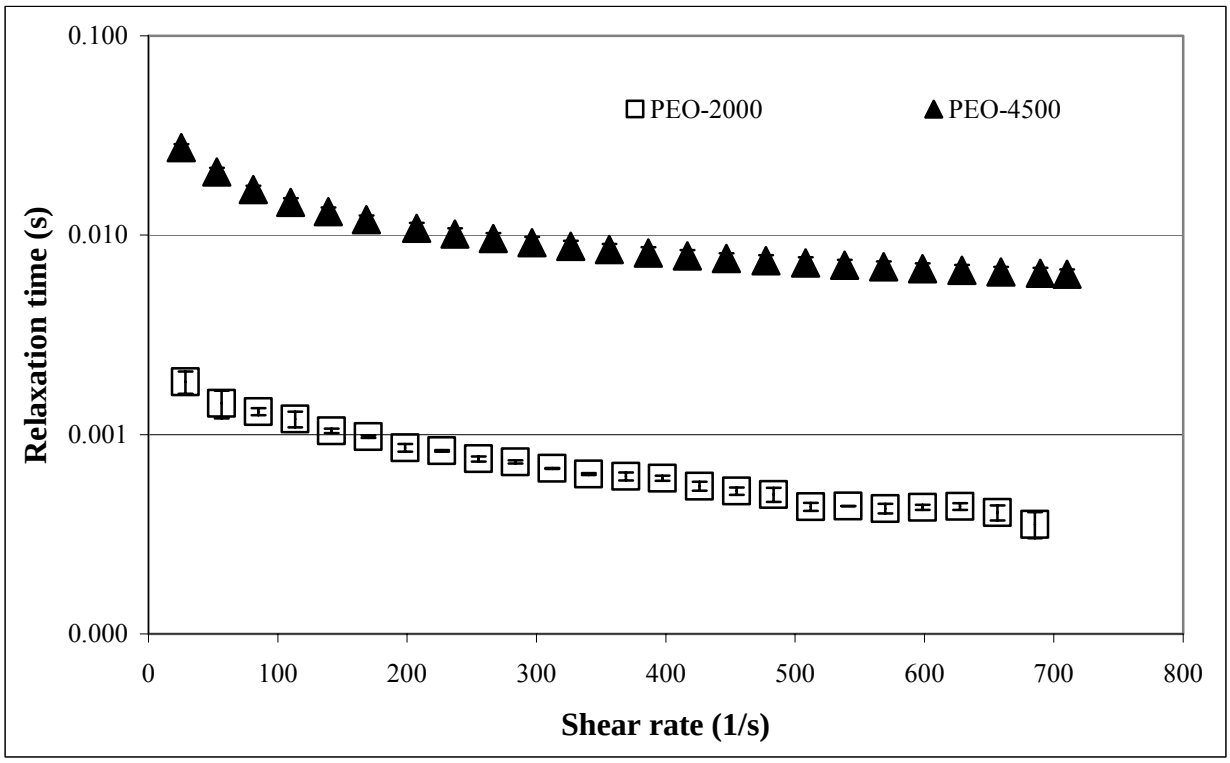

Figure 3-7. Relaxation times for PEOs at 2.5 mg/ml obtained using a viscoelastometer (Vilastic)

Table 3-3. Asymptotic viscosities of PEOs measured by a capillary viscometer at a concentration of 0.1 mg/ml at 22 °C ± 1 °C.

	Capillary Viscosity (cP) at 0.1 mg/ml
PEO-200	1.08
PEO-600	1.10
PEO-1000	1.10
PEO-2000	1.22
PEO-4500	1.25
Dextran	1.07

3.2.5 DRP Degradation Studies

PEO-4500 initially produced a significant reduction in resistance to flow of saline and of RBC suspensions when it was added to flowing fluid. However, the drag reducing efficiency of this polymer decreased rapidly with increased time of exposure to flow. In saline, the PEO-4500 completely lost its drag reducing ability after about an hour of flow. The presence of RBCs, however, significantly accelerated the polymer degradation rate, as shown in Figure 3-8. Additionally, an increase in RBC concentration led to an increase in degradation rate. In a 20% suspension of RBCs, the PEO-4500 completely lost its drag reducing effectiveness in three minutes (compared to ~60 minutes in saline alone).

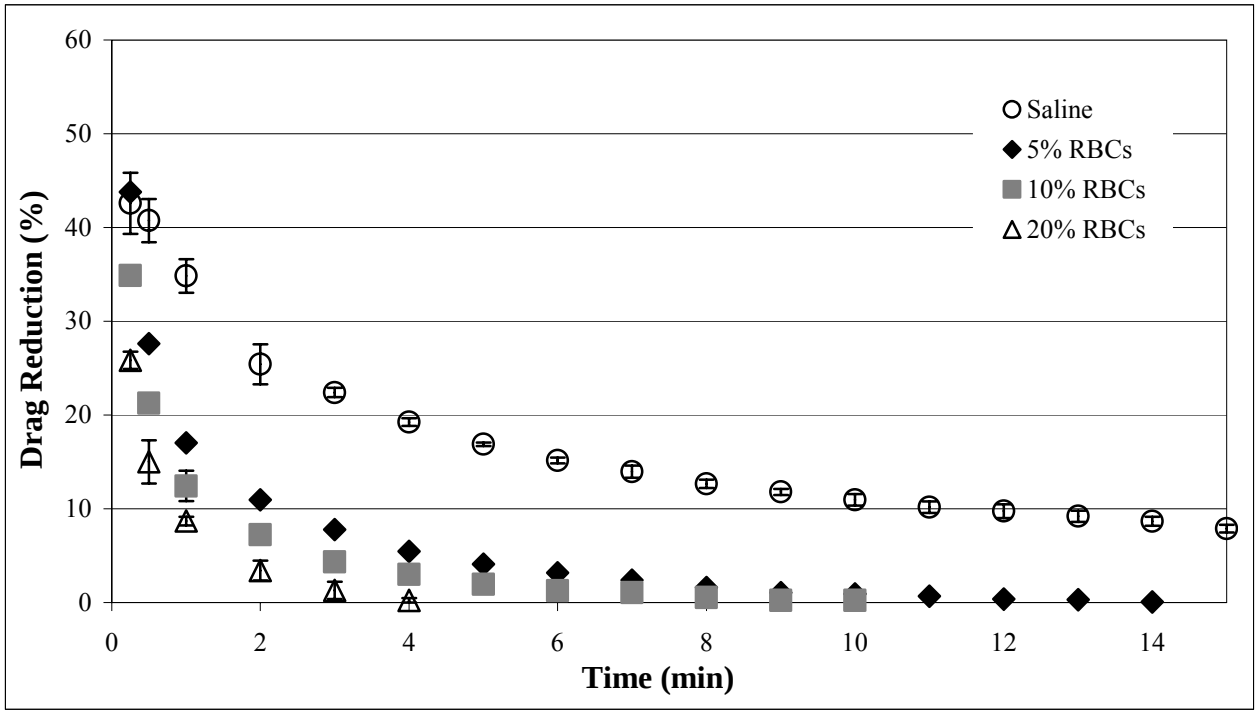

Figure 3-8. Drag reduction vs. time for PEO-4500 at a concentration of 0.1 mg/ml in saline and in the presence of RBCs at several concentrations. The rate of DRP degradation increases with an increase in RBC concentration

A similar effect was observed for PEO-4500 degradation in suspensions of rigid glass particles. Polymer degradation rate increased with an increase in particle concentration (Figure 3-9). While the polymer degraded much faster in either type of suspension than in saline, rigid particles caused a greater increase in PEO-4500 degradation rate than deformable RBCs at the same concentration (Figure 3-10). The matching viscosity control tests showed that while PEO-4500 degraded slightly faster in a 15% glycerol solution than in saline, the degradation was significantly slower in glycerol than in the 20% RBCs, which had the same viscosity (Figure 3-11).

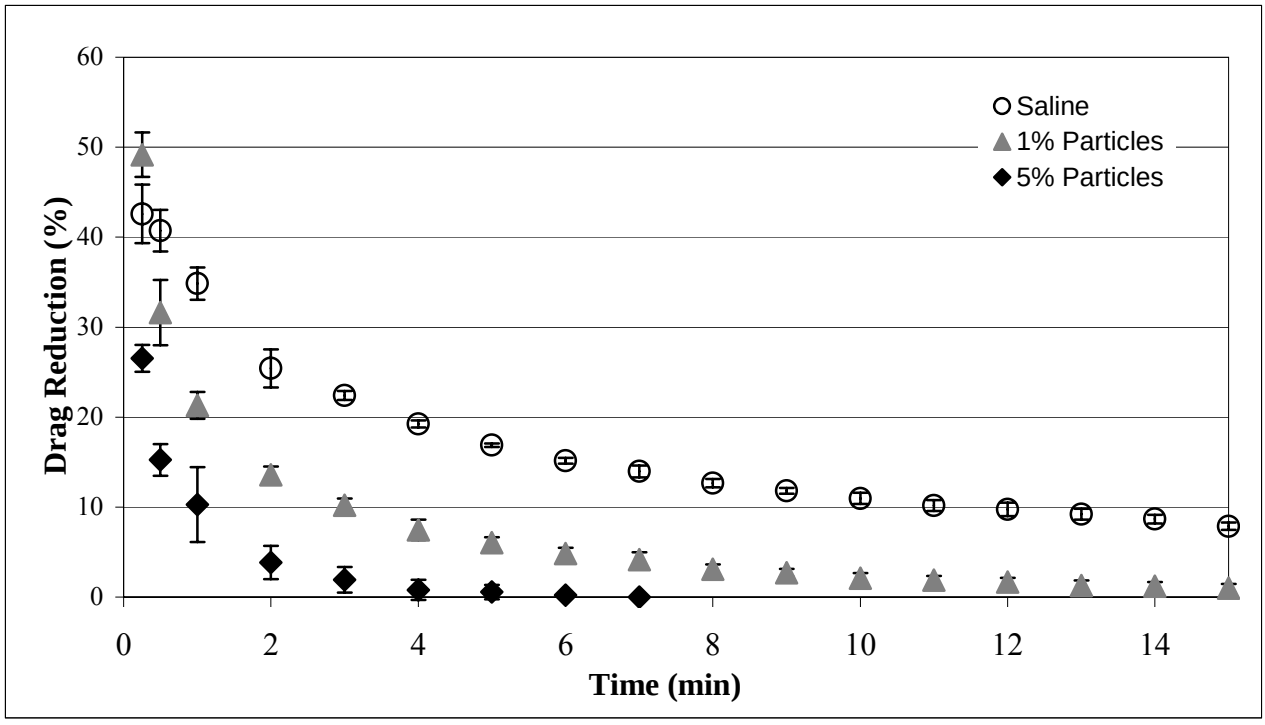

Figure 3-9. Drag reduction vs. time for PEO-4500 at a concentration of 0.1 mg/ml in saline and in the presence of rigid glass particles at two concentrations. The rate of PEO degradation increases with an increase in concentration of particles.

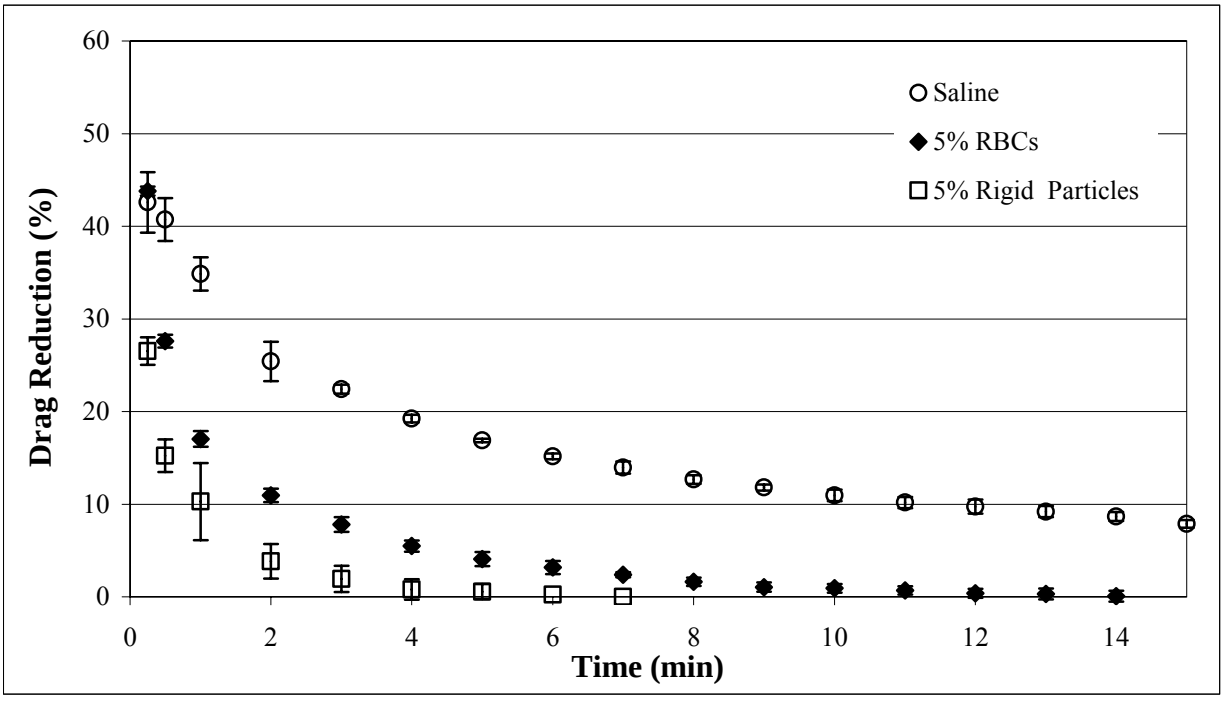

Figure 3-10. Drag reduction vs. time for PEO-4500 at a concentration of 0.1 mg/ml in saline compared to that in 5% RBCs or 5% rigid glass particles. The rate of polymer degradation is higher in a RBC suspension than in saline, and further increases in a suspension of rigid particles.

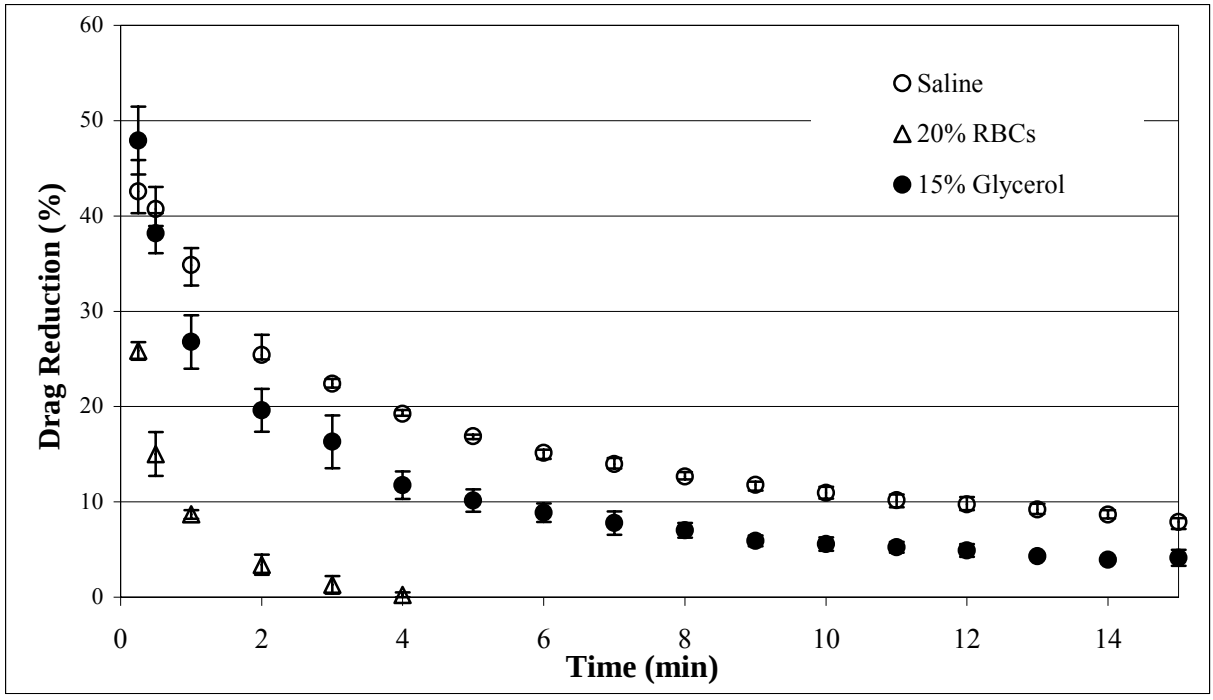

Figure 3-11. Drag reduction vs. time for PEO-4500 at a concentration of 0.1 mg/ml in saline compared to that in a 20% RBC suspension and an equiviscous glycerol solution. The rate of degradation of PEO-4500 at 0.1mg/ml in a 15% glycerol solution, having the same viscosity as a 20% RBC solution is slightly higher than in saline, but much lower than in the 20% RBC suspension

The MW of PEO-4500, determined by GPC, decreased significantly with increased exposure to flow. M_w of the PEO-4500 was initially 4.4 x 10^6 Da, but decreased to 2.5 x 10^6 Da within one hour and 1.5 x 10^6 Da following five hours of exposure to turbulent flow in saline. It is known that, as DRPs decrease in molecular weight, the onset of drag reduction occurs at higher Reynolds numbers [27]. Therefore, although polymers with molecular weights above 10^6 Da can still produce drag reduction, the Reynolds number in this case may not be high enough for the PEO with a molecular weight of 2.5 x 10^6 Da to produce significant drag reduction. IV also decreased significantly throughout the five hour study. IV of PEO was initially 9.8 dl/g but decreased to 7.7 dl/g within one hour and to 5.8 dl/g in five hours. The initial measurements for

this study were taken after one minute of exposure to turbulent flow. Although this initial M_w is similar to that given for undegraded PEO-4500 in Table 3-2, the PDI is much higher in this case. Therefore, there is a larger fraction of low MW polymer which would account for the lower IV and R_g. The discrepancy between the initial values of the molecular parameters measured in this study and the values in Table 3-2 may be due to the fact some degradation likely occurred during the first minute of exposure to flow. The molecular characteristics of PEO-4500 following exposure to turbulent flow in saline for a series of times are shown in Table 3-4.

Table 3-4. Molecular characteristics and drag reduction (DR) of PEO-4500 at 0.1 mg/ml during turbulent flow degradation in saline

Time (min)	**M_w** (Da)	**IV** (dl/g)	**Rg** (nm)	**PDI**	**DR** (%)
1	4.4×10^6	9.8	101	3.4	34
5	3.7×10^6	9.4	95	3.5	28
15	3.2×10^6	8.6	88	3.6	17
30	2.8×10^6	8.1	84	3.1	8
60	2.5×10^6	7.7	80	2.9	3
120	2.0×10^6	6.9	72	2.9	1
180	1.8×10^6	6.3	67	3	0
240	1.7×10^6	6.2	66	2.5	0
300	1.5×10^6	5.8	63	2.7	0

The single relaxation decay model, described in Section 3.1.5, fit the data well for PEO degradation in any of the tested solutions or suspensions (saline, RBCs, rigid particles, glycerol) for short term exposure to flow. DRP degradation rate (k) increased linearly with an increase in particle concentration as seen in Figure 3-12.

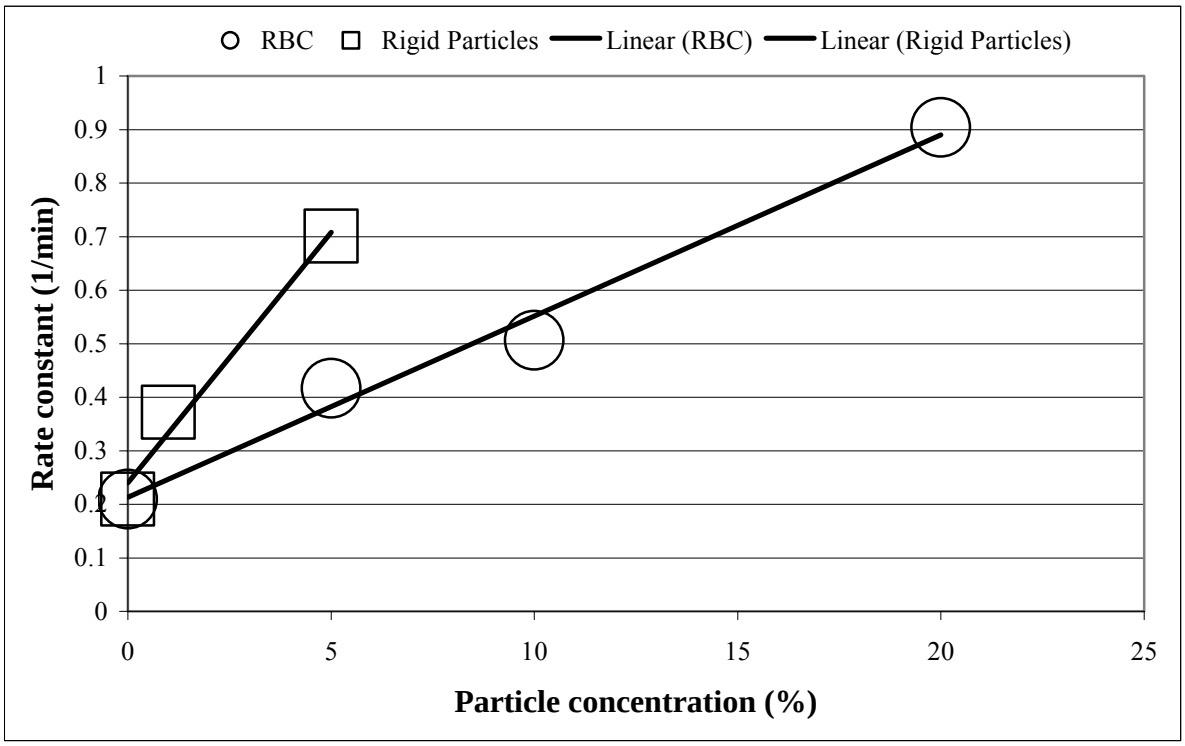

Figure 3-12. The rate of PEO degradation rate increases linearly with an increase in particle concentration. Rigid particles cause a larger increase in degradation rate than flexible RBCs for a given concentration increase.

3.3 DISCUSSION

As described in sections 3.1.1 – 3.1.4 and 3.2.1 – 3.2.4, a series of tests was created to characterize and evaluate the effectiveness of a polymer as a DRP, and the test protocol was validated using well characterized polymers, PEOs and high MW dextran. The results obtained in this specific aim for a well known DRP, PEO, and a high molecular weight polymer which is not a drag reducer, high MW dextran, agreed well with the literature. These tests verified that high molecular weight in combination with linear structure and non-Newtonian behavior in relatively concentrated solution are essential for drag reduction and that these properties could be

accurately evaluated using the protocol developed in this aim. Evaluation of DRP efficacy in turbulent blood flow showed that the presence of RBCs, which would be encountered *in vivo,* does not prevent the studied DRPs from reducing flow resistance. This test could be used to ensure that the effectiveness of newly developed DRPs would not be destroyed by RBCs. Overall, this series of experiments could be applied to new polymers to determine their potential to be used as DRPs for biomedical applications. One limitation of this test protocol is that, since the mechanism of the intravascular DRP effect is likely different from that in turbulent flow, proving that a DRP is effective in turbulent flow may not be enough to ensure that it will be effective *in vivo*. However, considering that the PEOs described above were tested in animal models, and there was a certain correlation found between intravascular effectiveness of these polymers and their physicochemical characteristics including drag reducing ability, it can be concluded that the developed set of tests is predictive for the *in vivo* behavior of new DRP candidates. This concern will be addressed more thoroughly in Specific Aims 2 and 3.

Mechanical degradation studies of DRPs, described in section 3.1.5 and 3.2.5, are also essential in characterizing DRPs as well as predicting their potential for use *in vivo*, especially in treating chronic circulatory disorders such as atherosclerosis or complications of diabetes. Determination of degradation behavior in the presence of particles such as RBCs is especially useful in predicting how DRPs will behave in the body, specifically how quickly their effects will diminish and therefore how often they may have to be administered. The observed increase in degradation rate of PEO in the presence of particles is a concern that must be considered in choosing DRPs for use *in vivo.*

The results discussed in Section 3.2.5 suggested that the increased degradation in suspensions is likely due to the combination of increased viscosity and the presence of particles,

with the particles playing the larger role. It has been shown that the intensity of turbulence of blood at hematocrits lower than 30% is greater than that of plasma adjusted to the same viscosity at a given Reynolds number [80]. Collisions between cells and their tumbling result in changes of direction of motion and, thus, the development of additional vortices. These vortices might be responsible, at least in part, for the increased PEO degradation rate observed in the presence of particles. Rigid RBCs are known to increase turbulence intensity even more than normal, flexible cells. The deformation of RBCs may absorb some of the kinetic energy from the turbulent flow and therefore reduce the size of these vortices to some extent [80]. This may explain the increase in PEO degradation rate in the presence of rigid particles compared to that in deformable RBCs.

The developed test provides a useful method for comparing the degradation behavior of various DRPs or a DRP in different solvents. Contribution of the shear stresses in the pump head to the mechanical degradation of PEO should be considered in the future in order to quantitatively determine the stresses which cause DRP degradation, but does not play a major role in this comparative study since the studies were performed at the same pump speed. It has been suggested that mechanical degradation of DRPs could be used as a model to study shear induced RBC damage [81]. It was also shown in an *in vitro* study that the Biomedicus pump did not produce significant hemolysis [82], and therefore it can be hypothesized that the major DRP degradation did not occur in the pump.

A single relaxation decay model was effective in predicting degradation behavior of PEO in all tested suspensions. Rate constant increased linearly with an increase in particle concentration, and was much higher for rigid particles than for deformable RBCs. This model could be applied to predict the time course of degradation of PEO. This has little practical use for PEO, however, since PEO degradation, especially in suspensions, occurs very quickly and can be

easily studied experimentally. A similar model was considered for predicting the mechanical degradation of other DRPs which degrade much more slowly. This is discussed in section 5.2.1.5.

Overall, the methods devised in this aim provided a strong basis for characterization of DRPs and determination of their efficacy. The combination of these tests can be used to evaluate the potential of candidate polymers to be effective in improving blood flow in the vascular system.

4.0 *IN VITRO* MICROSCALE STUDIES OF POTENTIAL MECHANISMS OF THE INTRAVASCULAR EFFECTS OF DRAG REDUCING POLYMERS

Elucidation of the mechanisms of the DRP effects on hemodynamics is essential from a scientific point of view as well as for their progress toward potential clinical use. The effects of DRPs on blood flow over a range of macro and microflow conditions similar to those found in the vascular system were studied using straight tubes of various lengths and diameters as well as fabricated models of microvessel bifurcations. In this specific aim, microchannel flow systems simulating the microflow environment of RBCs encountered in small arteries, arterioles and capillaries were designed and fabricated. The effects of DRPs on blood microflow were quantified using pressure and flow measurements as well as blood hematocrit measurements and microscopic flow visualization methods.

4.1 METHODS

4.1.1 Microchannel fabrication

Standard photolithography techniques and replica molding were used to fabricate bifurcated microchannels. Systems with channels ranging in diameter from 25 to 200 μm, one bifurcation or multiple bifurcations, and channel expansions and contractions were fabricated for these

studies. Relative flow resistances were calculated using the Poiseuille equation (Equation 8) to ensure that each branch will get sufficient flow.

$$Q = \frac{\pi \cdot r^4 \cdot \Delta P}{8 \cdot \mu \cdot L} \tag{8}$$

The channel design was drawn using a computer-aided design program (Adobe Illustrator) and was initially printed on a transparency using a high-resolution commercial printer to create a photolithographic mask. Preliminary fabrication using a transparency mask produced channels with rather rough edges. Therefore, in order to obtain channels with smooth, straight walls necessary for clear visualization of a developed near wall plasma layer, a chrome mask (fabricated at Penn State University), which significantly improved the resolution, was used. A resolution of ~ 500 nm can be obtained using a chrome mask compared to > 20 μm with a transparency mask [83]. Sample microchannel system designs are shown in Figure 4-1.

A negative photoresist, SU-8 2050 (Microchem), was spin-coated on either a three or four inch silicon wafer at a spin speed of 3000 rpm in order to control the channel height close to 100 μm. The resist was then soft baked in order to evaporate solvent and increase film density. The mask and wafer were exposed to near ultra-violet light, which produced the pattern of the mask in the photoresist. After exposure, the wafer was baked and submerged in a developer in order to remove unexposed photoresist. Since SU-8 is a negative resist, exposed areas were cross-linked and remained on the wafer after development. Following development, the patterned wafer was hard baked to remove remaining solvent from the photoresist.

A replica molding technique was then used to create a negative replica of the master in polydimethyl siloxane (PDMS). PDMS was an excellent choice for this application since it is strong, inexpensive, transparent, non-toxic, and can effectively reproduce features on the micron scale using replica molding [83]. The PDMS was poured over the mold, placed under vacuum to

remove air bubbles, cured in an oven at 60ºC for four hours, and then peeled from the master. This step provided three of the four walls of the channels. Access holes were then punched using a blunt needle, and the PDMS replica was sealed to a flat glass surface (cover glass) using an irreversible sealing technique where both surfaces were exposed to an air plasma, which introduced silanol groups on the surfaces, which in turn formed covalent bonds creating an irreversible seal [83]. Finally, the channels were placed in an oven at 60ºC overnight in order to strengthen the bond between the glass and PDMS

.

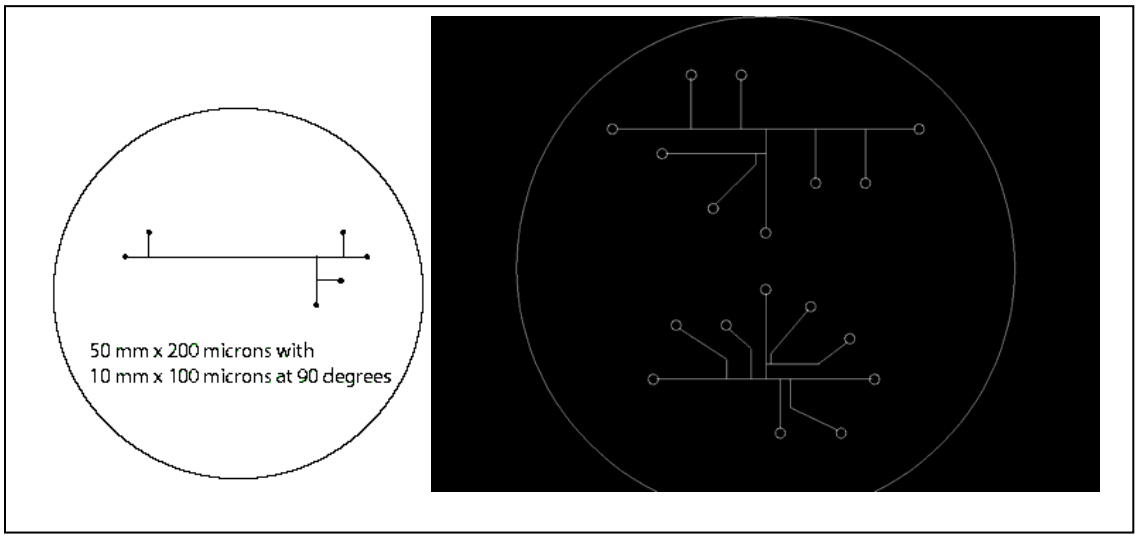

Figure 4-1. Sample microchannel design (left) and the chrome mask used for microchannel fabrication (right)

Cross sections of unsealed PDMS channels and of photoresist designs on the silicon wafer were cut, and light microscopy (PDMS channels) and scanning electron microscopy (silicon wafer) were used to verify the shape and dimensions of the channels. Figure 4-2 shows a cross section of a 100 μm segment of a PDMS channel (top left), an intact channel contraction

from 200 μm to 100 μm (top right), and scanning electron micrographs of cross sections of 200 μm and 50 μm segments of the photoresist on the silicon wafer (bottom left and right, respectively). All channel heights were verified to be ~ 100 μm.

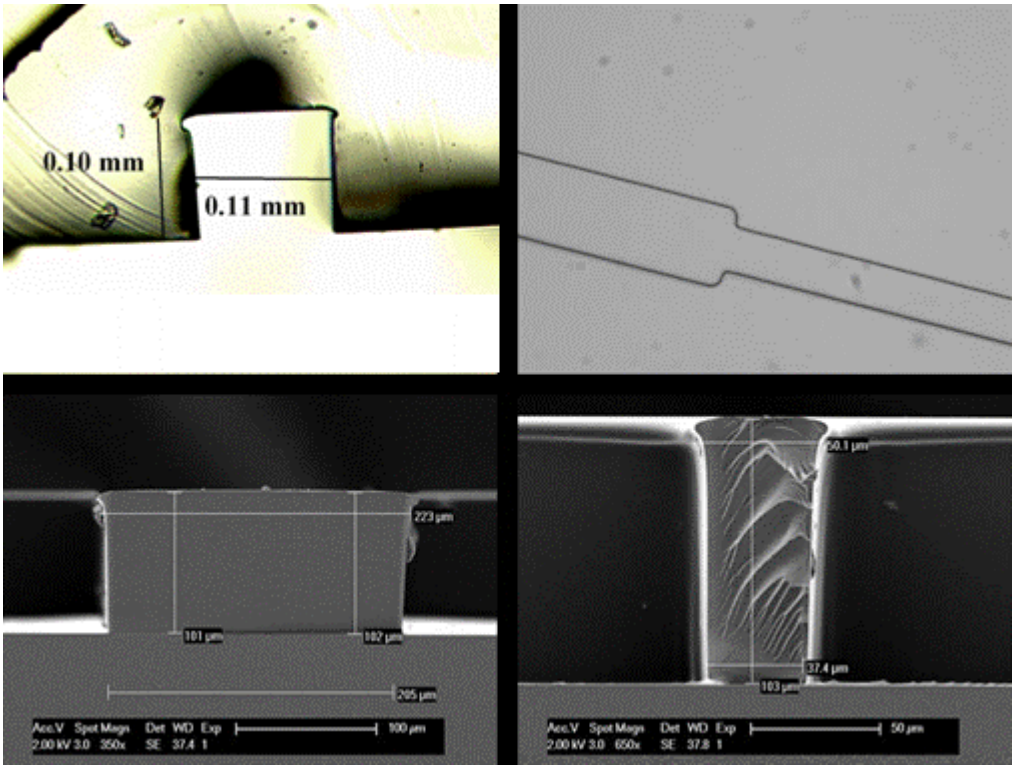

Figure 4-2. Micrographs of PDMS microchannels and the silicon wafer/photoresist master

4.1.2 Preparation of a red blood cell (RBC) suspension

Bovine blood was obtained from a local slaughterhouse. Bovine blood was chosen since it is easier to obtain and work with and less expensive than human blood and is often used in *in vitro* modeling of physiological and pathophysiological effects in the cardiovascular system [54, 87-89]. The RBCs were washed three times with phosphate buffered saline (PBS) and resuspended at a hematocrit of either 20% or 40% in PBS with 1% bovine serum albumin added to preserve

the biconcave shape of the cells. A hematocrit of 20% was chosen for the majority of the studies in capillary tubes and microchannels since *in vivo* microcirculatory hematocrit ranges between 20 and 50% of systemic hematocrit [56, 84] due to the Fåhraeus Effect which is more pronounced at lower hematocrit for a given vessel diameter [56]. A hematocrit of 40% also was used for several studies in order to mimic physiological hematocrit in the larger vessels since studies were performed in capillary tubes with a wide range of diameters. DRP (saline in controls) was added to the suspension at various concentrations and incubated at room temperature for at least one hour. Light microscopy was used to verify normal biconcave shape of the RBCs.

All *in vitro* blood flow experiments were performed at room temperature. Previous experiments, where blood viscosity with and without polymer was measured in a rotational viscometer at both room temperature and 37°C, showed that the addition of polymer did not change the temperature dependence of blood viscosity. Therefore, it was appropriate to perform the experiments at room temperature.

4.1.3 Effects of DRPs on blood flow in straight capillary tubes

The effects of DRPs on the flow of RBCs in a straight channel in laminar flow were studied using a flow system (Figure 4-3) consisting of a syringe pump (Harvard Apparatus), a pressure transducer (PCB Piezotronics), and a capillary tube with a known diameter ranging from 115-1300 μm in order to test the hypothesis that DRPs attenuate the Fåhraeus-Lindquist Effect. Experiments were performed using tubes with a wide range of diameters and lengths in order to determine how the DRPs' influence on blood flow is affected by capillary tube dimensions. In order to prevent RBC sedimentation, the suspension in the syringe was kept well mixed by

placing a small magnetic stir bar inside the syringe, and manually agitating it using another magnet on the outside. Length of collective tubing was minimized to avoid cell settling in the tubing as much as possible.

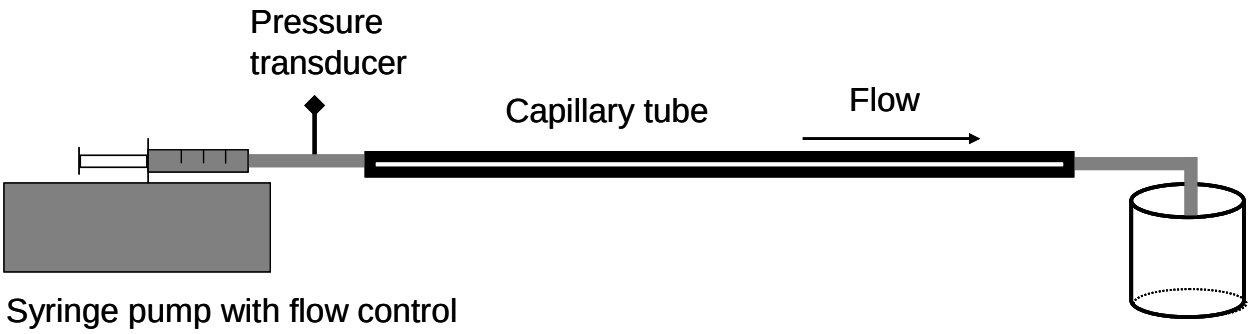

Figure 4-3. Schematic of capillary flow system.

Flow rates varied from 0.05 to 20 ml/min in order to match physiological shear rates and Reynolds numbers. Reynolds number was calculated using Equation 3, and wall shear stress (τ_w) was calculated using

$$\tau_w = \frac{\Delta P * d}{4 * L} \tag{9}$$

where ΔP is the pressure drop across the tube, *d* is tube diameter, and *L* is tube length. Reynolds number and calculated wall shear stress values for the tubes used in this study are shown in Table 4-1. *In vivo*, small arteries and arterioles have diameters ranging from 0.02 to 0.1 cm, flow rates ranging from 0.004 to 5 ml/min, and Reynolds numbers ranging from 0.4 to100 [85].

Table 4-1. Reynolds number and calculated wall shear stress for blood flow in capillary tubes

Diameter μm	Reynolds Number	Wall Shear Stress (N/m^2)
115	1-20	10-70
220	5-30	3-20
410	10-260	2-50
560	30-380	5-40
860	20-250	1-11
1300	10-170	0.3-3

RBC suspensions with a hematocrit of 20% were used for all studies. For the experiments run in the 115 μm tube, a suspension with a hematocrit of 40% was tested as well. DRP concentrations of 2, 10, 20, and 100 μg/ml were applied in this study. A concentration of 2 μg/ml represents an effective concentration for *in vivo* use, while slightly higher concentrations led to a stronger effect and therefore easier quantification of the DRP effect on microscale blood flow. Pressure vs. flow relationship was determined for each polymer concentration and compared to the control RBC suspension. Friction factor was calculated using Equation 4 as described in 3.1.1 and compared to a theoretical friction factor for laminar flow calculated by Equation 10,

$$\lambda = \frac{64}{\mathrm{Re}} \tag{10}$$

which can be derived by substituting the Poiseuille equation into the Darcy-Weisbach equation. An increase in pressure gradient, and therefore friction factor, indicated attenuation of the Fåhraeus-Lindquist Effect. Mean friction factors were compared using one-way ANOVA and unpaired, two-sample Student's *t*-tests assuming unequal variances with two-tail distribution. Data are presented as mean ± standard deviation.

While physiological blood flow is pulsatile, steady flow was chosen for the current studies since it is much easier to quantify and model, and since pulsatility is significantly diminished in microvessels [59, 86]. Although real blood vessels are distensible, the current

microflow studies were performed in tubes with rigid walls in order to be able to quantify DRP effects on the wall shear stresses via measurements of pressure gradients across a microchannel. If an increase in pressure gradient is seen after the addition of DRP to blood, it can be assumed that in an *in vivo* situation this would cause vasodilation. However, to quantitatively characterize the changes in the microchannel flow produced by DRP additives, application of channels with rigid walls is valuable. Pressure versus flow relationships were determined for both control and DRP suspensions in the same tubes at the same flow rates in order to ensure that there is no difference in surface roughness between tests.

Entrance length (l_e), defined as the length needed for the velocity profile to become fully developed, was calculated [74] using

$$l_e = 0.06 \cdot \mathrm{Re} \cdot d \ , \qquad (11)$$

where d is tube diameter. Tubes were selected to be sufficiently long, and therefore the assumption of fully developed, steady, laminar flow is valid.

Entrance and exit effects were also considered. It was shown that drag reducing ability correlates well with elongational viscosity [87], and, since the flow at the entrance to a tube is highly elongational, the effects of this elongational viscosity on the pressure versus flow relationship in the tube must be determined. These effects were examined through capillary blood flow experiments in tubes of the same diameter with different lengths. Since the flow is laminar, the pressure drop per unit length along the tube should be constant for a constant flow rate. If this is not the case in the tubes of different length, the difference can be attributed to entrance effects. Mean pressure drop per unit length was calculated for a 220 μm diameter tube with a length of 50 mm and one with the same diameter but a length of 100 mm and compared

using an unpaired, two-sample Student's *t*-test assuming unequal variances with two-tail distribution. Exit effects can be assumed to be negligible since tubes exited to the atmosphere.

4.1.4 Effects of DRPs on blood flow in bifurcated microchannels

The effect of DRPs on the flow of RBCs in microchannels was studied using the PDMS channels fabricated in 4.4.1. Bovine RBC suspensions were prepared using the method outlined in 4.1.2. It was previously shown that feed hematocrit, diameter, and flow rate distribution between branches are the most important factors in determining RBC distribution at a bifurcation [57], and therefore these parameters were carefully considered in experimental design. Cell distensibility, suspension medium, flow rate in the parent branch, and bifurcation geometry, on the other hand, were shown to have little or no influence on RBC distribution at the bifurcation [57]. In channels with parent branch diameters greater than 50 μm, it was also shown that ratio of parent channel diameter to daughter channel did not affect RBC distribution between the branches [88]. All experiments in this study were performed with parent channels having diameters of 50 μm or greater. A syringe pump (Harvard Apparatus) in infuse mode was used to generate flow of the RBC suspensions through the channels fabricated in 4.1.1. Flow rates ranging in the parent channel from 0.01 to 0.2 ml/min, depending on channel dimensions, were used for these experiments. Reynolds numbers ranged from 1 – 20. A schematic of the microchannel flow system is shown in Figure 4-4.

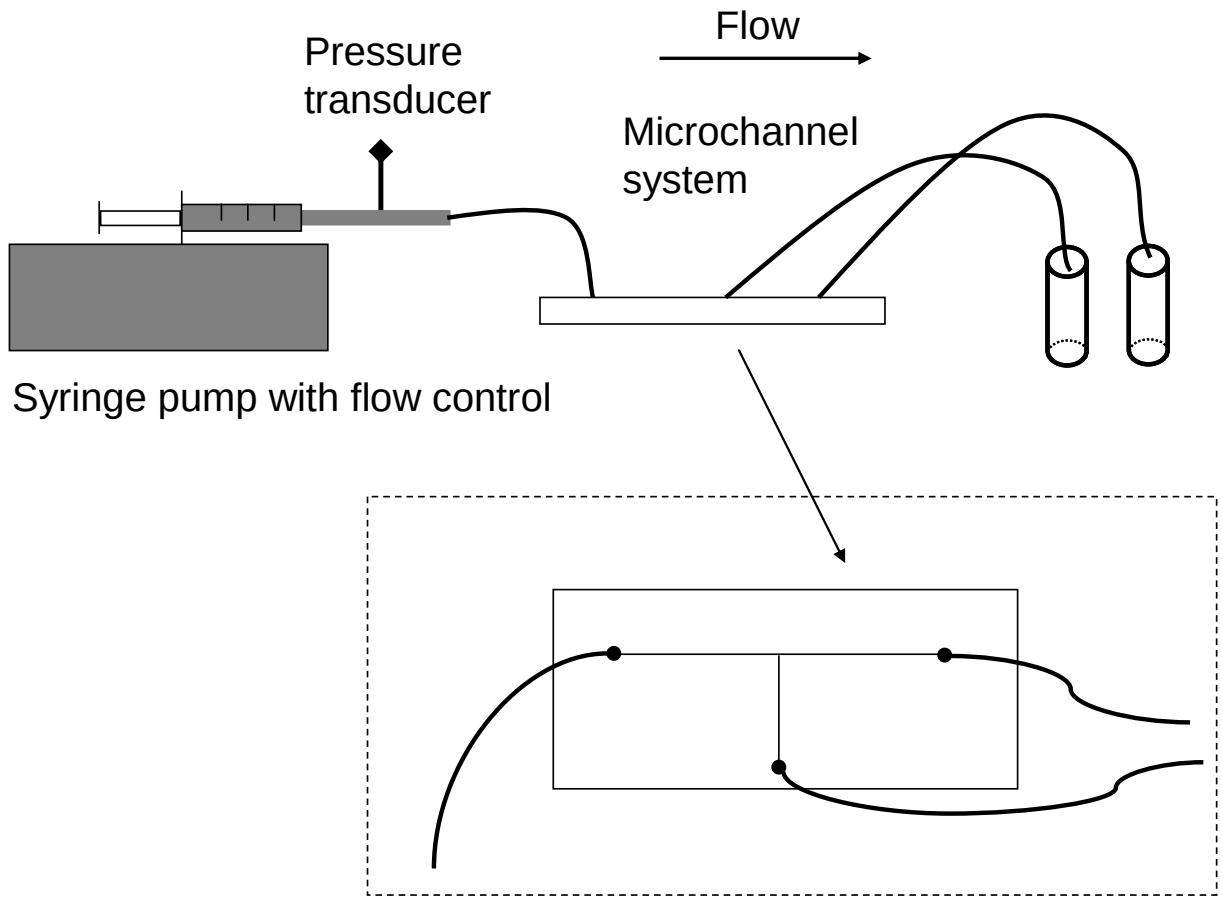

Figure 4-4. Schematic of microchannel flow system

In a separate set of experiments blood samples were collected from each outlet, and hematocrits were measured using a standard microcapillary technique. These experiments were performed in bifurcated channels with a parent branch diameter of 50 μm and a daughter branch diameter of 25 μm since the Fåhraeus, Fåhraeus-Lindquist, and plasma skimming effects become more pronounced as tube diameter is decreased. Depth of both channels was 100 μm. A flow rate of 0.1 ml/min was used for this experiment giving Re ~ 15 in the channel upstream of the bifurcation. It was estimated that almost 90% of the flow went through the parent channel. Wall shear stress was calculated to be ~ 250 N/m^2. Blood samples were collected directly into microcapillary tubes in order to minimize sedimentation in connective tubing. The outlet

hematocrit values from the parent and daughter branches were compared to each other using an unpaired, two-sample Student's *t*-test assuming unequal variances with two-tail distribution. These values were compared in both the DRP and control samples in order to directly determine whether the DRPs were attenuating the plasma skimming effect. Data are presented as mean hematocrit ± standard deviation.

As the RBCs flowed through the microchannels under physiologically relevant pressures and flow rates ranging from 0.01 to 0.2 ml/min, their flow behavior was recorded with a microscopic flow imaging system (Figure 4-5), which consists of an inverted research microscope (IX70, Olympus, NJ), a cooled CCD camera (MicroMax DIF, Roper Scientific, NJ), and an associated image acquisition board hosted in a PC. The illuminated flow field was imaged and recorded by the CCD camera. At least twenty images were recorded at each condition. The control RBC suspension with no polymer added was run first in order to adjust the depth of focus to visualize a clear near-wall plasma layer. The suspension was then replaced with RBC samples containing DRP without moving the channel or changing the focus. Finally, the control suspension was tested again to ensure that the plasma layer was still visible. Image J (a version of NIH image software) was used to quantify the size of the cell free plasma layer in each image. In each image, the cell free area along a given length of the channel was identified manually and quantified using the Analyze Particle tool. Mean plasma layer size was compared between the control and DRP case using an unpaired, two-sample Student's *t*-test assuming unequal variances with two-tail distribution. At least five images were analyzed in each case. Results are presented as mean plasma layer size ± standard deviation. Areas in the main channel and the smaller branch, as well as the bifurcation itself and channel expansions/contractions were imaged.

Images were also taken in a straight glass microchannel having a diameter of 100 μm since its dimensions were well defined, and the plasma layer could be easily observed and quantified. Reynolds numbers in this channel ranged from 1 – 20 and shear stress ranged from 5 – 70 N/m^2. At least five images were analyzed in each case. Results are presented as mean plasma layer size ± standard deviation.

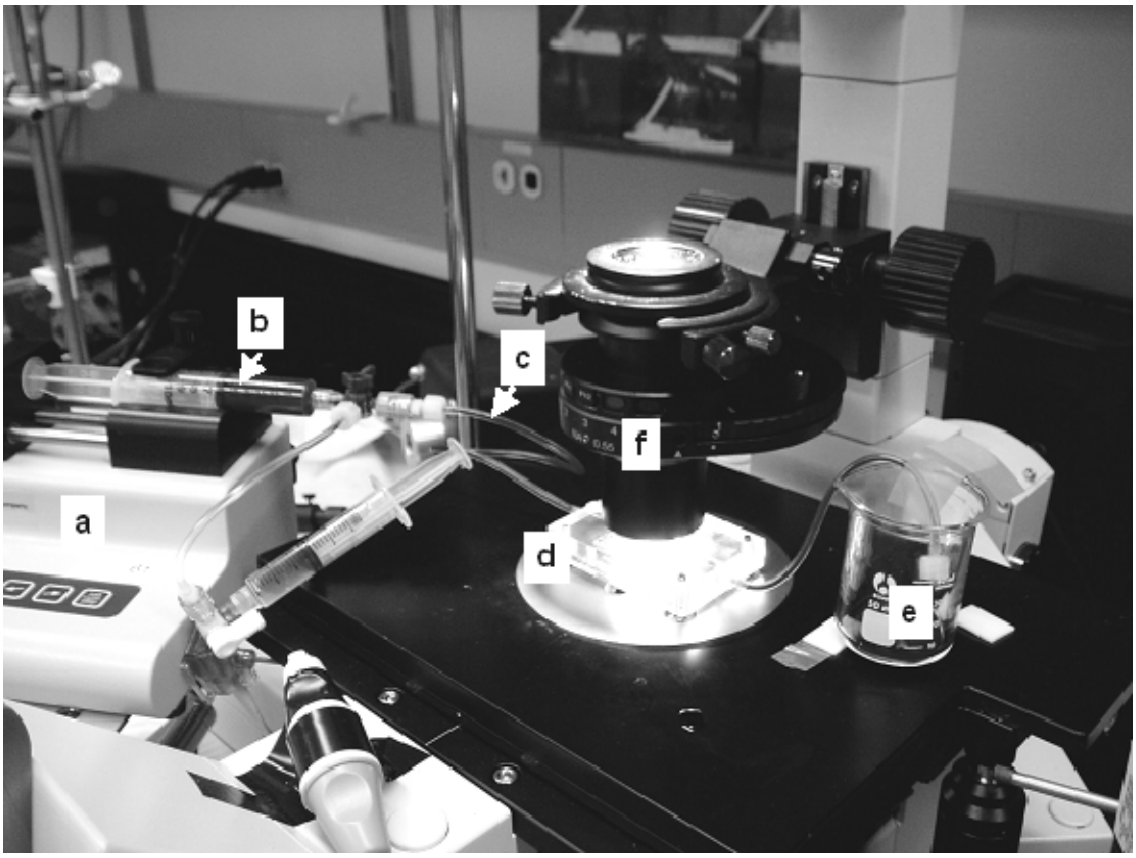

Figure 4-5. System for microflow experiments consisting of: a) syringe pump, b) syringe, c) PVC tubing, d) microchannel, e) reservoir, and f) inverted microscope

4.1.5 Model for DRP effects on microcirculation

Using the marginal zone model developed by Haynes [89], blood flow in small capillary tubes (diameter < ~ 500 μm) can be described and size of the near wall plasma layer can be

predicted with and without DRP additives. Blood flow was modeled as steady flow of a two-phase fluid through a cylindrical tube with a core region of RBCs and a cell free plasma region near the wall. A schematic is shown in Figure 4-6

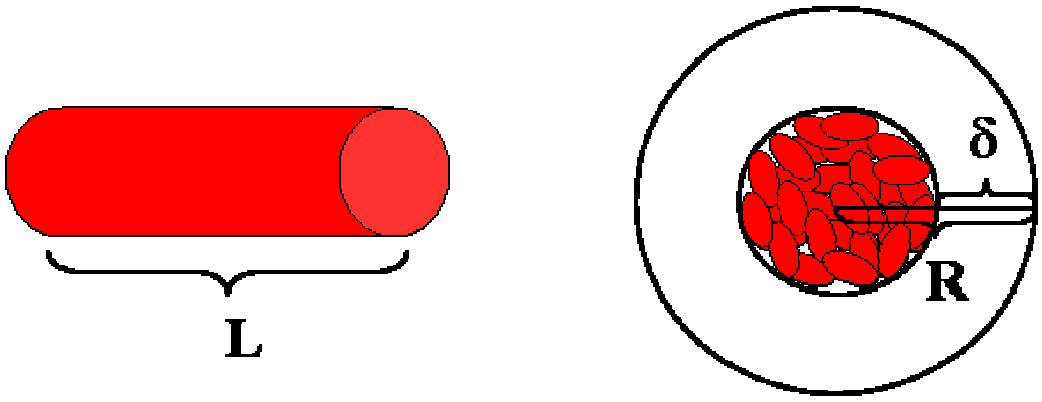

Figure 4-6. Schematic used for marginal zone model of capillary blood flow

Newtonian behavior was assumed in each region. Therefore, in the core RBC region

$$\tau_{rz} = -\mu_{RBC}\frac{dv_z^{RBC}}{dr} = \frac{(P_0 - P_L)\cdot r}{2\cdot L} \qquad (12)$$

where τ_{rz} is the shear stress, μ_{RBC} is the viscosity of the RBC region, v_z^{RBC} is the axial component of the velocity, (P_0-P_L) is the pressure drop over the tube, r is the tube radius, and L is the tube length. μ_{RBC} was assumed to be equal to bulk viscosity of the blood measured using a rotational rheometer. Boundary conditions can be written such that

$\frac{dv_z^{RBC}}{dr} = 0$ at r = 0 since axial velocity is at a maximum at the centerline of the tube and

$\tau_{rz}\big|_{RBC} = \tau_{rz}\big|_{p}$ at r = R - δ, where δ is the size of the plasma layer, since the transport of momentum must be constant across the interface between the RBC and plasma layer. For the plasma region

$$\tau_{rz} = -\mu_p \frac{dv_z^p}{dr} = \frac{(P_0 - P_L)\cdot r}{2\cdot L} \tag{13}$$

where μ_p is the plasma viscosity and v_z^p is the axial component of the velocity. In this case, experimental data were collected using RBCs suspended in PBS, and, therefore, μ_p is equal to the viscosity of water. Boundary conditions can be written as

$v_z^{RBC} = v_z^p$ at r = R - δ since the velocity in each region must be the same at the interface and

$v_z^p = 0$ at r = R because of the no slip boundary at the tube wall. Integration of Equations 11 and 12 gives the axial velocity profile in each region given in Equations 14 and 15.

$$v_z^p(r) = \frac{(P_0 - P_L)\cdot R^2}{4\cdot \mu_p \cdot L}\cdot\left[1-\left(\frac{r}{R}\right)^2\right]$$

$$\text{when } R-\delta \le r \le R \tag{14}$$

$$v_z^{RBC}(r) = \frac{(P_0 - P_L)\cdot R^2}{4\cdot \mu_{RBC} \cdot L}\cdot\left[1-\left(\frac{r}{R}\right)^2 - \frac{\mu_p}{\mu_{RBC}}\left(\frac{r}{R}\right)^2 + \frac{\mu_p}{\mu_{RBC}}\left(\frac{R-\delta}{R}\right)^2\right]$$

$$\text{when } 0 \le r \le R-\delta \tag{15}$$

Flow rates (Q) for each region can then be obtained using Equations 16-19.

$$Q_p = 2\pi \int_{R-\delta}^{R} v_z^p(r) r dr \tag{16}$$

$$Q_{RBC} = 2\pi \int_{0}^{R-\delta} v_z^{RBC}(r) r dr \tag{17}$$

$$Q_p = \frac{\pi\cdot(P_0 - P_L)}{8\cdot\mu_p\cdot L}\cdot\left[R^2 - (R-\delta)^2\right]^2 \tag{18}$$

$$Q_{RBC} = \frac{\pi\cdot(P_0 - P_L)}{4\cdot\mu_p\cdot L}\cdot\left[(R-\delta)^2 - \left(1-\frac{\mu_p}{\mu_{RBC}}\right)\cdot\frac{(R-\delta)^4}{R^2} - \frac{\mu_p}{\mu_{RBC}}\cdot\frac{(R-\delta)^4}{R^2}\right] \tag{19}$$

The sum of the two fractions Q_{RBC} and Q_p gives the total flow rate in the tube, Q.

$$Q = \frac{\pi \cdot R^4 \cdot (P_0 - P_L)}{8 \cdot \mu_p \cdot L} \cdot \left[1 - \left(1 - \frac{\delta}{R} \right)^4 \cdot \left(1 - \frac{\mu_p}{\mu_c} \right) \right] \tag{20}$$

Using the Poiseuille equation, $Q = (P_0 - P_L)\ \pi r^4 / 8\ \mu L$, and Equation 20, the apparent viscosity in the tube can be calculated as

$$\mu_{apparent} = \frac{\mu_p}{1 - \left(1 - \frac{\delta}{R} \right)^4 \cdot \left(1 - \frac{\mu_p}{\mu_{RBC}} \right)} \tag{21}$$

Using these equations and the experimental data obtained from capillary and microchannel blood flow experiments, the effects of DRPs on the size of the near wall plasma layer in tubes of different diameter can be calculated.

4.2 RESULTS

4.2.1 Effects of DRPs on blood flow in straight capillary tubes

Preliminary studies of the effects of DRPs on blood flow in straight capillary tubes were conducted using tubes ranging in diameter from 0.41 to 1.3 mm. All data were normalized for solution viscosity calculated using the Poiseuille equation and data obtained by running suspension media with no RBCs through the flow system. Table 4-2 shows specifications for the tubes tested and the increase in wall shear stress observed in each case. In the larger tubes, where the Fåhraeus-Lindquist Effect did not occur (0.86 and 1.3 mm), the DRPs had no effect on the

wall shear stress. In the smaller tubes (0.41 and 0.56 mm), the DRPs produced a significant increase in wall shear stress due to the attenuation of this effect.

Table 4-2. Tube specifications and increase in wall shear stress caused by DRPs in blood flow in a straight channel

Diameter	Length	Flow Rates	Reynolds Numbers	Shear Rates	Increase in wall shear stress (%)				
(mm)	(cm)	(ml/min)		(1/s)	No DRP	10 μg/ml PEO-4500	20 μg/ml PEO-4500	20 μg/ml AVP	100 μg/ml PEO-4500
0.41	3.5	0.5-10	10-260	1200-67000	0	42	40	18	N/A
0.41	12.7	0.5-2	10-60	1200-9000	0	N/A	23	15	22
0.56	7.5	2-20	30-380	1400-20000	0	15	N/A	N/A	N/A
0.86	13	2-20	20-250	400-5500	0	2	N/A	N/A	N/A
1.3	61.5	2-20	10-170	100-1600	0	0	0	0	N/A

Based on the results of these preliminary studies, which confirmed that the Fåhraeus-Lindquist Effect was more pronounced in smaller tubes, additional studies were performed in capillary tubes with diameters of 220 μm and 115 μm. In the 220 μm capillary with length of 50 mm, 10 μg/ml PEO-4500 caused an average increase in wall shear stress of 11%, and 20 μg/ml PEO-4500 caused an increase of 14% ($p < 0.01$ at all but the lowest flow rate). In the 220 μm capillary with length of 100 mm, PEO-4500 increased wall shear stress by 9% and 26% at concentrations of 10 and 20 μg/ml respectively ($p < 0.05$ at all flow rates and $p < 0.01$ at all but the lowest flow rate). Figure 4-7 shows friction factor vs. Reynolds number for blood flow in the tube with length of 100 mm. In the control case, the experimental friction factor was significantly lower than the theoretical due to lower near wall viscosity. When DRP was added,

however, the friction factor was significantly increased. Similar results were seen in the tube with length of 50 mm.

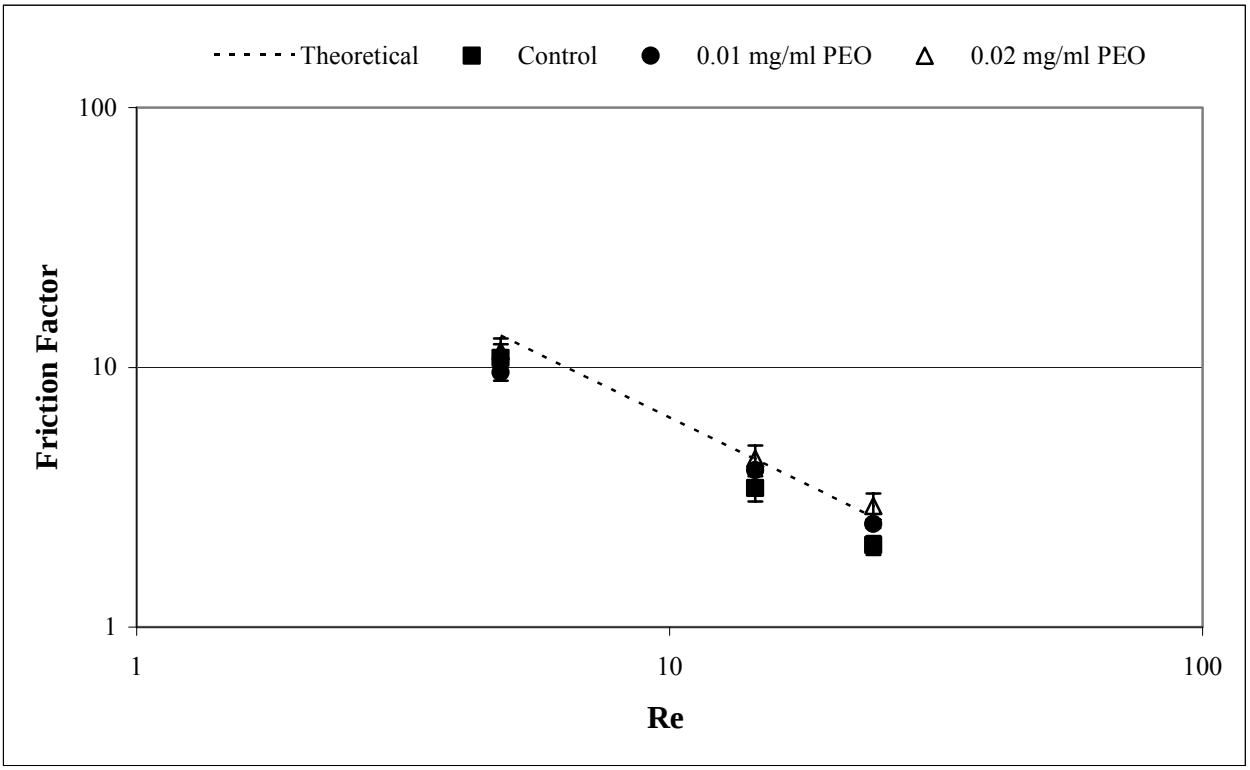

Figure 4-7. Friction factor vs. Re for RBCs flowing in a 220 μm capillary tube

An even more significant effect was seen in the 115 μm capillary tube where the addition of 10 μg/ml PEO-4500 caused an increase in wall shear stress of 24% at a hematocrit of 20% and 52% at a hematocrit of 40%. Figures 4-8 and 4-9 show friction factor vs. Reynolds number for flow of RBCs in this tube at hematocrits of 20% and 40% respectively. In the control case, the experimental friction factor is significantly lower than the theoretical. The experimental friction factor increased with the addition of 10 μg/ml DRP, likely due to RBCs relocating to the near

wall space. Similar effects were observed with the addition of other DRPs including PAM, HA, and AVP.

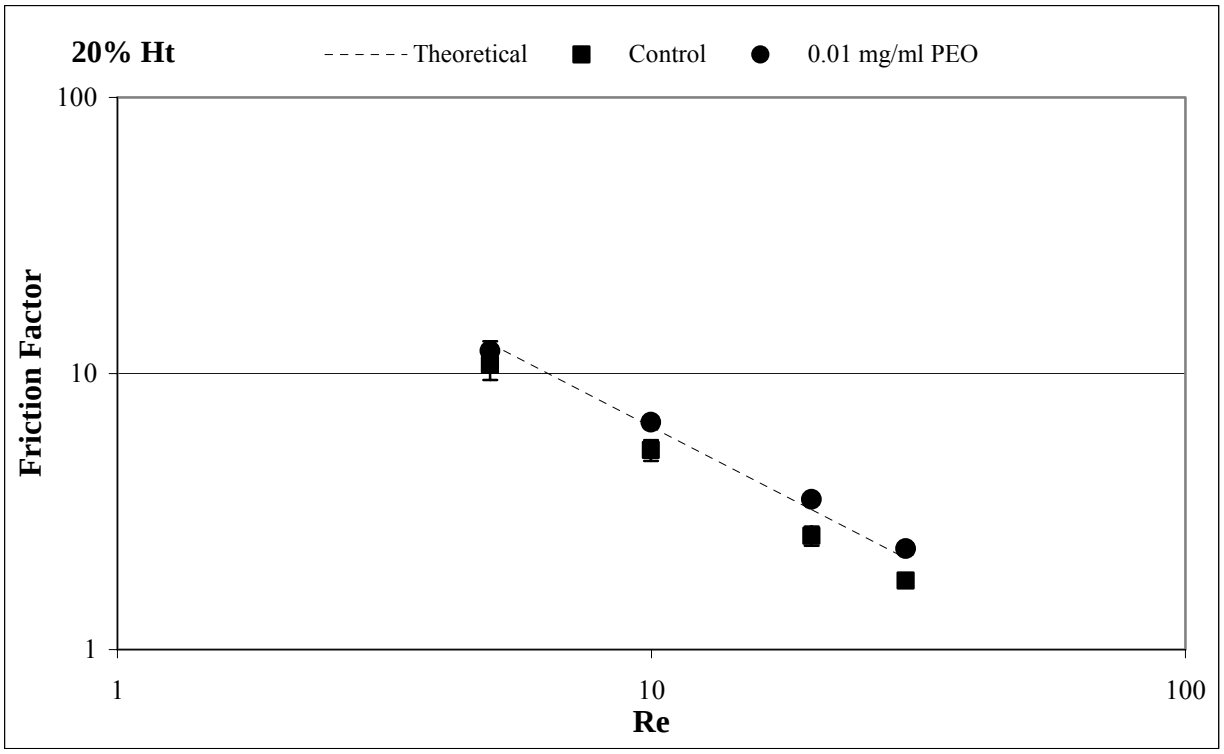

Figure 4-8. Friction factor vs. Re for RBCs (Ht = 20%) with 0 and 10 μg/ml PEO-4500 flowing in a 115 μm capillary tube

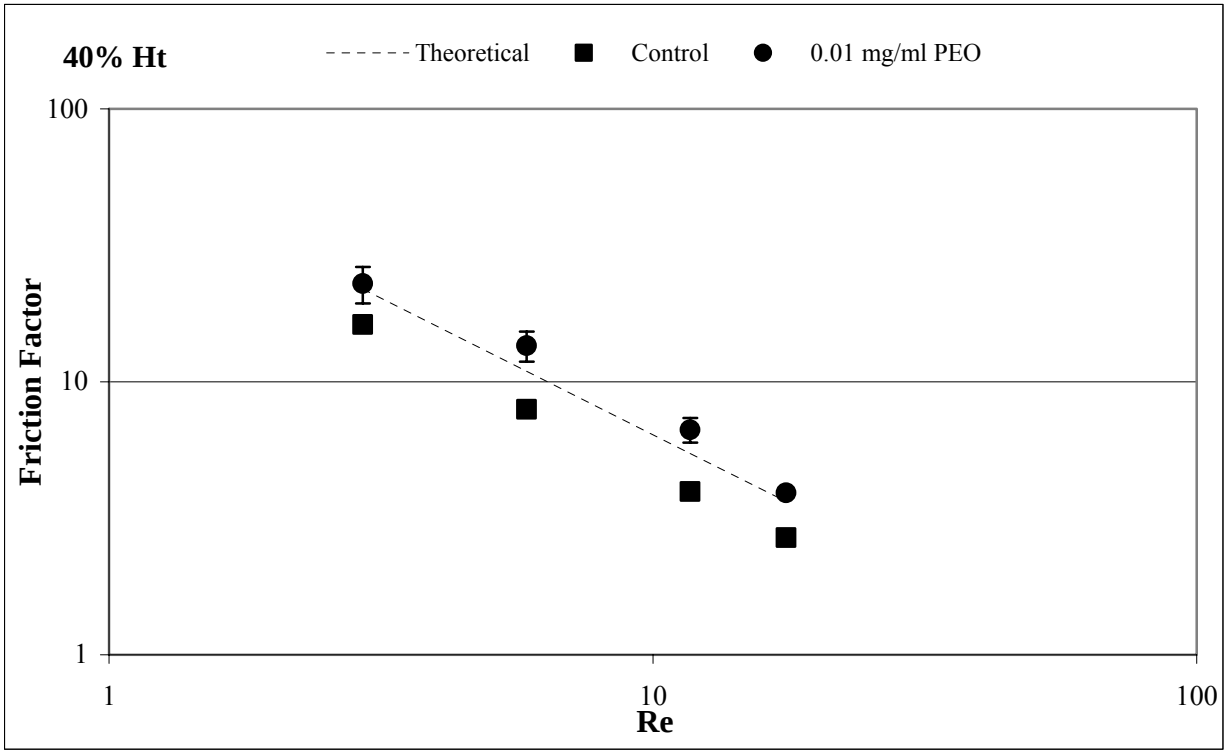

Figure 4-9. Friction factor vs. Re for RBCs (Ht = 40%) with 0 and 10 μg/ml PEO-4500 flowing in a 115 μm capillary tube

The effects of PEO-4500 at a concentration of 2 μg/ml in 115 μm capillary tube were also investigated since this concentration was found to be effective at improving hemodynamics *in vivo.* The addition of PEO caused an increase in wall shear stress of 8% at a hematocrit of 20% and 26% at a hematocrit of 40%. Figures 4-10 and 4-11 show friction factor vs. Reynolds number for flow of RBCs in this tube at hematocrits of 20% and 40% respectively. In the control case, the experimental friction factor is significantly lower than the theoretical. Although the effect was not as strong as in the 10 μg/ml case, the experimental friction factor significantly increased with the addition of 2 μg/ml DRP compared to control. This increase in friction factor was clearly due to reduction of near wall plasma layer size and increase in the near-wall viscosity.

ANOVA showed that the addition of DRPs had a significant effect on wall shear stress when RBCs flowed through the 115 μm tube at all flow rates ($p < 0.05$ in all cases and $p << 0.001$ for all flow rates at 40% Ht and all flow rates except 0.05 ml/min at 20% Ht). A Student's *t*-test showed that the addition of 10 μg/ml PEO to flowing RBCs produced a statistically significant increase in wall shear stress at all tested flow rates and hematocrits ($p<0.01$). The addition of 2 μg/ml PEO produced a statistically significant increase in wall shear stress at all tested flow rates at a hematocrit of 40% ($p<0.01$) and the all but the lowest flow rate at 20% Ht ($p<0.05$).

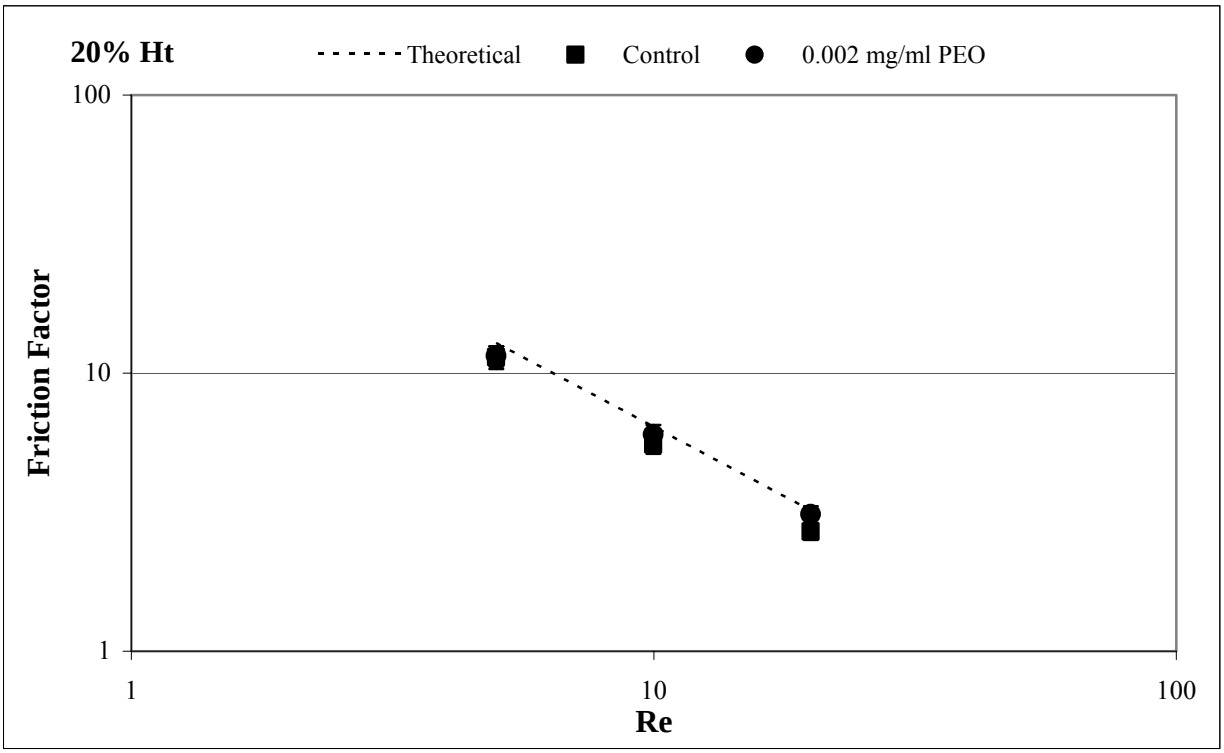

Figure 4-10. Friction factor vs. Re for RBCs (Ht = 20%) with 0 and 2 μg/ml PEO-4500 flowing in a 115 μm capillary tube

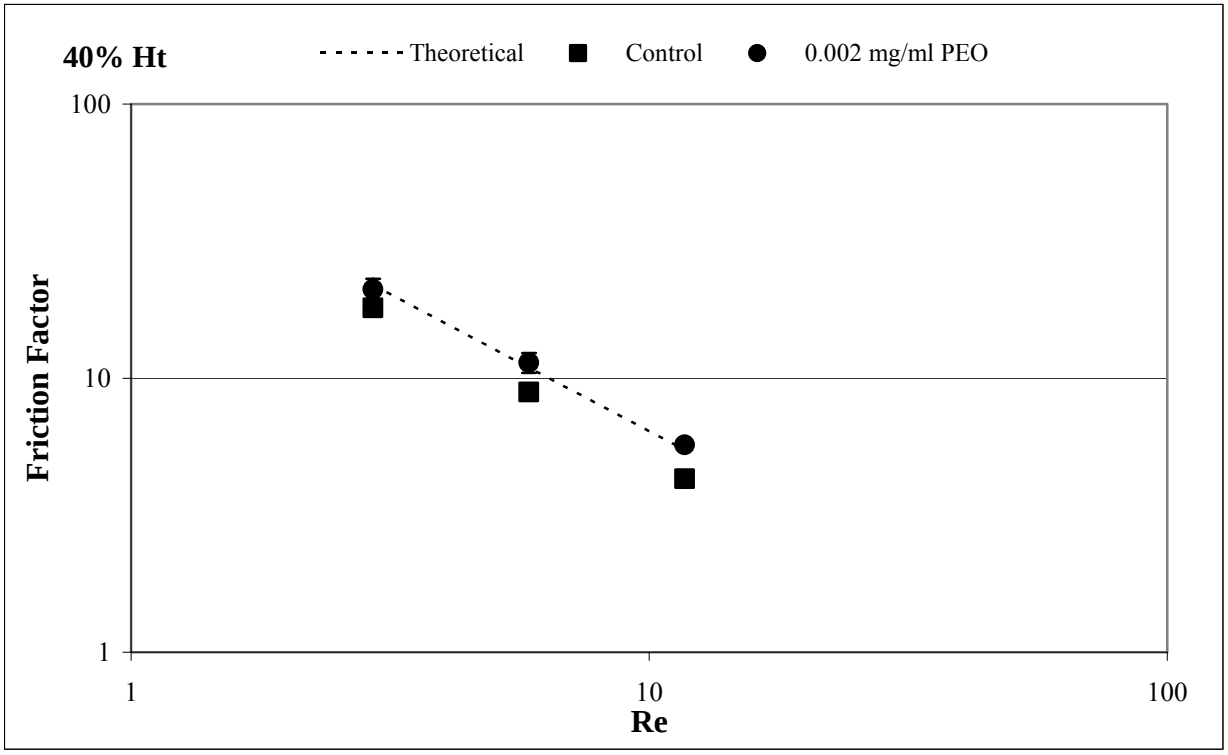

Figure 4-11. Friction factor vs. Re for RBCs (Ht = 40%) with 0 and 2 μg/ml PEO-4500 flowing in a 115 μm capillary tube

Additionally, in the 220 μm capillary tube, pressure drop per unit length was calculated in the tubes of different lengths (50 and 100 mm). No significant difference was seen between these values for the different length tubes ($p > 0.01$ in all cases). Therefore, it can be concluded that entrance effects were negligible for these studies.

4.2.2 Effects of DRPs on blood flow in straight glass microchannels

The effect of DRPs on the near wall plasma layer was investigated in a straight glass microchannel with a square cross section measuring 100 μm x 100 μm and a length of 2.5 cm (Figure 4-12). A developed near wall cell free plasma layer can be seen in the control suspension

of 20% Ht RBCs flowing at 0.2 ml/min. When a DRP, PEO-4500 in this case, was added to the suspension at a concentration of 10 μg/ml, the RBCs were shifted closer to the channel wall, significantly reducing the size of the plasma layer and became elongated. The RBC elongation likely occurred due to the increased stress on the RBCs caused by their proximity to the channel walls. However, there is also a possibility that the RBC elongation might be caused in part by some direct effect of the DRPs on the RBC membrane. When flow was stopped, there was a slight but statistically significant difference between plasma layer size in the control suspension (1.68 μm) and that with PEO (1.12 μm, $p<0.001$). The presence of a plasma layer, especially in the control case, is likely due to the fact that, although the pump was stopped, some flow still existed in the channel (a delay with imaging after stop of the pump would allow RBCs to settle). During flow, the plasma layer increase was significantly larger in the control suspension than in the PEO suspension ($p<0.001$ at 0.05 ml/min and at 0.1 ml/min). In the control suspension, the plasma layer sized increased from 1.68 μm to 5.5 μm when flow was increased from 0 to 0.1 ml/min. When 10 μg/ml PEO was added to the suspension, however, an increase in flow rate from 0 to 0.1 ml/min only caused the plasma layer to increase from 1.12 to 1.3 μm. Figure 4-13 shows the increase in plasma layer size with increase in flow rate for the control suspension, and the significant decrease in near wall plasma layer size caused by DRP addition. Data are presented as the average plasma layer size of five frames ± standard deviation. Similar results are seen with other DRPs including PAM, AVP, and HA. However, polymers that have no drag reducing ability, such as PEO-200 and high molecular weight dextran, produced no effect on the cell-free layer.

Pressure gradient was also measured over the 100 μm x 100 μm x 2.5 cm straight glass microchannel. In the control case, experimental pressure was found to be lower than theoretical.

The addition of a DRP, 10 μg/ml PEO-4500, led to an increase in pressure gradient, and thus in wall shear stress, compared to control RBCs at all but the lowest tested flow rate. Pressure increases were statistically significant ($p < 0.01$) at the higher flow rates. Figure 4-14 shows the friction factor vs. Re in the rectangular glass microchannel for both control RBCs and RBCs with 10 μg/ml PEO. These results confirm that the DRPs cause a similar phenomenon in rectangular channels to that observed in tubes with a circular cross section. This validates the use of bifurcated microchannels with rectangular cross sections to investigate the effects of DRPs on RBC behavior at bifurcations.

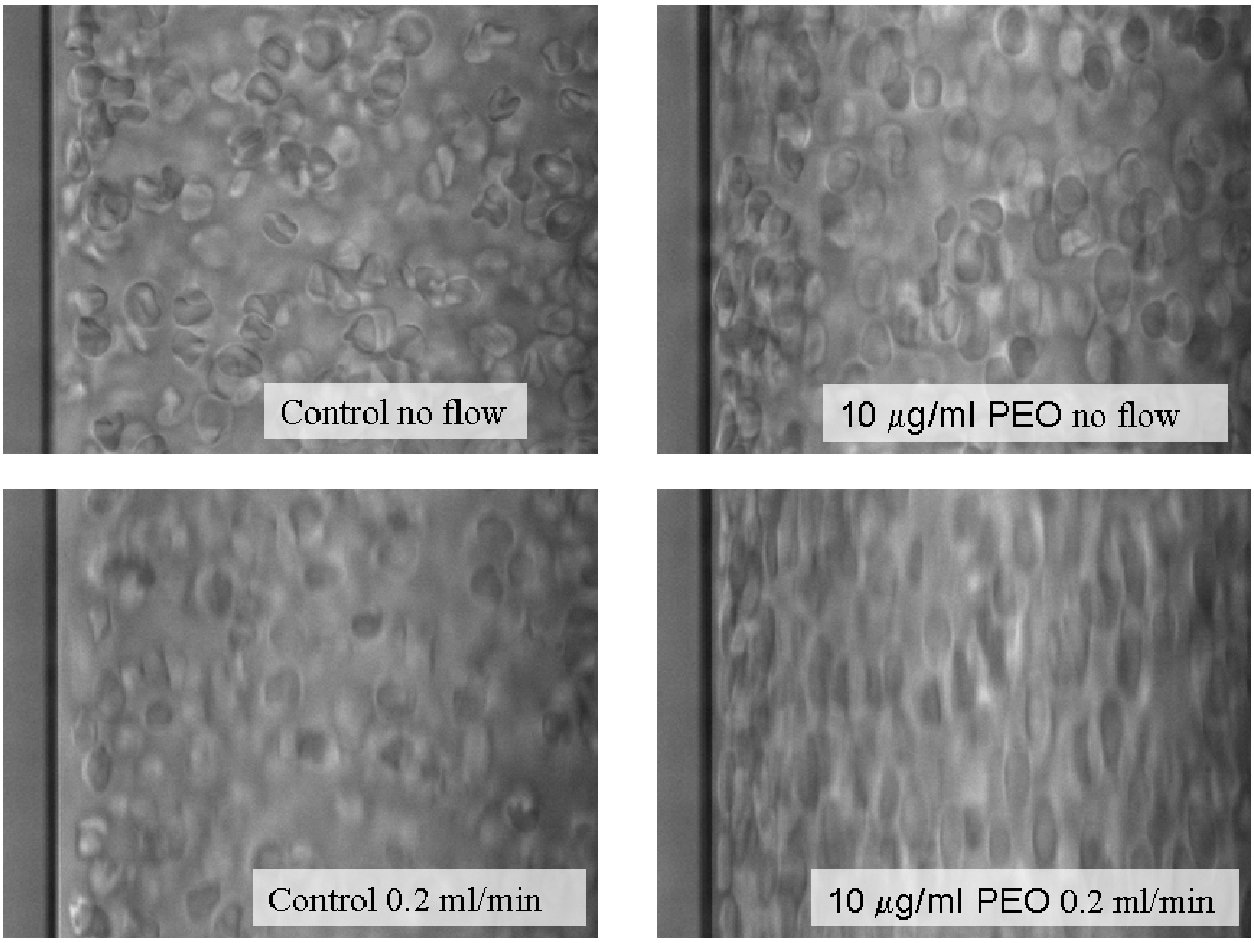

Figure 4-12. RBCs in a 100 μm straight, glass channel with no polymer and no flow (top left) and flowing at 0.2 ml/min (top right) and with 10 μg/ml PEO-4500 and no flow (bottom left) and flowing at 0.2 ml/min (bottom right)

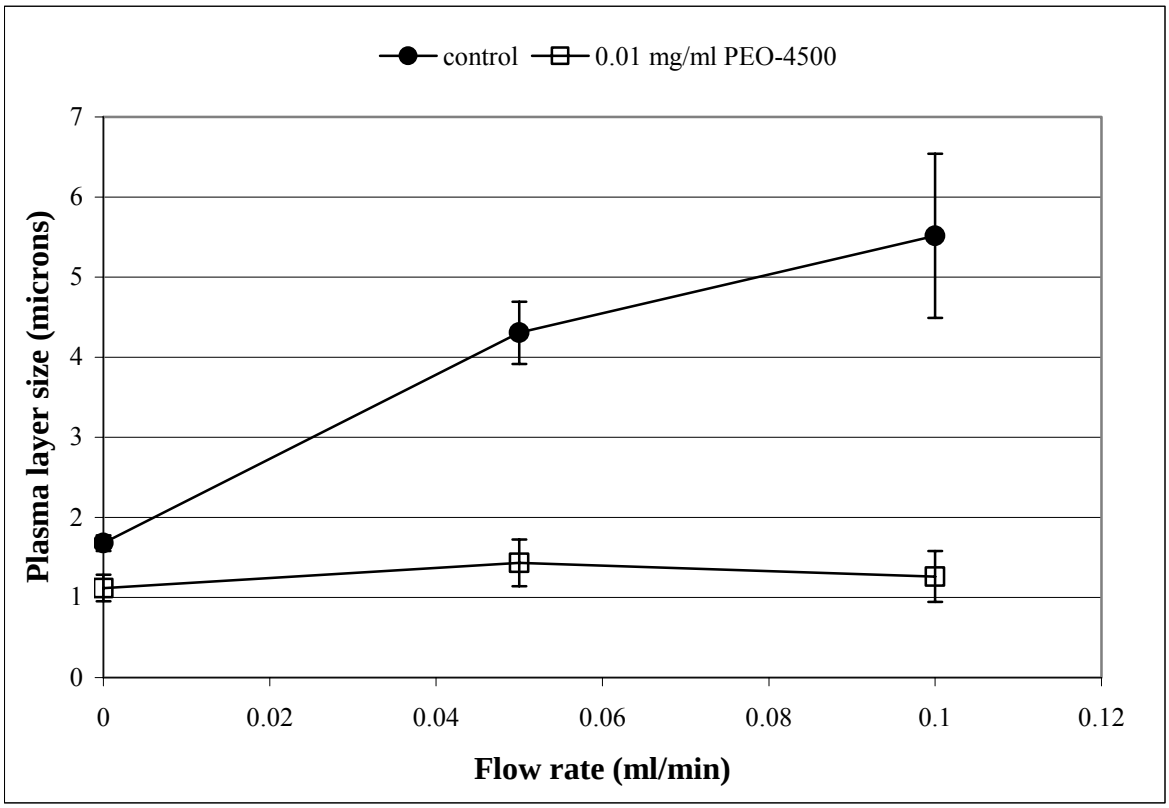

Figure 4-13. DRP (PEO-4500) caused a significant decrease in plasma layer size in a 100μm glass channel ($p<0.001$ at 0.05 ml/min and 0.1 ml/min)

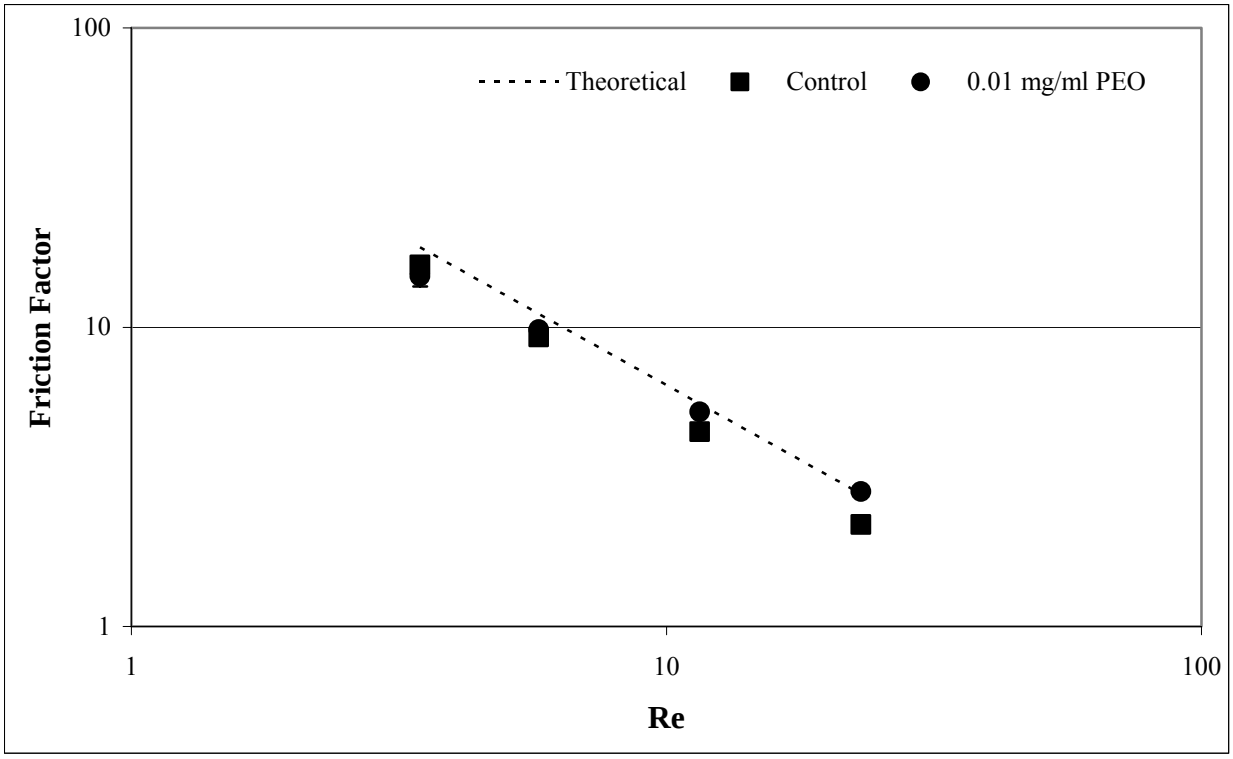

Figure 4-14. Friction factor vs. Re for RBCs (Ht = 20%) with 0 and 10 μg/ml PEO-4500 flowing in a 100 μm rectangular microchannel

4.2.3 Effects of DRPs on blood flow in bifurcated microchannels

The effect of DRPs on the flow of RBCs in PDMS microchannel systems was then studied in order to determine the potential effects that DRPs have on blood flow at bifurcations in the vascular system *in vivo*. Images were first taken upstream of the bifurcations, in the straight section of the PDMS microchannel to confirm that RBCs behaved the same in PDMS as in glass, and to ensure that a near wall plasma layer did form in the fabricated channels. Images such as those in Figure 4-15 verified that the PDMS channels could be used to visualize the near wall plasma layer. As in the glass channels, when PEO-4500 was added at a concentration of 10 μg/ml to the suspension of flowing RBCs (20% Ht) in the PDMS channel, the RBCs became

more elongated and moved closer to the channel wall, causing a reduction in size of the plasma layer. When flow was stopped, no significant difference in plasma layer size between the control and PEO ($p=0.76$) was seen. However, during flow, the plasma layer was significantly larger in the control suspension than in the suspension containing PEO ($p=0.01$ at 0.05 ml/min and $p<0.001$ at 0.1 ml/min). Figure 4-16 shows the increase in plasma layer size with increase in flow rate for the control suspension, and the decrease in near wall plasma layer size when DRP was added. Data are presented as the average plasma layer size calculated from frames ± standard deviation. Similar results were seen with the addition of other DRPs such as PAM, AVP, and HA.

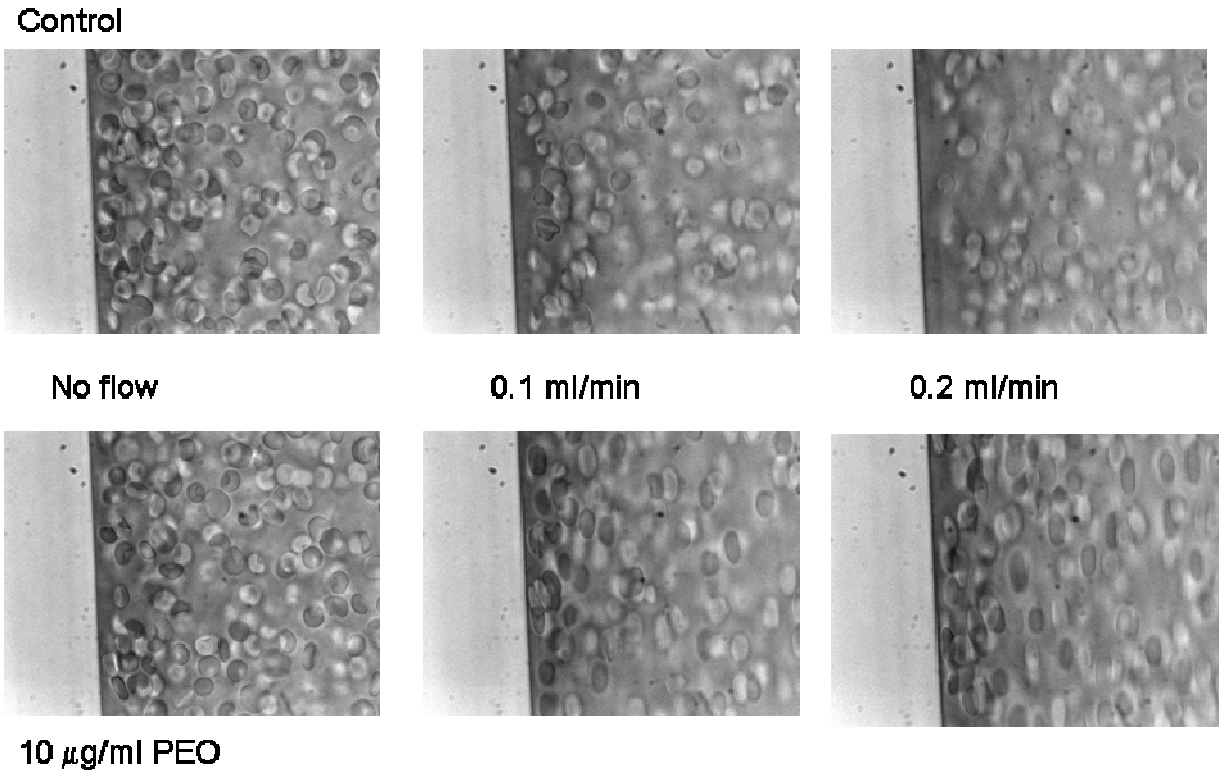

Figure 4-15. RBCs in a 100 μm PDMS channel upstream of the bifurcations with no polymer and no flow (top left) and flowing at 0.1 ml/min (top middle) and 0.2 ml/min (top right) and with 0.01 mg/ml PEO-4500 and no flow (bottom left) and flowing at 0.1 ml/min (bottom middle) and 0.2 ml/min (bottom right)

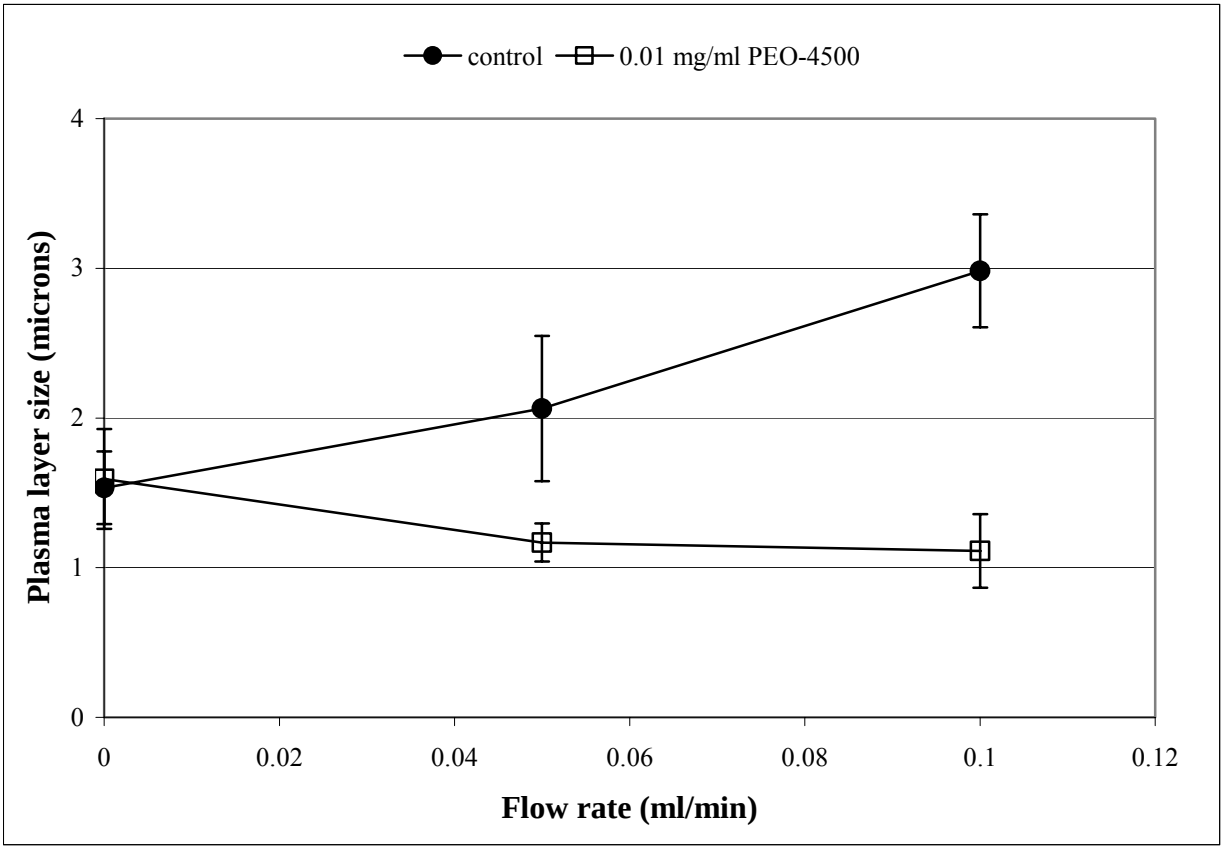

Figure 4-16. DRP (PEO-4500) caused a significant decrease in plasma layer size in a 100 μm section of a PDMS channel upstream of bifurcations (p=0.01 @ 0.05 ml/min and p<0.001 @ 0.1 ml/min)

Next, the DRP effects on RBC distribution at microchannel bifurcations were directly visualized using the methods described in 2.1.4. Figure 4-17 shows the locations in the channels where images were taken. Images were taken in both 100 μm to 100 μm (Figure 4-18) and 100 μm to 50 μm (Figure 4-19) bifurcations with bifurcation angles of 90º. In both cases, a developed near wall plasma layer can be seen as control RBCs flow through the bifurcations. Flow direction in each image is indicated by the arrows. When DRPs, either PEO-4500 or AVP, were added at a concentration of 10 μm/ml, the RBCs were relocated to this near wall region, greatly reducing the plasma layer size. Due to the decrease in the size of the near wall plasma

layer with the addition of DRPs, more RBCs would flow into the daughter branch, lessening the plasma skimming effect. When flow was stopped, no difference in plasma layer size was observed between RBCs with and without DRP.

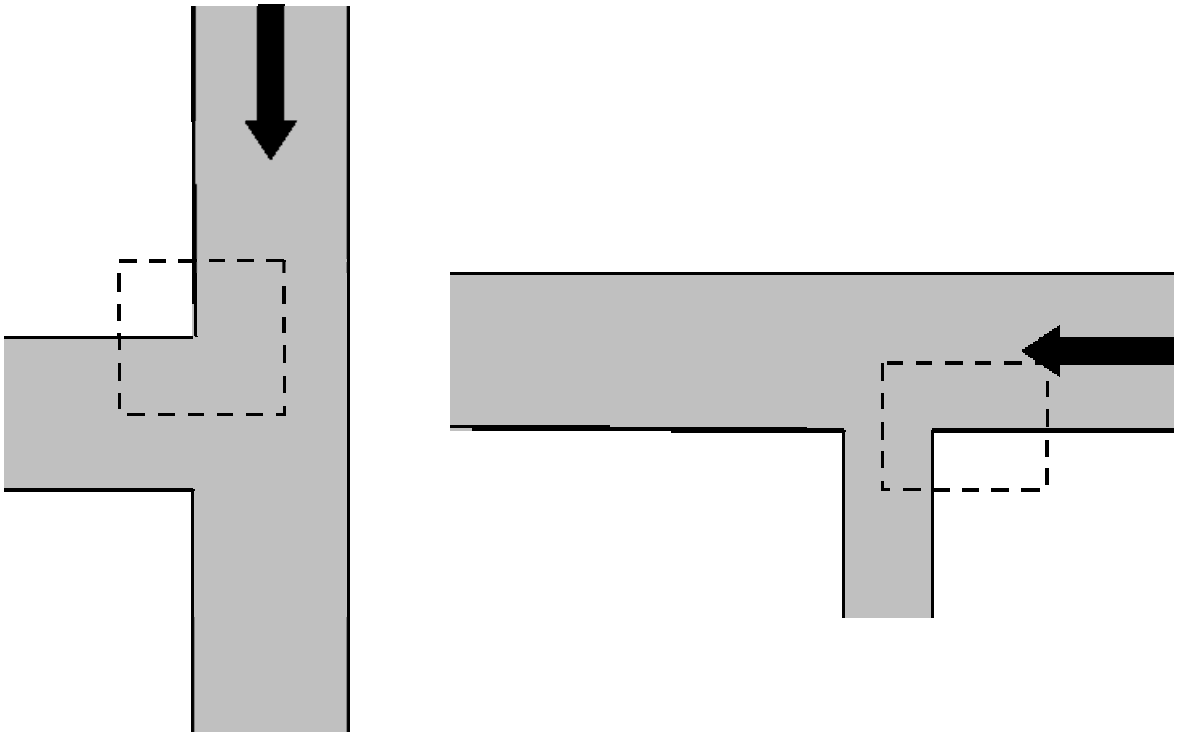

Figure 4-17. Schematic of microchannel systems highlighting regions where images were taken in 100 µm to 100 µm bifurcation (left) and 100 µm to 50 µm bifurcation (right). Arrows indicate direction of flow.

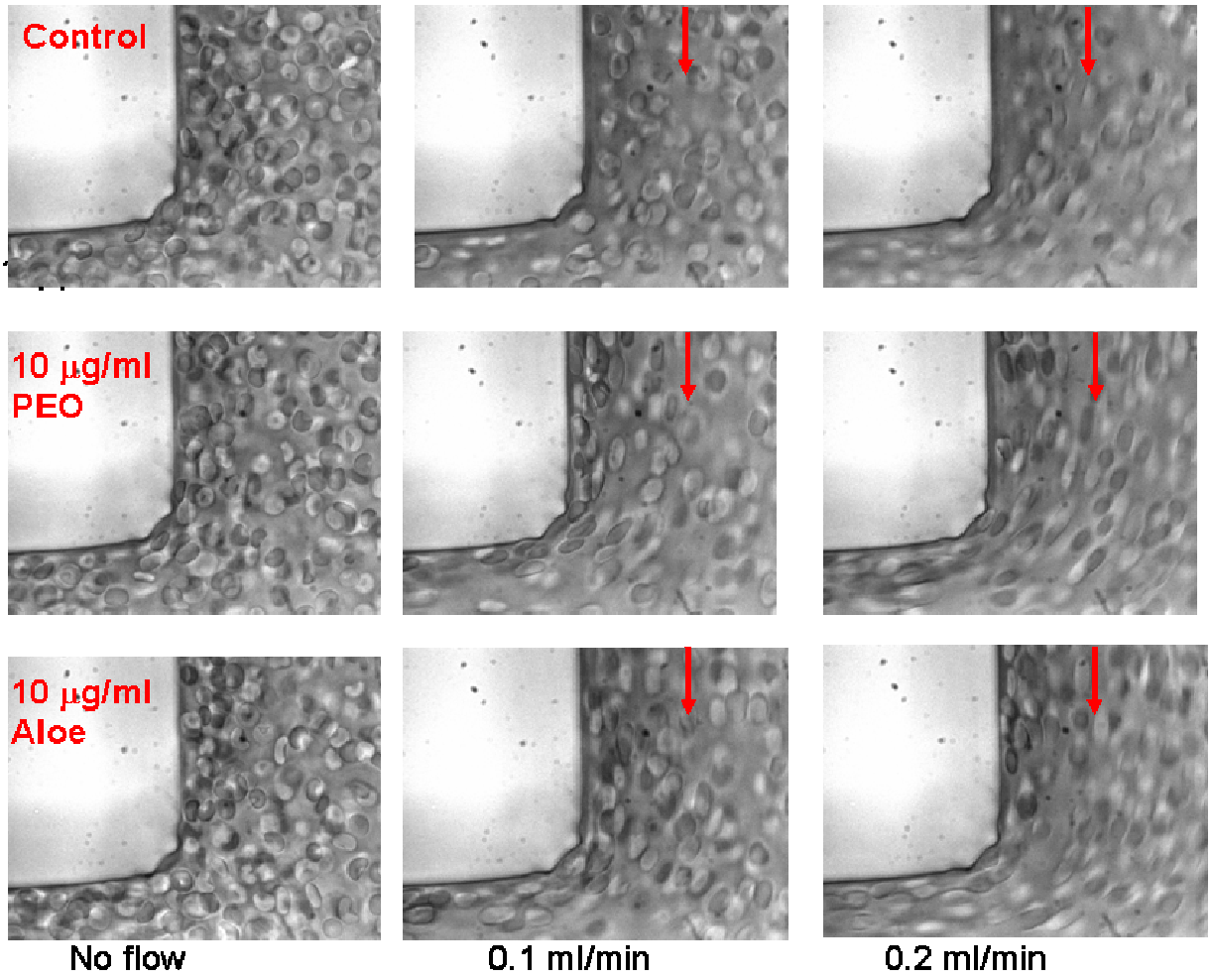

Figure 4-18. RBC suspensions in a 100 μm to 100 μm right angle bifurcation with no polymer and no flow (top left) and flowing at 0.1 ml/min (top middle) and 0.2 ml/min (top right) and with 10 μg/ml PEO-4500 and AVP and no flow (middle and bottom left, respectively) and flowing at 0.1 ml/min (middle and bottom middle) and 0.2 ml/min (middle and bottom right)

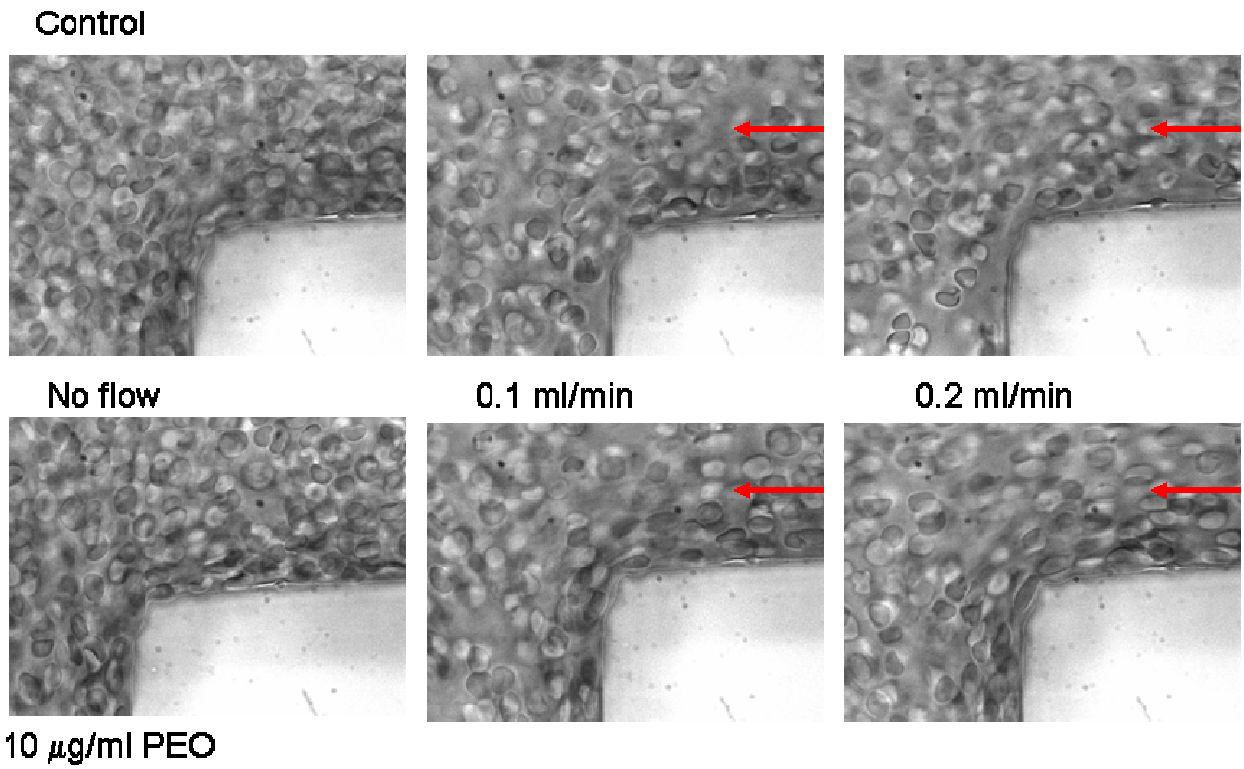

Figure 4-19. RBC suspensions in a 100 μm to 50 μm right angle bifurcation with no polymer and no flow (top left) and flowing at 0.1 ml/min (top middle) and 0.2 ml/min (top right) and with 10 μg/ml PEO-4500 and no flow (bottom left) and flowing at 0.1 ml/min (bottom middle) and 0.2 ml/min (bottom right)

Finally, in a 50 μm to 25 μm bifurcation, blood samples were collected from the outlets of both the parent and daughter branch as well as from the feed syringe. Hematocrit was measured for each sample. In the control case, the parent hematocrit was found to be significantly higher than that in the daughter branch ($p < 0.001$), showing that plasma skimming was occurring in this system. Parent branch hematocrit was 19.0% ± 1.1%, while the daughter branch hematocrit was 17.1% ± 1%. When 10 μg/ml PEO-4500 was added, however, the plasma skimming effect was attenuated, and no significant difference was observed between parent and daughter branch hematocrit ($p = 0.6$). Hematocrit in the parent channel and daughter channel were 18.3% ± 1.3% and 18.6% ± 2.2% respectively. Feed hematocrit was 18.6% ± 1.3%, and no

significant difference between feed hematocrit in the control and polymer RBC suspensions was observed ($p > 0.1$). Figures 4-20 and 4-21 compare hematocrits measured from blood samples taken from the inlet and each outlet of the channel both in the control case and with the addition of DRP.

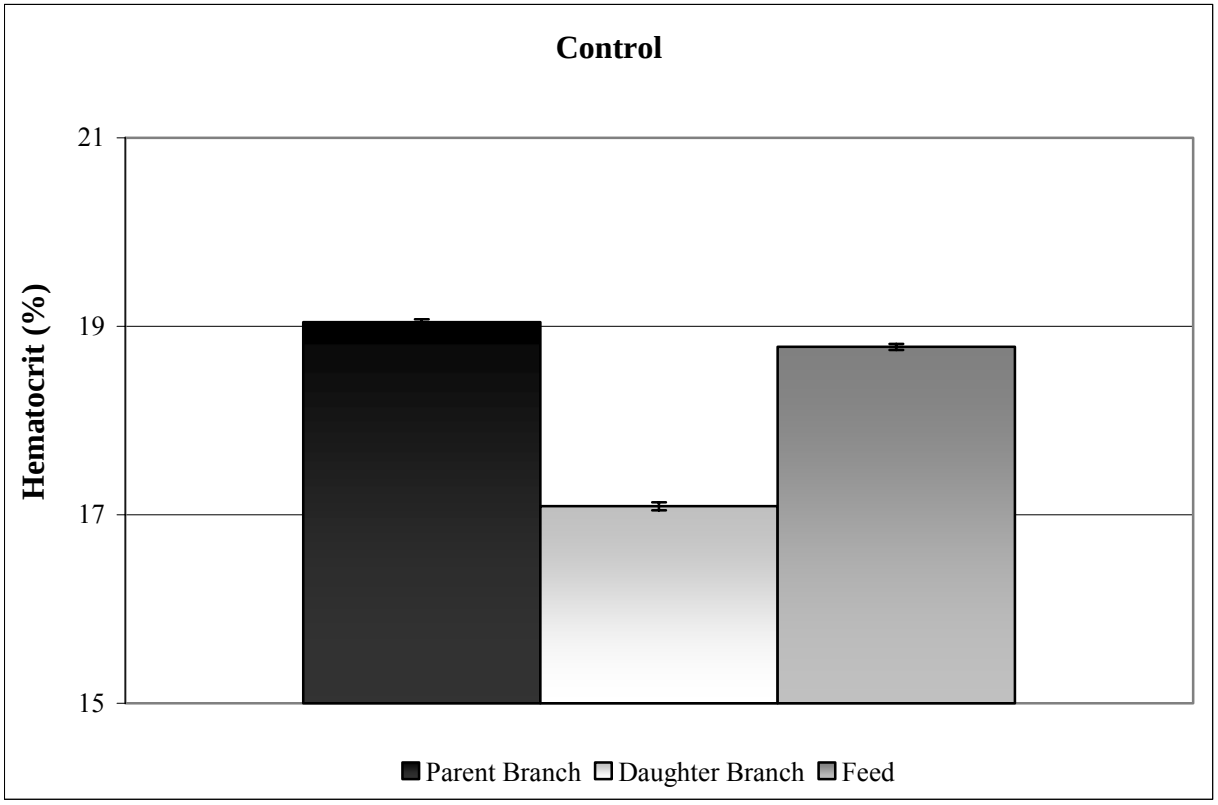

Figure 4-20. Comparison of hematocrits at the channel inlet and outlets of the parent and daughter branch. For RBC suspensions with no DRP flowing at 0.1 ml/min in a 50 μm to 25 μm bifurcation, parent branch hematocrit is significantly higher than that in the daughter branch indicating that plasma skimming is occurring

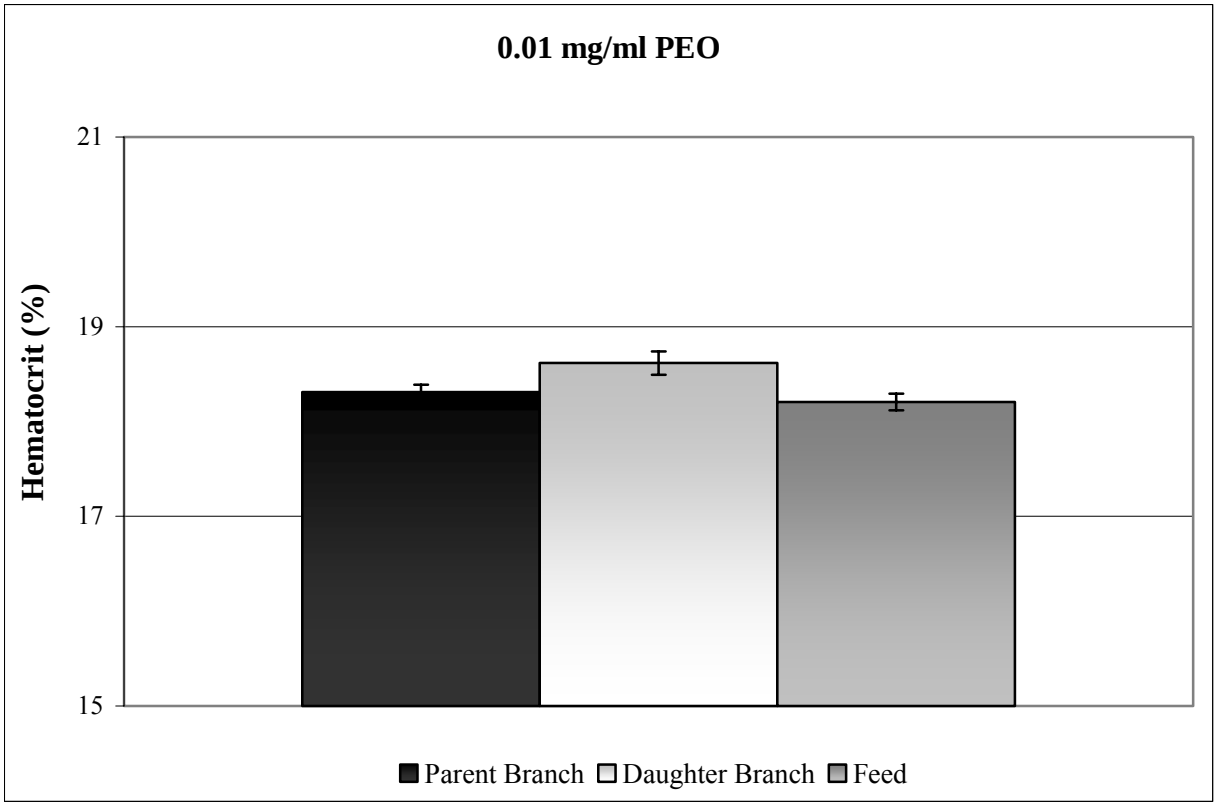

Figure 4-21. Comparison of hematocrits at the channel inlet and outlets of the parent and daughter branch. For RBC suspensions with 10 μg/ml PEO-4500 flowing at 0.1 ml/min in a 50 μm to 25 μm bifurcation, the plasma skimming effect is attenuated and no significant difference is observed between parent and daughter hematocrit.

An interesting effect was observed when DRPs were added to RBCs (20% Ht) flowing through a channel expansion. The addition of 10 μg/ml PEO-4500 to RBCs flowing through the expansion caused a redistribution of RBCs at flow separations. As shown in Figure 4-22, at a channel expansion from 50 μm to 200 μm with flow from top to bottom, significant flow separation and formation of pockets of plasma can be seen in the control blood at the expansion. When DRP was added, however, the RBCs were relocated to the near wall region eliminating the plasma pockets at the expansion, and the flow separation was reduced. This effect became more

apparent as flow rate was increased, and no difference was seen between the control and DRP case when flow was stopped. A similar effect was observed in a 100 μm to 200 μm expansion, both with 20% hematocrit (Figure 4-23) and 40% hematocrit (Figure 4-24) RBCs, although the recirculation zone was much smaller in the 40% Ht case.

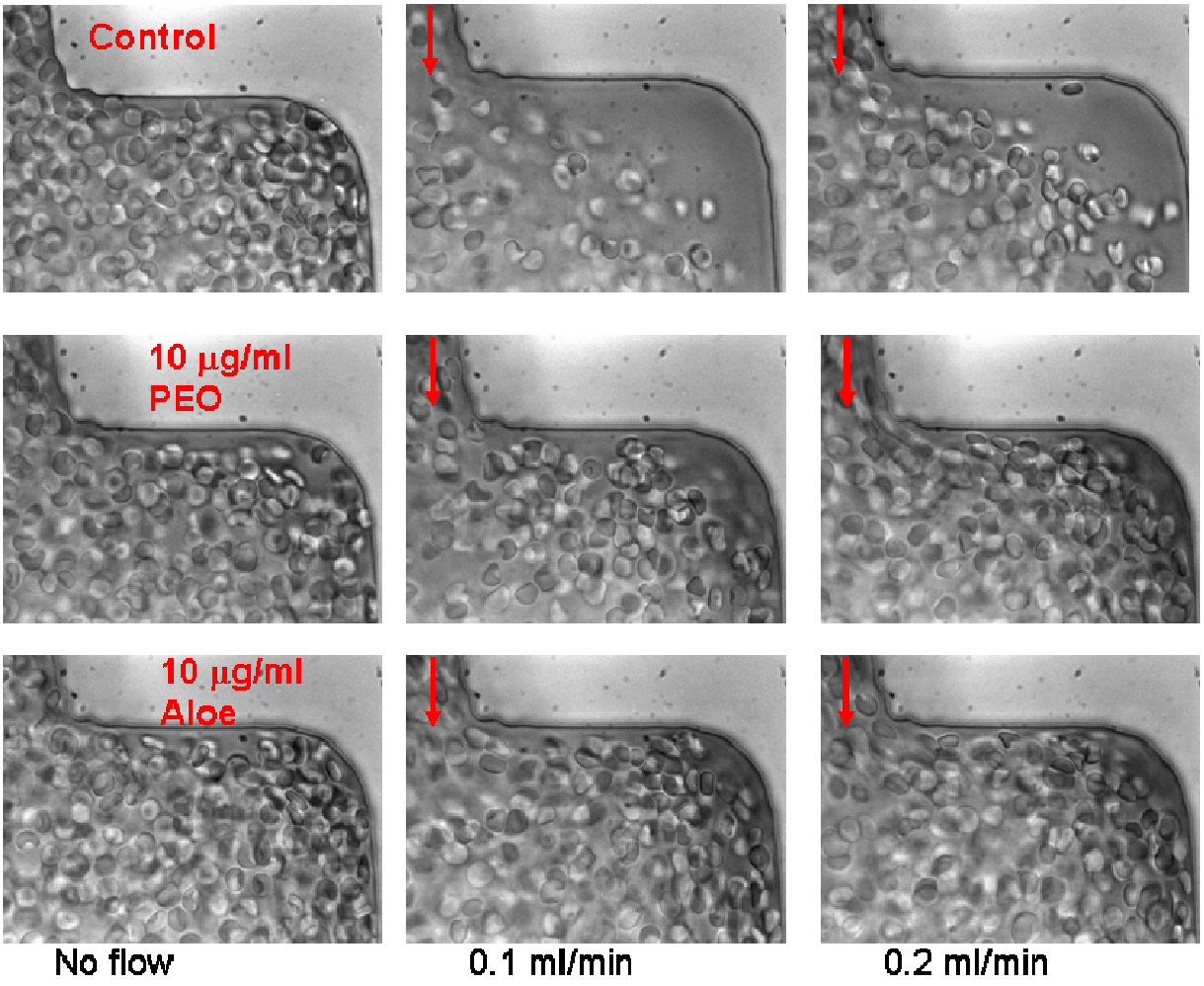

Figure 4-22. 20% hematocrit RBC suspension in a 50 μm to 200 μm expansion with no polymer and no flow (top left) and flowing at 0.1 ml/min (top middle) and 0.2 ml/min (top right) and with 10 μg/ml PEO-4500 and AVP and no flow (middle and bottom left, respectively) and flowing at 0.1 ml/min (middle and bottom middle) and 0.2 ml/min (middle and bottom right)

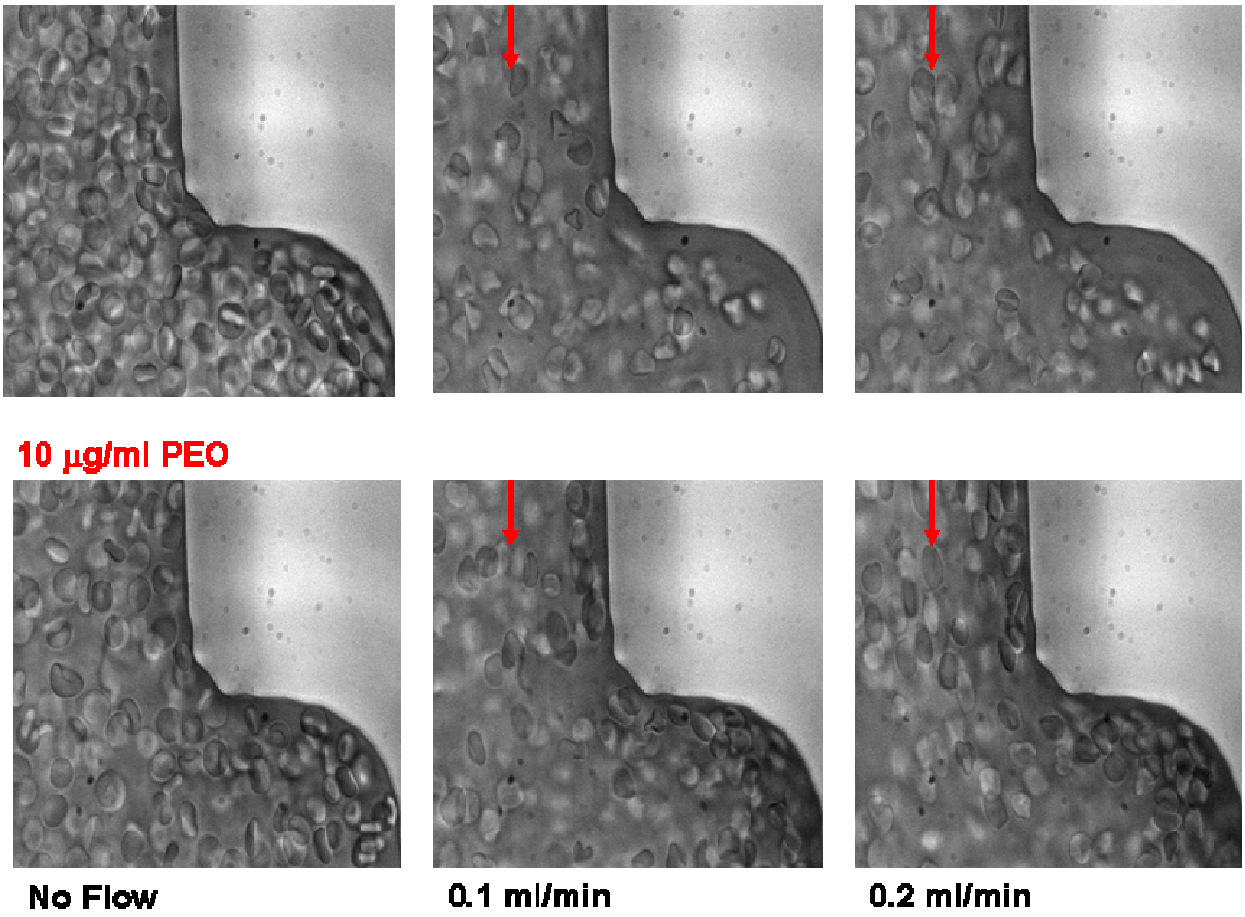

Figure 4-23. 20% hematocrit RBC suspension in a 100 μm to 200 μm expansion with no polymer and no flow (top left) and flowing at 0.1 ml/min (top middle) and 0.2 ml/min (top right) and with 10 μg/ml PEO-4500 (bottom left) and flowing at 0.1 ml/min (bottom middle) and 0.2 ml/min (bottom right)

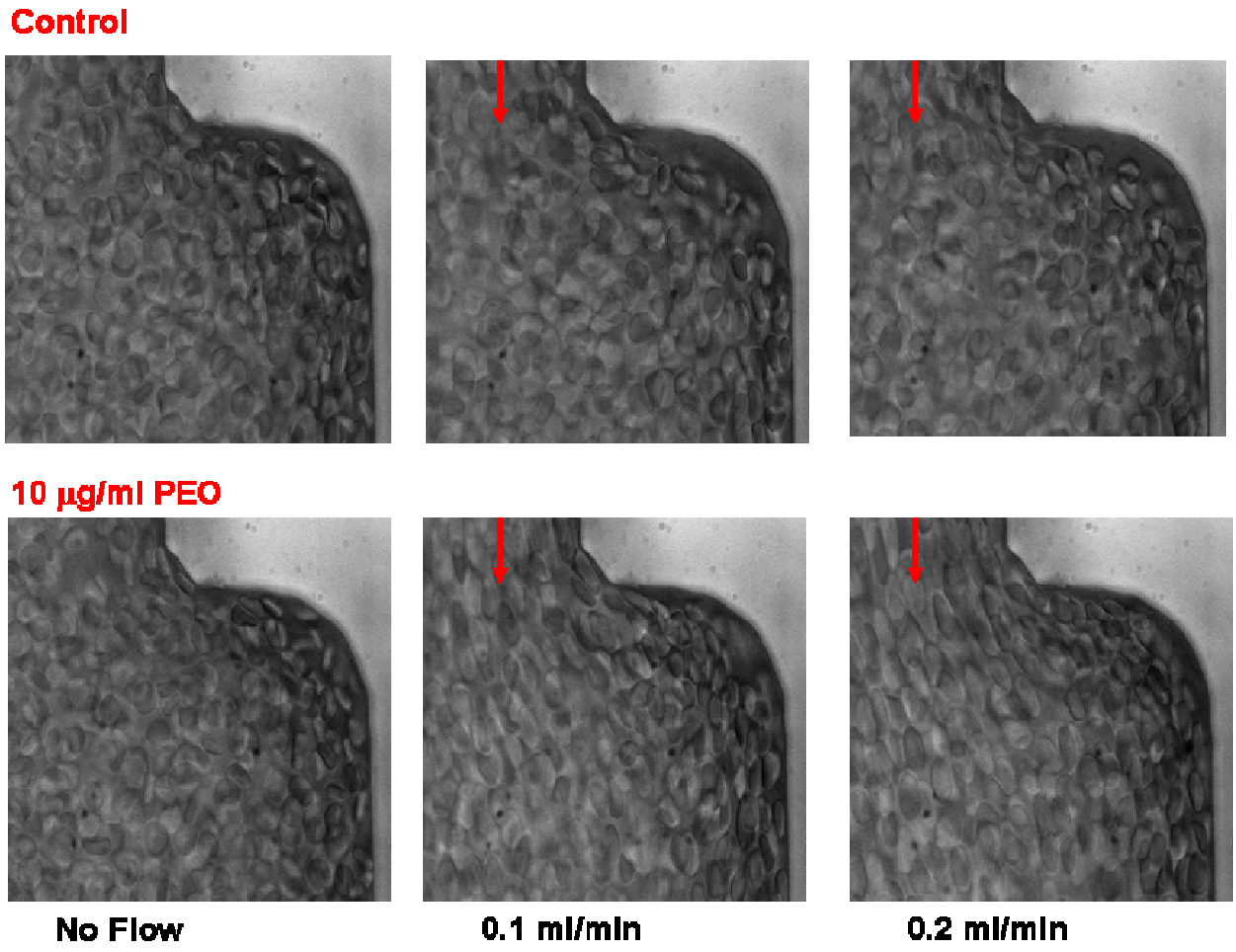

Figure 4-24. 40% hematocrit RBC suspensions in a 100 µm to 200 µm expansion with no polymer and no flow (top left) and flowing at 0.1 ml/min (top middle) and 0.2 ml/min (top right) and with 10 µg/ml PEO-4500 (bottom left) and flowing at 0.1 ml/min (bottom middle) and 0.2 ml/min (bottom right)

4.2.4 Model for DRP effects on microcirculation

Based on *in vitro* and *in vivo* experiments, in vessels with diameters greater than 100 µm at a hematocrit of ~ 40 % and flow rates high enough to prevent aggregation, the size of the near wall plasma layer is likely to be no larger than 4 µm [56]. This agrees well with the plasma layer sizes calculated using Equation 21, derived from the marginal zone theory, for the studies of flow of

RBCs through the 115 μm capillary tube which range from 1 to 4 μm depending on flow rate and hematocrit. When DRP was added to the RBCs, plasma layer size calculated using this model was reduced. When 10 μg/ml PEO-4500 was added to RBCs flowing in the 115 μm capillary tube, plasma layer size was calculated to be between -2 and 1 μm depending on flow rate and hematocrit. The negative plasma layer size, while physically impossible, may indicate that RBCs are actually more concentrated in the near wall region than in bulk flow. This is qualitatively supported by the imaging studies described in 4.2.1, where the RBCs appear to be more concentrated in the near wall region than in the bulk flow when DRP is added to the RBC suspension. Using the same method for RBCs flowing in the 100 μm microchannel, plasma layer size was calculated to be 3.4 μm for control RBCs flowing at 0.05 ml/min and 4.4 μm at 0.1 ml/min. When 10 μg/ml PEO-4500, calculated plasma layer size was reduced to 2.0 μm and 0.6 μm at 0.05 and 0.1 ml/min respectively. These results agree relatively well with the measured plasma layer size (4.3 μm for control RBCs flowing at 0.05 ml/min and 5.5 μm at 0.1 ml/min and 1.4 μm at 0.05 ml/min and 1.3 μm and 0.1 ml/min with 10 μg/ml PEO-4500).

4.2.5 Results Summary

Overall, the following major results were obtained through the studies performed in this specific aim.

- The addition of DRPs to a RBC suspension flowing in a microchannel produced a significant increase in wall shear stress.
- A significant decrease in near wall plasma layer size was observed when DRPs were added to a RBC suspension flowing in a microchannel.

- When DRP was added to a RBC suspension flowing through a channel expansion, RBCs were relocated to the near wall region, eliminating the plasma pockets at the expansion and reducing flow separation in this area.
- DRPs significantly decreased the plasma skimming effect at a channel bifurcation increasing the hematocrit of the blood flowing through the daughter branch.

4.3 DISCUSSION

At the present time, neither the Fåhraeus and Fåhraeus-Lindquist (F-L) Effects nor the drag reducing polymer phenomenon is fully understood. Although the drag reducing phenomenon is completely different from the Fåhraeus and F-L effects, the studies performed in this specific aim indicate that these phenomena may unite in the vascular system to produce interesting consequences which can potentially be beneficial in both microfluidic technology and medicine.

The observed redistribution of RBCs across the microchannels and reduction of plasma layer size caused by DRPs are intriguing scientific phenomena. The prevention of RBC movement toward the center of the vessel by DRPs may improve the transport function of blood in the microcirculation and facilitate gas transport between RBCs and tissue *in vivo* by reducing diffusion distance. This effect could also potentially be extremely beneficial in facilitating gas exchange and reducing thrombosis (by reducing recirculation zones) in blood contacting artificial organs and bioreactors. The observed increases in the near-wall hematocrit and in local viscosity with the addition of DRPs produce an increase in wall shear stress in the microchannels. In microvessels, this increase in wall shear stress would cause release of endothelial-derived relaxing factor composed of nitric oxide [59], promoting vasodilatation and

thus decreasing overall vascular resistance. *In vivo* experiments have shown that DRPs cause a decrease in vascular resistance [12, 16, 38, 39], and local vasodilation caused by RBC redistribution could be one of the mechanisms responsible for this effect. The observed increase in wall shear stress caused by DRPs could also lead to an increase in number of functioning capillaries, which has been seen with the injection of DRPs in previous *in vivo* studies [3]. In the case of hemorrhagic shock, the reduction in plasma skimming at vessel bifurcations might improve microcirculation, delivering more RBCs to the capillaries, and acting as an autotransfusion. This is extremely promising since it has been previously shown that adequate functional capillary density is a major factor of survival in hemorrhagic shock [42].

The reduction of flow separations and elimination of the "plasma pocket" region observed at channel expansions has potential clinical significance as well. It is known that thrombi are likely to form in areas of flow separation [90-92]. Studies by Karino and Goldsmith, performed with human platelets flowing in an expansion with a diameter ratio of 3.33 (151 μm to 504 μm), suggested that the combination of long residence times, flow patterns, and fluid mechanical stresses present in vortices associated with flow separation lead to platelet aggregation and thus thrombus formation [91]. Moving RBCs closer to the wall would wash platelets out of this recirculating plasma zone and therefore could decrease thrombus formation. This would be beneficial not only in the vessels, but also in medical devices where thrombosis is one of the major concerns. Atherogenesis is known to occur in areas of flow separation where low flow and low shear stress conditions are present. The reduction in flow separation caused by DRPs and the movement of RBCs to the vessel wall and resulting increase in shear stress supports the results of previous studies which showed that DRPs can prevent and delay the development of atherosclerotic legions [2, 4, 9]. These findings suggest that DRPs produce a

novel phenomenon in blood flow in microvessels which could provide an exciting new avenue for the treatment of cardiovascular disorders.

5.0 DEVELOPMENT AND TESTING OF NEW DRAG REDUCING POLYMERS FOR POTENTIAL BIOMEDICAL APPLICATIONS

Several DRPs, including high molecular weight PEOs, PAMs, and plant-derived polysaccharides were applied in previous *in vivo* studies and shown to have beneficial effects on blood circulation, but currently none is being clinically used . PAM was applied in many animal studies and shown to be very effective, but it is not ideal for use *in vivo* because of the known toxicity of the acrylamide monomer as well as certain biocompatibility issues [9, 93]. PEO was also shown to be effective in animal studies and is a good candidate for certain biomedical applications, but its rapid mechanical degradation, especially in the presence of RBCs, may present a major obstacle for use in treating chronic pathologies. Certain polysaccharides have also shown promise, but lack of consistency between preparations and of a method for production of large quantities are hurdles that must be overcome. Therefore, the search continues for new DRPs, which are biocompatible, mechanically stable, well defined, and easily manufactured, to be proposed for clinical uses. Three potential candidate DRPs have been identified that may meet criteria necessary for use *in vivo*. These include a natural DRP extracted from the aloe vera plant; poly(N-vinylformamide), a high molecular weight polymer synthesized from a non-toxic isomer of acrylamide; and hyaluronic acid, a high molecular weight polysaccharide known to have drag reducing properties and already approved by the FDA for some clinical uses (especially in the

veterinary practice) [73]. Each of these polymers was characterized and evaluated for its efficacy as a drag reducer and ability to withstand stress induced degradation.

5.1 METHODS

5.1.1 Development and characterization of an aloe vera based DRP

Aloe vera DRP (AVP) was shown to be a very effective DRP, reducing resistance to turbulent flow *in vitro* by up to 50% at a concentration of 10 μg/ml, but is not well characterized or reproducible. It has long been known that plant components vary from plant to plant depending on plant age, part used, or where it was grown [94, 95]. A standard protocol for AVP preparation, which provides a relatively reproducible polymer, has been developed [34]. The AVP was extracted from freshly cut leaves of aloe vera plants obtained from Silverthorn Ranch Nursery (Fallbrook, CA). Leaves were removed from the aloe vera plant and sliced open lengthwise, and the exposed gel scraped from the interior of the leaves. The gel was then mixed with sterile saline. This mixture was filtered through several layers of cheesecloth and the resulting filtrate collected and stirred. The aloe vera extract was then centrifuged at 14,000 rpm for one hour at 4 °C. The resulting supernatant was collected and tested for drag reducing effectiveness *in vitro* using a circulating flow loop as described in 3.1.1. The DRP was then selectively precipitated from the supernatant using 100% ethanol. The precipitate was collected and dried overnight in a vacuum. The dried precipitate was then dissolved at a concentration of 2.5 mg/ml in sterile saline with 0.1 mg/ml Gentamicin added as an antibacterial agent. Several days of slow stirring at 4 °C were required to dissolve the precipitate. When completely

dissolved, the polymer solution was again centrifuged and the supernatant was dialyzed against sterile saline using a Spectra/Por regenerated cellulose membrane (Spectrum Laboratories, Inc.) with a molecular weight cutoff of 50,000 Da. Dialysis removed any low molecular weight polymer or other low molecular weight impurities.

The effect of lyophilization (freeze-drying) of the AVP on its efficacy upon reconstitution was investigated, since lyophilization of aloe might be beneficial for storage, transport, or sterilization. AVP solution was lyophilized using a Labconco Freezone 4.5 freeze dryer. Following lyophilization, the dry polymer was redissolved in normal saline.

AVP was characterized using hydrodynamic and rheological methods as well as GPC as described in 3.1.1 – 3.1.5. Additional characterization was performed in an attempt to determine the chemical structure of the active, drag reducing component of AVP. Proteinase K and trypsin assays were used to rule out the presence of polypeptides in the active components of the preparation. Since trypsin and proteinase K are both serine proteases which digest proteins by hydrolyzing peptide bonds [96, 97], degradation of the polymer by these enzymes would indicate peptide bonds were present in the active DRP component of aloe. Then, an approach similar to that used in Chow et al [60], enzymatic digestion with endo-β-D-mannanse was used to make a preliminary determination of the residues and linkages in the backbone of AVP. After treatment with each enzyme, drag reduction tests of the AVP were used to determine enzymatic cleavage in the polymer backbone. A decrease in drag reducing ability, likely caused by a decrease in molecular weight, was used to indicate cleavage of the polymer.

5.1.2 Synthesis and characterization of poly(N-vinylformamide)

An inverse emulsion polymerization technique described by Badesso et al. [68] was used to synthesize high molecular weight poly(N-vinylformamide) (PNVF). N-vinylformamide (NVF) monomer (Sigma-Aldrich) was distilled at 80°C under vacuum. The distilled NVF monomer (25 ml), sorbitan monostearate (4.02 g), octane (145 ml), water (48 ml), and 2,2'-azobis(2,4-dimethylpentanenitrile) (Vazo 52, 0.048 g, DuPont) reacted in a high-speed stirrer (500 rpm) at 50°C for three hours under nitrogen. The reaction produced an emulsion, which was broken with excess acetone to yield high molecular weight PNVF. The PNVF was dried and then dissolved in distilled water at a concentration of 5 mg/ml. The PNVF solution was then dialyzed against distilled water using a Spectra/Por polyvinylidine difluoride membrane (Spectrum Laboratories, Inc.) with a $1x10^6$ Da molecular weight cutoff to remove any unreacted monomer, low molecular weight polymer, and other impurities. The dialyzed PNVF was lyophilized and redissolved at a concentration of 5 mg/ml in distilled water or saline. Three lots of the polymer were synthesized. Each preparation was characterized using the hydrodynamic, rheological, and chemical methods described in 3.1.1 to 3.1.5. The preparation which was shown to have the best drag reducing properties was selected for the further studies, and results of these studies are presented in 5.2.2. ^{1}HNMR spectrum was recorded on a Bruker Avance 300 spectrometer, using deuterium oxide as a solvent. ^{1}HNMR was used to confirm that the tested polymer was indeed PNVF and not the hydrolyzed form, poly(vinyl amine).

5.1.3 Characterization of hyaluronic acid (HA) as a DRP

Several HA samples with various MWs were obtained from Lifecore Biomedical. The polymers were characterized, and their drag reducing efficacy and mechanical stability were investigated using the methods described in 3.1.1 – 3.1.5 in order to assess the potential of HA as a DRP for use in biomedical applications.

5.1.4 Comparison and correlation of DRP physicochemical and rheological properties with their drag reducing activity and their effects on microchannel blood flow

Correlations between physicochemical and rheological properties of the polymers and their drag reducing efficiency were evaluated. PEO-4500, AVP, PNVF, and HA, as well as PAM, were all included in the correlations. High molecular weight dextran was included as a negative control. Correlations with drag reducing ability were tested for molecular parameters including molecular weight, intrinsic viscosity, radius of gyration, and hydrodynamic radius, as well as viscoelastic properties of concentrated solutions including viscosity, elasticity, and relaxation time at low and high shear rates in order to show which properties correlated best with a polymer's drag reducing efficiency. Correlations were also evaluated between these same molecular and rheological parameters and the DRP effects in microchannel blood flow studies. These correlations provided a better understanding of which properties best define and predict a polymer's ability to improve microcirculation.

Degradation behavior of the various DRPs in response to mechanical stresses was compared. This allowed for the prediction of the ability of the DRPs to withstand the mechanical

stresses of the vascular system when injected intravenously and thus, at least in part, their ability to be used to treat chronic circulatory disorders.

5.2 RESULTS

5.2.1 Development and characterization of an aloe vera based DRP

Since high MW polysaccharides are known to be effective drag reducers [1, 6, 17] that are resistant to mechanical degradation [21-23], and a polysaccharide extracted from the aloe vera plan was found to have low systemic toxicity when injected either intraperitoneally or intravenously [24], it was hypothesized that AVP would be a good candidate DRP for use in the medical field. Previous studies have shown that AVP was an effective DRP both *in vitro* and *in vivo* [1, 34]. AVP, however, had not been fully characterized, and production methods were not reproducible. Therefore, it was important to attempt to standardize AVP extraction methods in order to eliminate variability between preparations, as well as to characterize this DRP. The results presented in Sections 5.2.2.1 to 5.2.2.5 show certain progress made toward this standardization and characterization of this novel DRP. Figure 5-1 shows an image of a molecule of AVP obtained using an atomic force microscope (AFM).

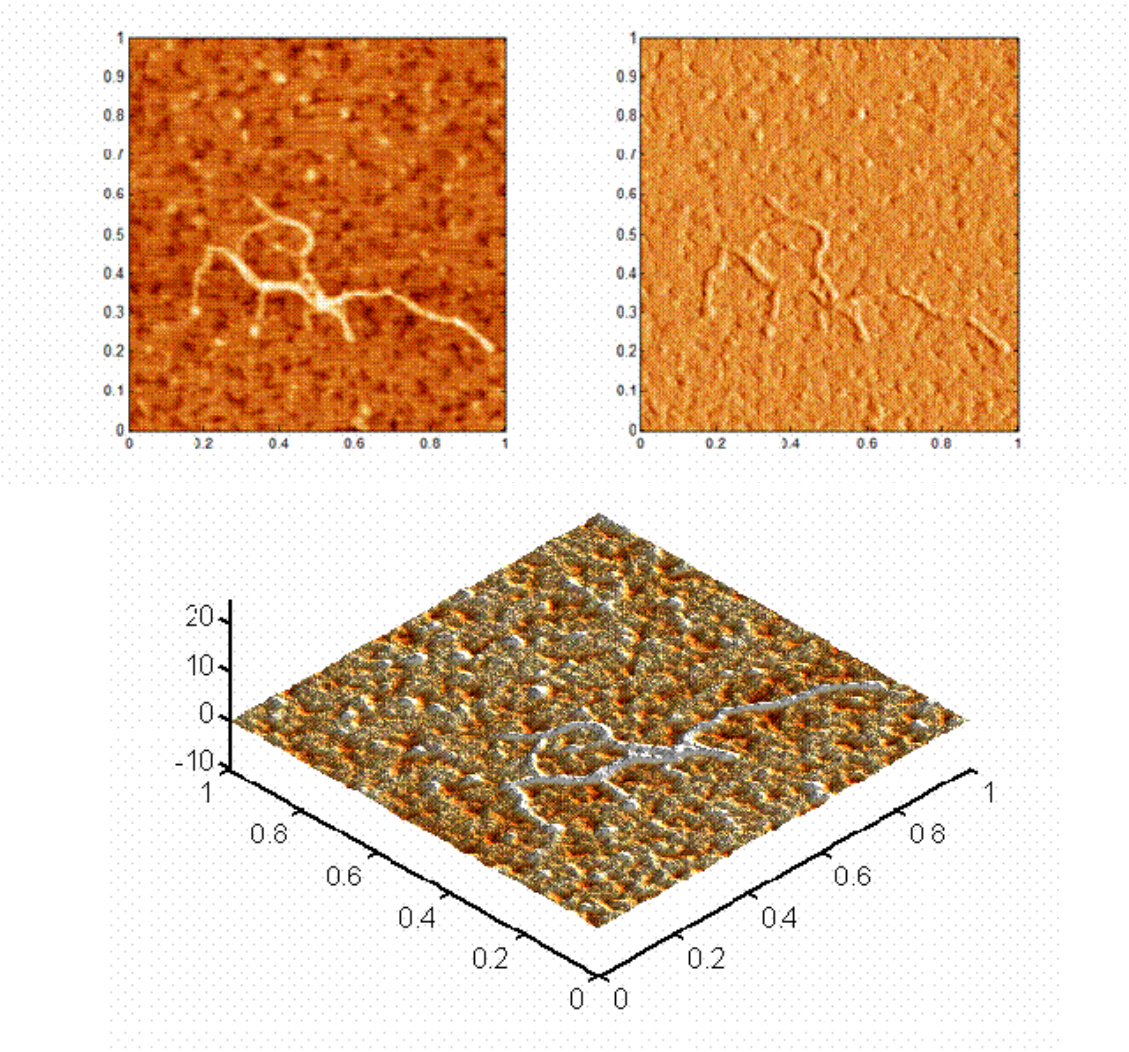

Figure 5-1. AFM of aloe-derived DRP molecule (image was obtained by Brian Cusick in Dr. Tomasz Kowalewski's laboratory at Carnegie Mellon University)

5.2.1.1 Chemical characterization of AVP

Identification of the chemical structure of the active drag reducing component of AVP is necessary before this DRP can be approved for use in the clinical setting. Using a trypsin based assay as well as a proteinase K based assay, the possibility that the active drag reducing component of aloe was a protein was ruled out. Trypsin and proteinase K are both serine

proteases which digest proteins by hydrolyzing peptide bonds [96, 97]. AVP maintained its drag reducing activity when tested in the turbulent flow system at 10 μg/ml following treatment with either trypsin or proteinase K. Since neither enzyme degraded the polymer, it was concluded that the aloe-derived DRP did not contain peptide bonds. Based on these studies and the literature [24, 60, 61, 63, 64, 95], it is reasonable to conclude that the drag reducing component of aloe is a polysaccharide residue.

Treatment of AVP with endo-β-D-mannanse, however, did cause degradation of the DRP. Following treatment with endo-β-D-mannanse, the drag reducing efficiency of AVP was diminished. Before enzyme treatment, the AVP reduced resistance to flow by ~ 40% at a concentration of 10 μg/ml; after treatment, the AVP produced no drag reducing effect. Since endo-β-D-mannanse is known to hydrolyze mannans (galactomannans, glucomannans, and galactoglucomannans) containing β-1,4 linkages, it can be inferred that the drag reducing element of aloe likely contains a backbone comprised of β-1,4 linked mannose residues.

5.2.1.2 GPC

Mean weight average molecular weight of the AVP determined by GPC was 8.4×10^6 Da ± 3.0×10^6 Da. Intrinsic viscosity was 29.3 dl/g ± 3.2 dl/g. Radius of gyration and hydrodynamic radius were 199 nm ± 26 nm and 153 nm ± 20 nm respectively. Polydispersity index was calculated to be 1.17 ± 0.17. These molecular characteristics are indicative of effective DRPs, but standard deviations are high. This may be due to the fact that components vary among plants depending on factors such as plant age [94, 95], or that slight variations may have still existed in the extraction procedure leading to different actual concentrations of DRP in the final preparation.

5.2.1.3 *In vitro* test of drag reducing ability

Drag reducing ability of AVP was assessed at 10 μg/ml in turbulent flow. At a Re of 22,000, AVP reduced resistance to flow by 31% ± 6%. Figure 5-2 shows friction factor vs. Re for 10 μg/ml AVP in the recirculating turbulent flow system compared to pure saline and the friction factor obtained using the Blasius equation (Equation 5). At a higher concentration, 100 μg/ml, AVP was found to reduce friction by up to 50%. At a concentration of 10 μg/ml, AVP produced a statistically significant reduction in friction factor compared to saline (control) at all tested Reynolds numbers ($p < 0.001$)

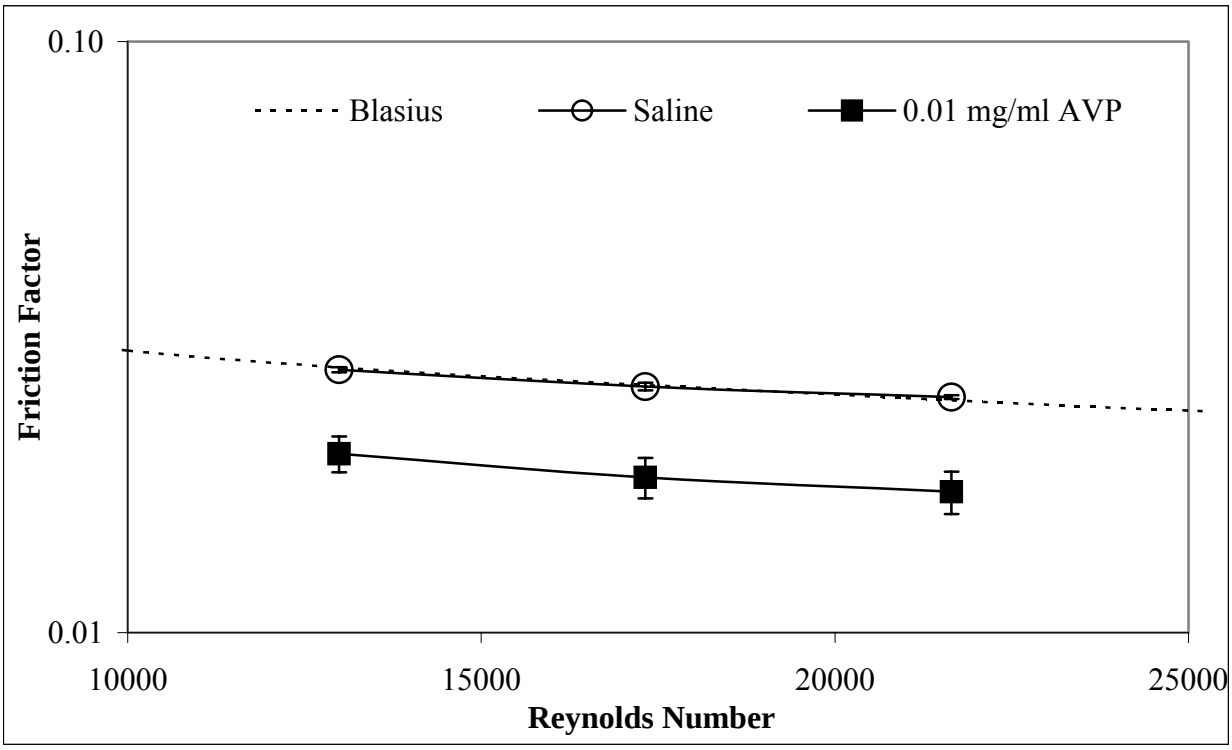

Figure 5-2. Drag reducing effect of AVP

As described in section 5.1.1.1, the effect of lyophilization of the drag reducing effectiveness of AVP was also studied. It was found that the process of lyophilization produced no change in the aloe polymer's drag reducing activity. At a concentration of 10 μg/ml, the tested

AVP reduced resistance by 30.6% ± 2.1% prior to lyophilization compared to 29.3% ± 5.1% following the lyophilization process. Therefore, lyophilization could be used to provide a safe storage or transport method for AVP preparations.

5.2.1.4 Viscoelasticity

Concentrated AVP solutions demonstrated pronounced non-Newtonian behavior and high viscosity, which are defining characteristics of all effective DRPs. Average viscosity, elasticity, and relaxation time, determined at a concentration of 2.5 mg/ml in saline using the Brookfield cone and plate rheometer and the Vilastic 3 viscoelastometer, are shown in Figures 5-3 through 5-6. At low concentrations AVP solutions had Newtonian flow behavior. Average asymptotic viscosity at a concentration of 0.1 mg/ml was found to be ~ 1.2 cP.

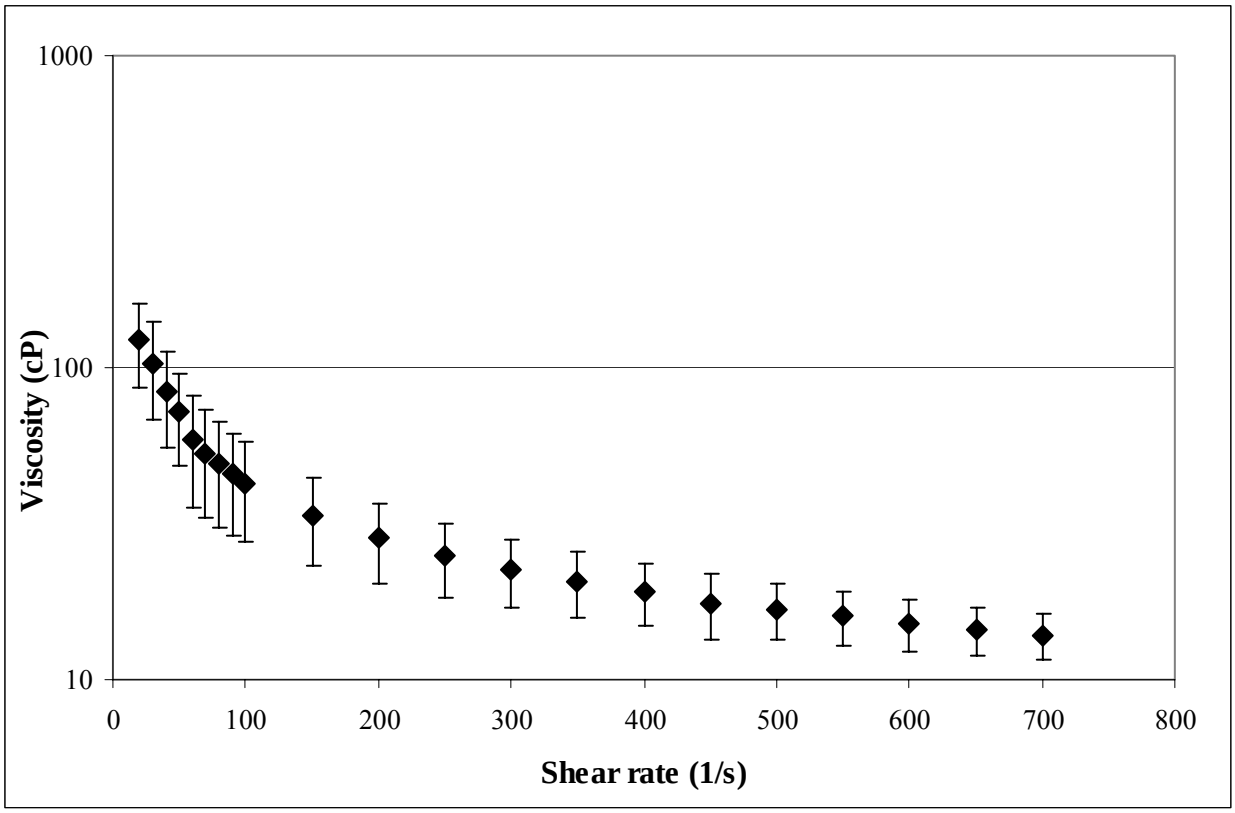

Figure 5-3. Viscosity of AVP measured in the Brookfield cone and plate rheometer at a concentration of 2.5 mg/ml

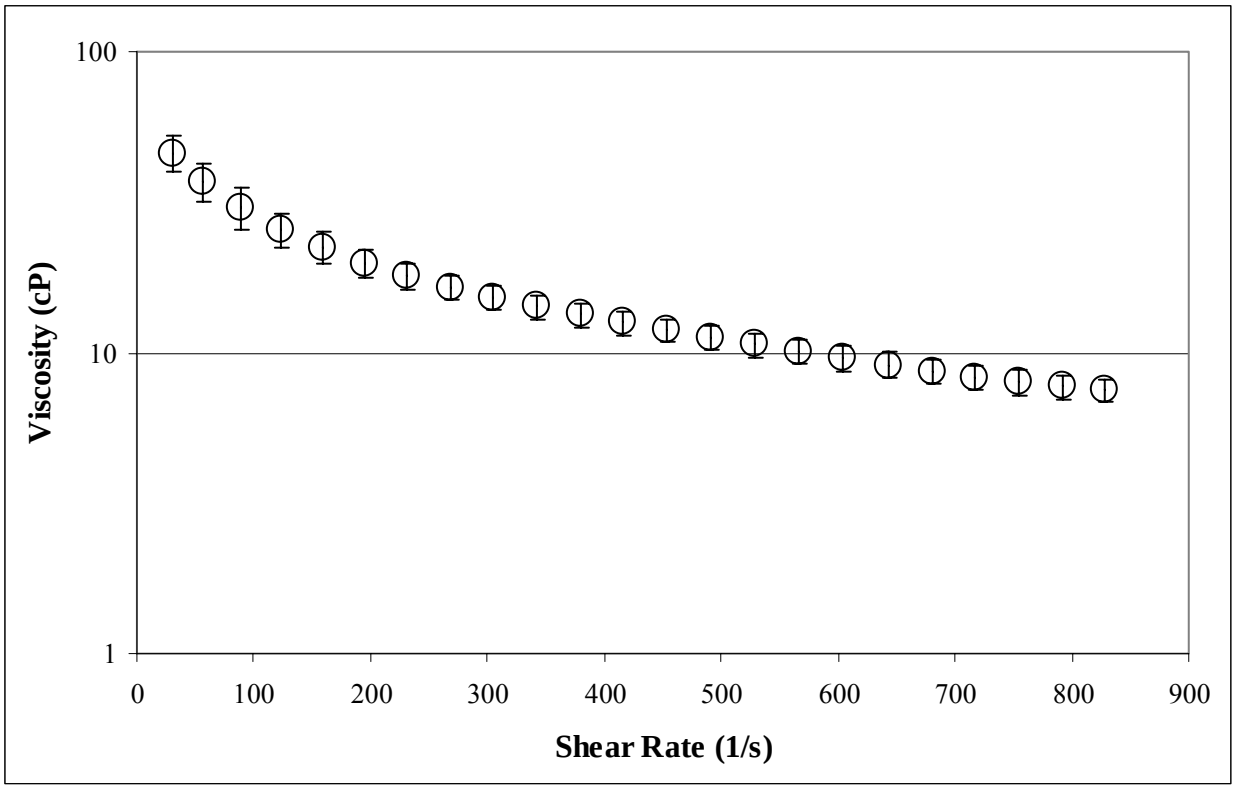

Figure 5-4. Viscosity of AVP measured in a viscoelastometer (Vilastic) at a concentration of 2.5 mg/ml

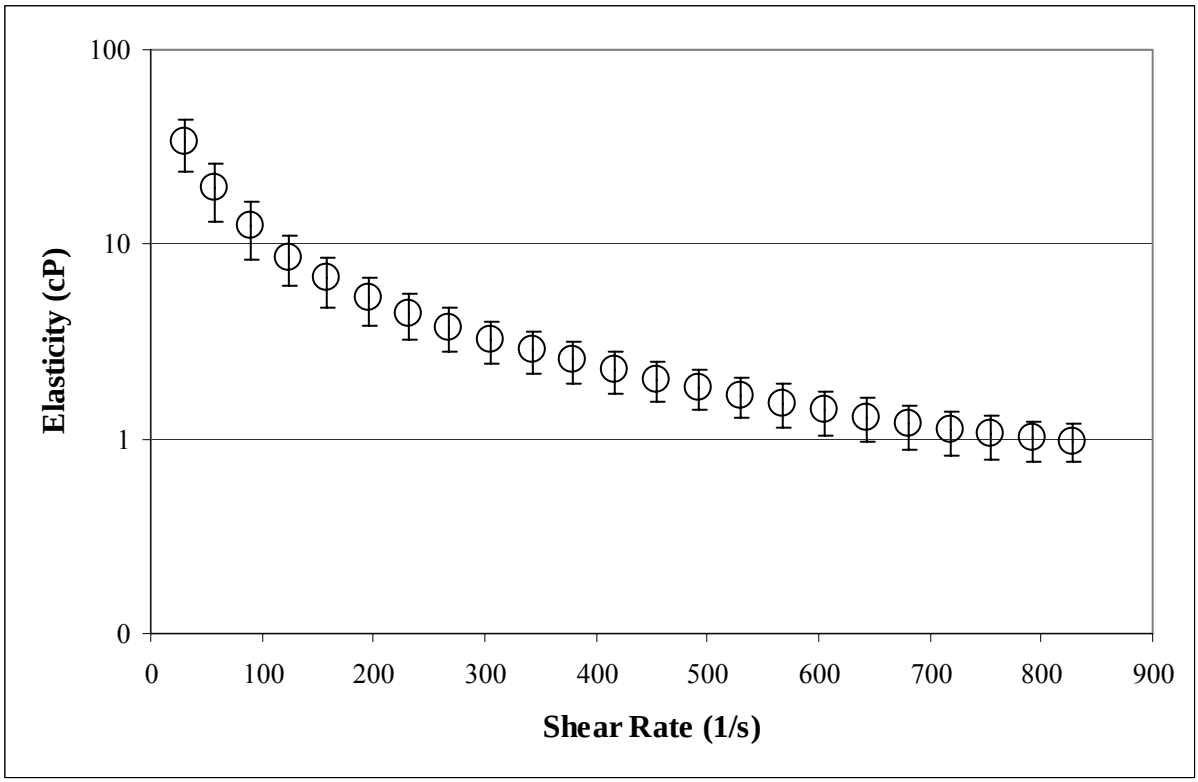

Figure 5-5. Elasticity of AVP measured in a viscoelastometer (Vilastic) at a concentration of 2.5 mg/ml

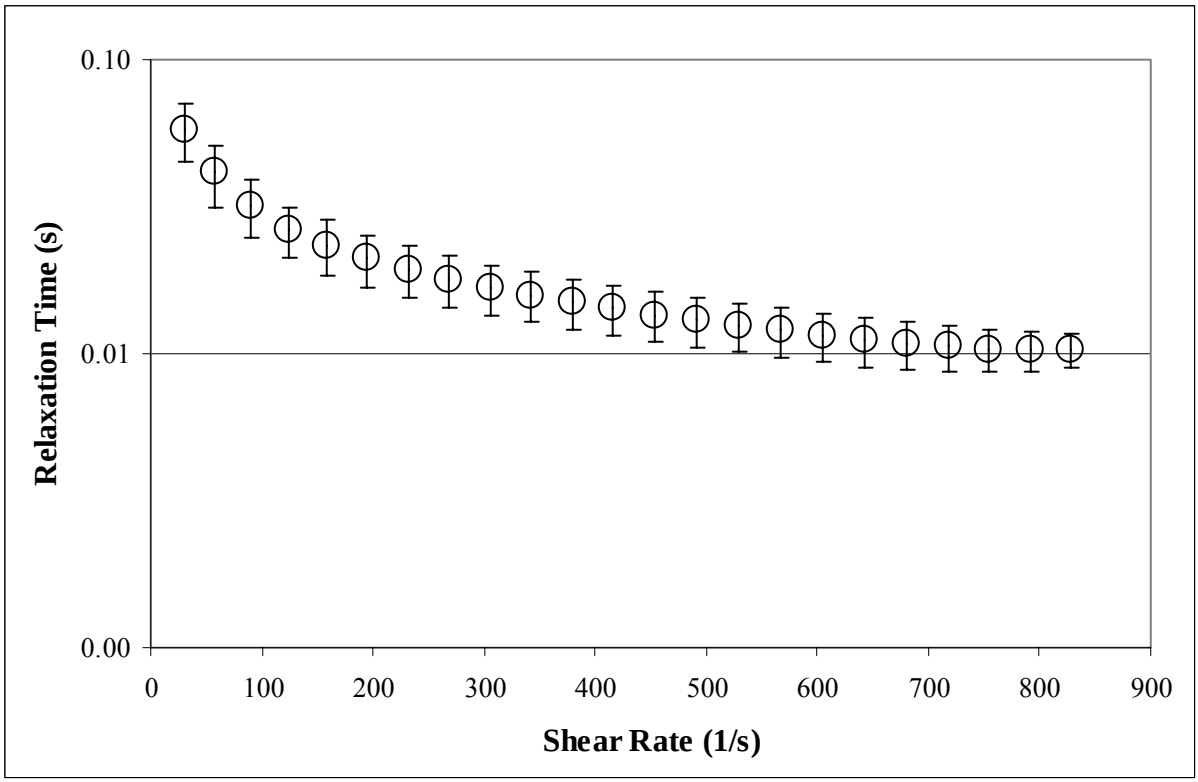

Figure 5-6. Relaxation time of AVP measured in a viscoelastometer (Vilastic) at a concentration of 2.5 mg/ml

5.2.1.5 Mechanical degradation studies

AVP was found to be much less susceptible to mechanical degradation than PEO in both saline and in the presence of RBCs. In saline, AVP retained over 50% of its original drag reducing efficiency after five hours of exposure to turbulent flow. The degradation rate of AVP was slightly faster in a 20% RBC suspension, but 40% of its original drag reduction was still maintained in the suspension after five hours of exposure to turbulent flow (Figure 5-7). Molecular characteristics of AVP, measured using GPC, did not change significantly following exposure.

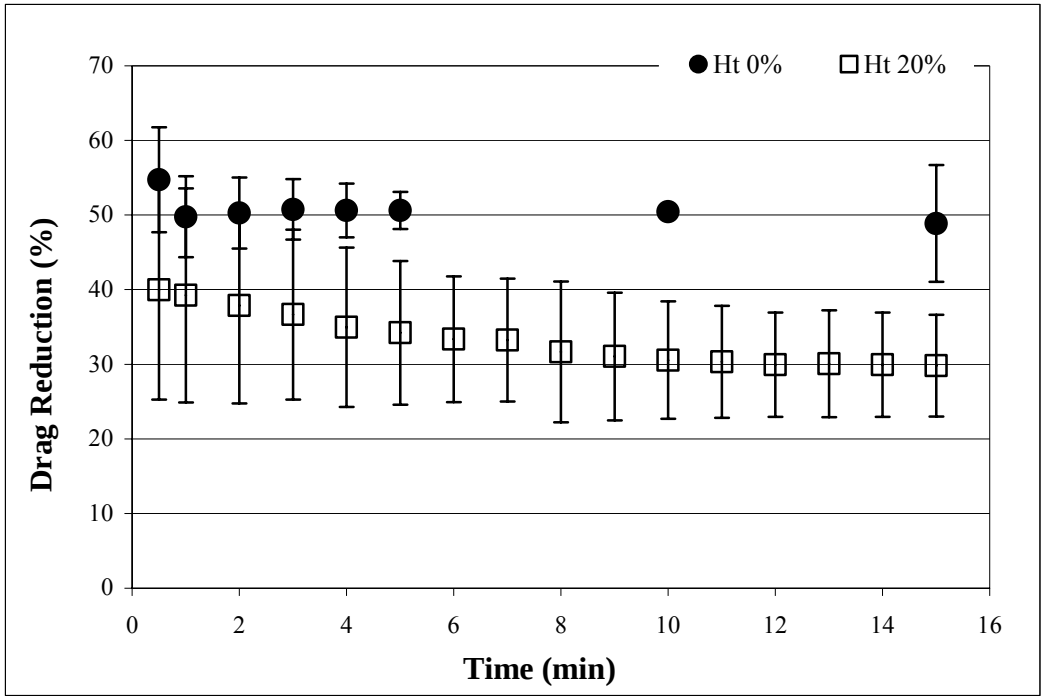

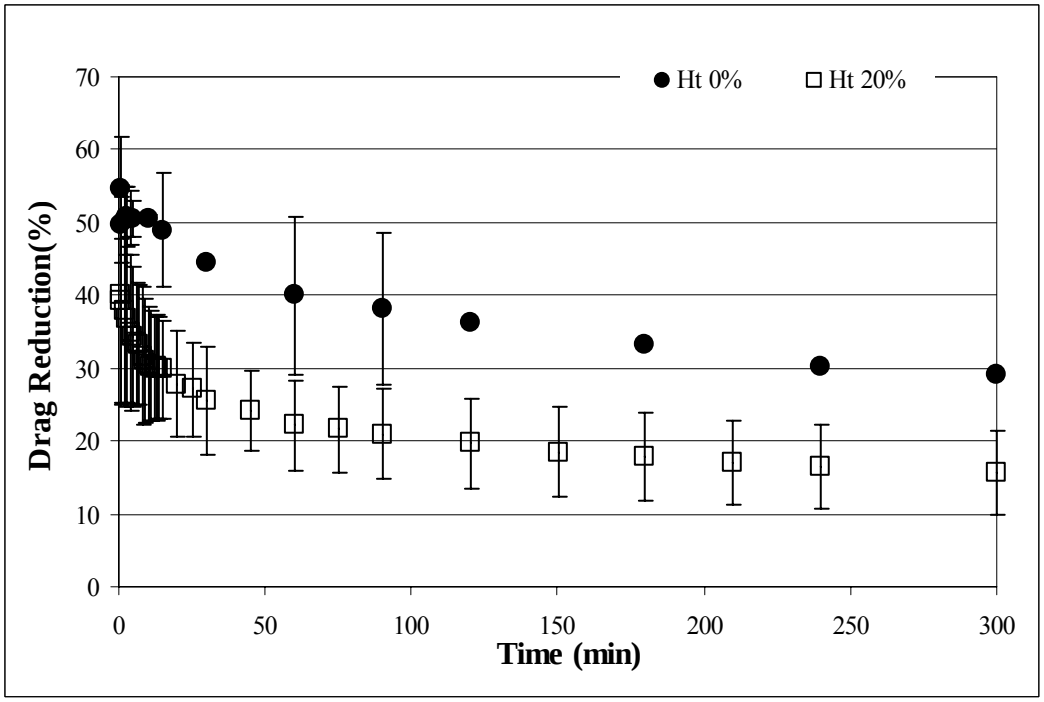

Figure 5-7. The rate of degradation of AVP at 0.1mg/ml is higher in a RBC suspension than in saline, but AVP maintains drag reducing ability in both saline and RBC suspensions following 15 min (top) and 5 hr (bottom) of exposure to turbulent flow.

The single relaxation decay model, which was applied to PEO degradation and described in Section 3.1.5, model was also tried for AVP degradation, where it could be used to predict degradation over longer time periods than can be practically studied. However, this model did not fit well. Therefore, it was determined that the single relaxation decay model could not be used universally to predict degradation of any DRP at least in the studied recirculating flow system.

5.2.2 Synthesis and characterization of poly(N-vinylformamide)

High MW PNVF was synthesized using an inverse emulsion technique, and tested as a potential DRP. Since PNVF is synthesized from a non-toxic isomer of acrylamide [66, 67], and polyacrylamide is known to be an effective DRP, high MW PNVF was considered to have potential for DRP applications *in vivo*.

5.2.2.1 ^{1}HNMR

The synthesis of PNVF was confirmed by NMR, ^{1}HNMR (D_2O) δ 1.68 (br s, 2H, methylene), 3.89 (br s, 1H, methine), and 8.0 ppm (m, 1H, formyl H). The shift at 8.0 ppm, which represents the formyl hydrogen, confirmed that the tested polymer was indeed PNVF and not the hydrolyzed form, poly(vinyl amine).

5.2.2.2 GPC

The synthesized PNVF had a weight average molecular weight, measured by GPC, of 4.2×10^6 Da ± 1.7×10^5 Da with a polydispersity index of 4 prior to dialysis. Following dialysis against a membrane with a 1×10^6 Da molecular weight cutoff, the weight average molecular weight

increased to $4.5x10^6$ Da ± $3.1x10^5$ Da, and the polydispersity index was reduced to 1.4. The intrinsic viscosity was 4 dl/g ± 0.1 dl/g and the radius of gyration was 82 nm ± 2.4 nm. In comparison, PEO-4500 had a much higher intrinsic viscosity (13 dl/g) and radius of gyration (120 nm).

5.2.2.3 *In vitro* test of drag reducing ability

The addition of PNVF to turbulent flow produced a marked reduction in resistance to flow. Figure 5-8 shows the pressure vs. flow relationship for water with 0.1 mg/ml PNVF and 0.5 mg/ml of PNVF compared to that of pure water. At a given flow rate, the PNVF solution required a significantly lower driving pressure than the pure water, representing the Toms effect. PNVF reduced resistance to turbulent flow by a maximum of 20% at a Reynolds number of 20,000 when added into the circulating system at a concentration of 0.1 mg/ml and 32% at a concentration of 0.5 mg/ml. At a concentration of 0.1 mg/ml, PEO-4500 reduced drag by 36% while PEO-1000 and PEO-2000 reduced drag by 17% and 23% respectively. A dimensionless friction factor vs. Reynolds number curve for these experiments is shown in Figure 5-9. PNVF produced a statistically significant reduction in friction compared to saline (control) over the entire range of studied Reynolds numbers at both 0.1 mg/ml and 0.5 mg/ml ($p < 0.001$).

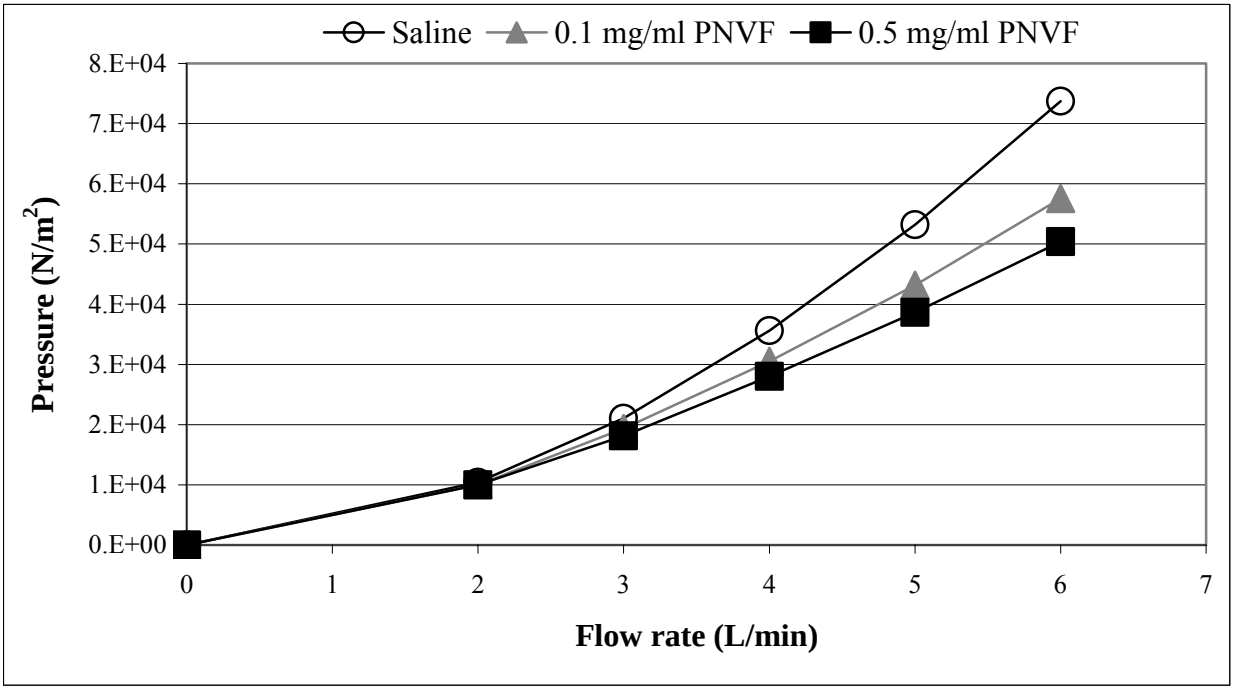

Figure 5-8. Pressure vs. flow characteristics of PNVF solutions obtained in the turbulent flow system.

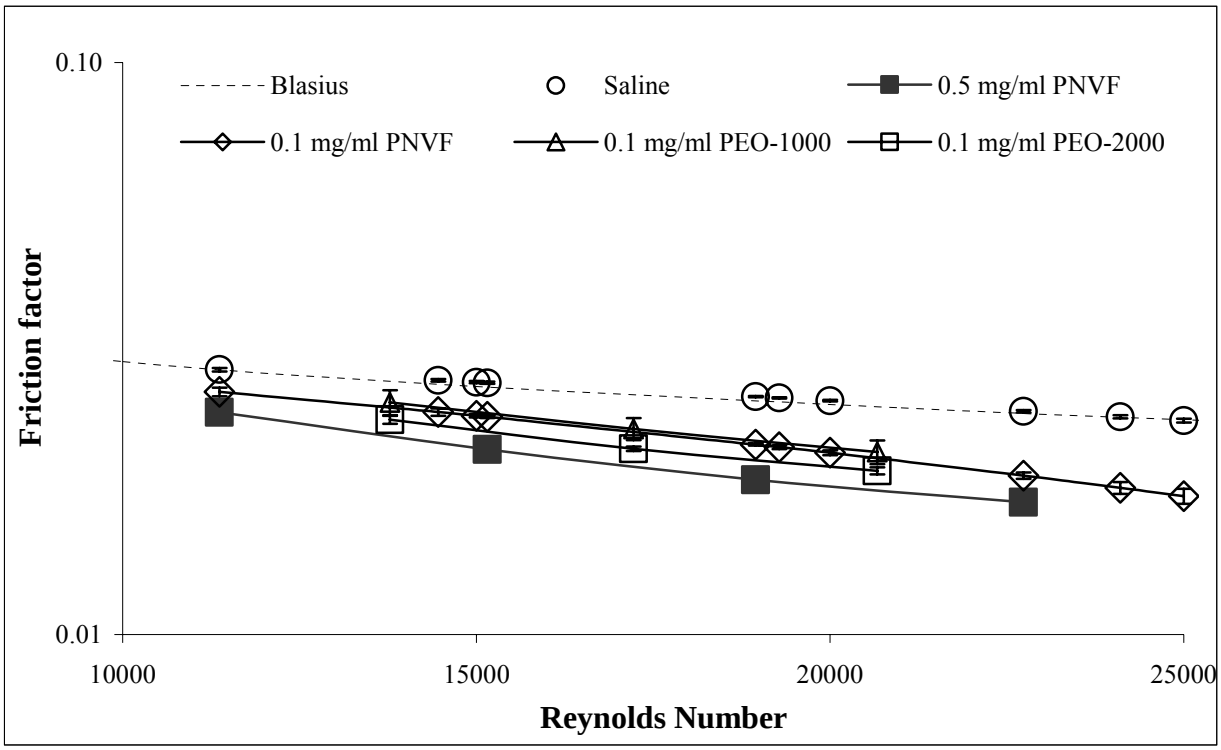

Figure 5-9. Dimensionless friction factor vs. Reynolds number obtained for saline, PNVF (two concentrations) and two PEO solutions

5.2.2.4 Viscoelasticity

Concentrated PNVF solutions exhibited non-Newtonian behavior, a characteristic demonstrated by DRPs. High shear viscosity of a 5 mg/ml PNVF solution dissolved in saline was ~6 cP at a shear rate of 400 s^{-1}. The viscosity vs. shear rate curves for this solution, determined using a viscoelastometer and a cone and plate viscometer are shown in Figure 5-10. The viscosity, elasticity, and relaxation time vs. shear rate curves for the PNVF, PEO-1000, and PEO-2000 solutions dissolved in saline are shown in Figures 5-11, 5-12, and 5-13. Asymptotic viscosity of a 0.5 mg/ml PNVF solution was 1.3 cP and asymptotic viscosity of a 0.1 mg/ml solution was 1.05 cP.

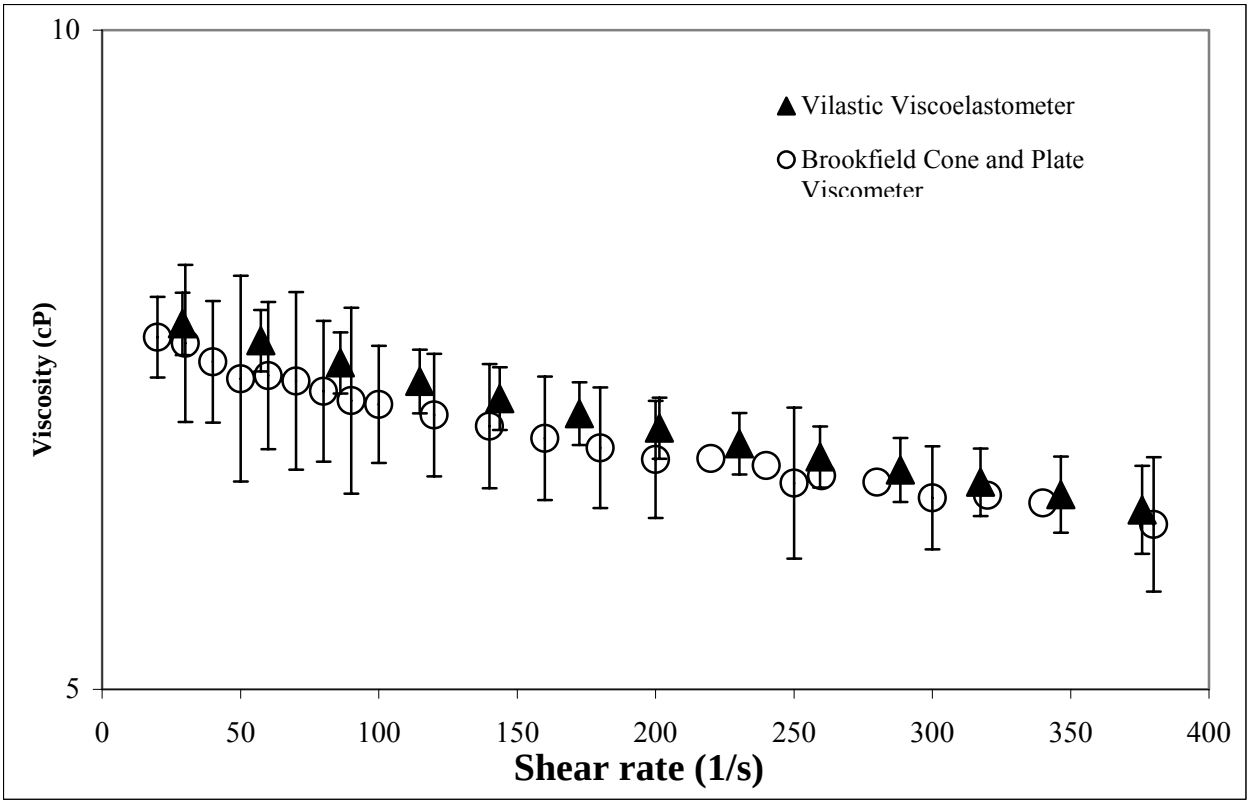

Figure 5-10. Viscosity of PNVF solution at the concentration of 5 mg/ml compared to that of two PEOs

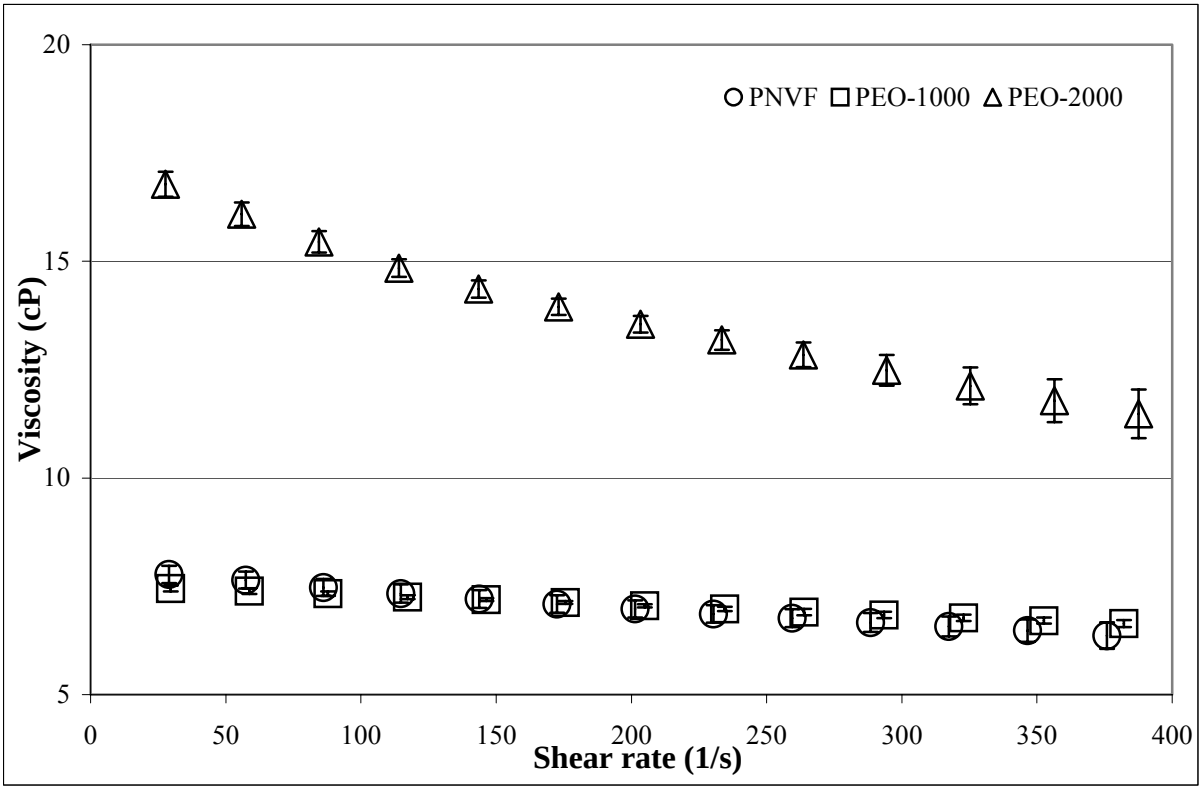

Figure 5-11. Viscosity of PNVF solution measured in viscoelastometer at a concentration of 5 mg/ml compared to that of two PEOs

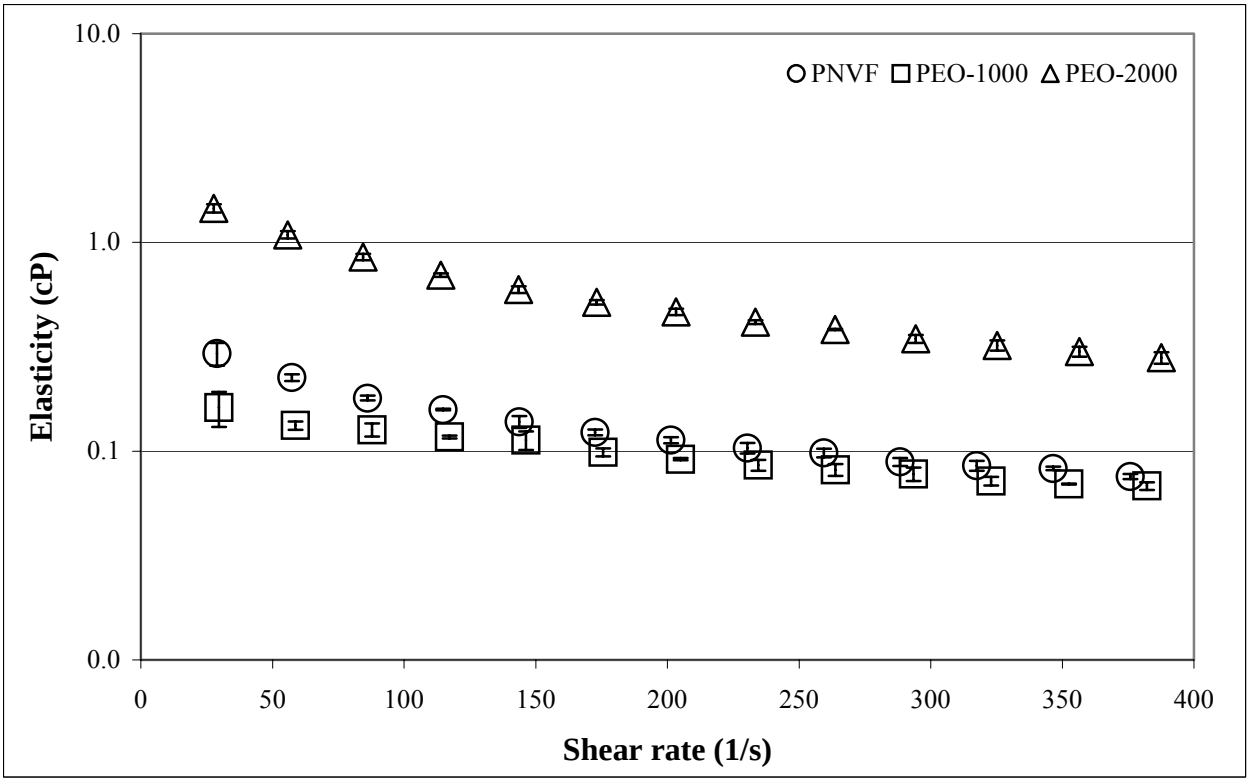

Figure 5-12. Elasticity of PNVF solution measured in viscoelastometer at a concentration of 5 mg/ml compared to that of two PEOs

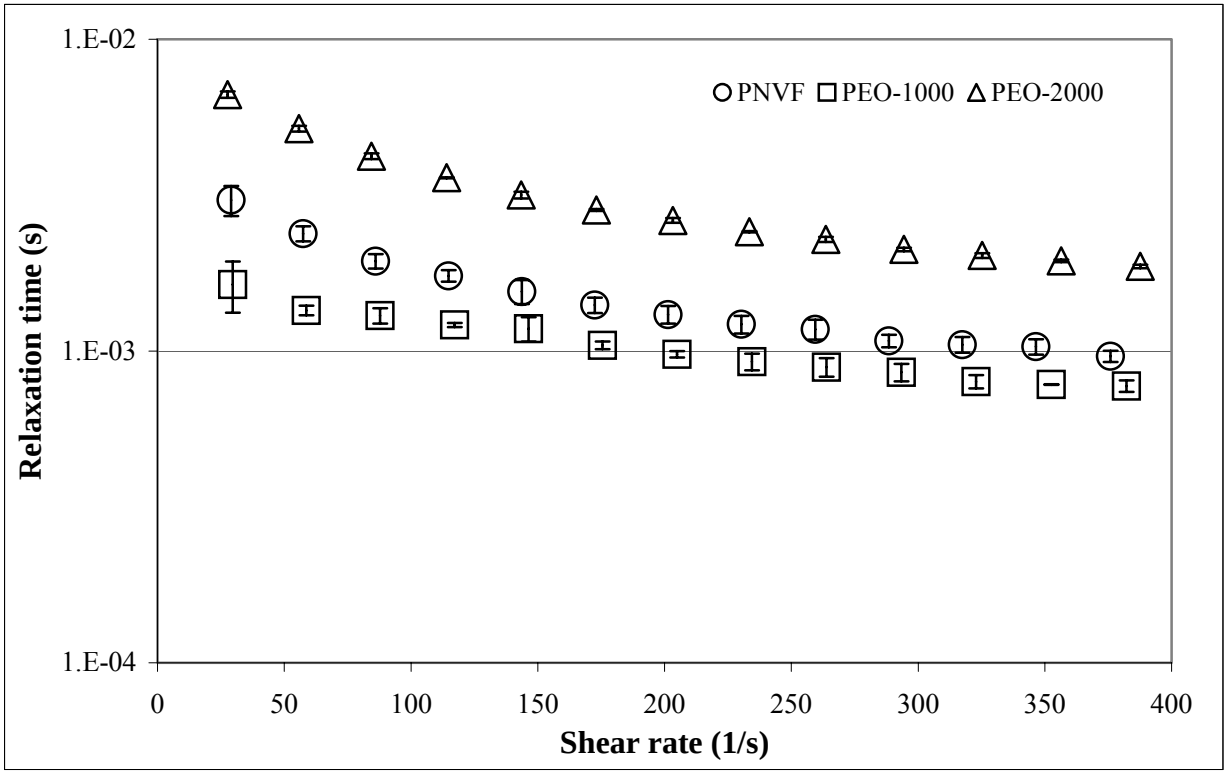

Figure 5-13. Relaxation time of PNVF solution measured in viscoelastometer at a concentration of 5mg/ml compared to that of two PEOs

5.2.2.5 Mechanical degradation studies

The PNVF initially reduced resistance to flow by 15% when added into the recirculating flow system at a concentration of 0.1 mg/ml and a Reynolds number of 15,000. However, the drag reducing efficiency of the PNVF decreased with continuing exposure to flow, vanishing within 90 minutes of exposure. The degradation of PNVF was compared to that of PEO-1000 and PEO-2000, which exhibited similar initial drag reducing efficiency. Figure 5-14 shows the drag reduction produced by these DRPs following exposure to flow induced shear stresses. PNVF retained over 40% of its ability to reduce resistance to flow after 30 minutes of exposure to flow induced shear stress and almost 25% after an hour of exposure, while the PEO-1000 lost its drag

reducing ability completely within 30 minutes and PEO-2000 within one hour. Average molecular weight of the PNVF, however, decreased only slightly over time. The change in molecular weight versus time of exposure to flow is shown in Figures 5-15 and 5-16. Both weight average (M_w) and z average (M_z) molecular weight, which represents the higher end of the molecular weight distribution, are shown.

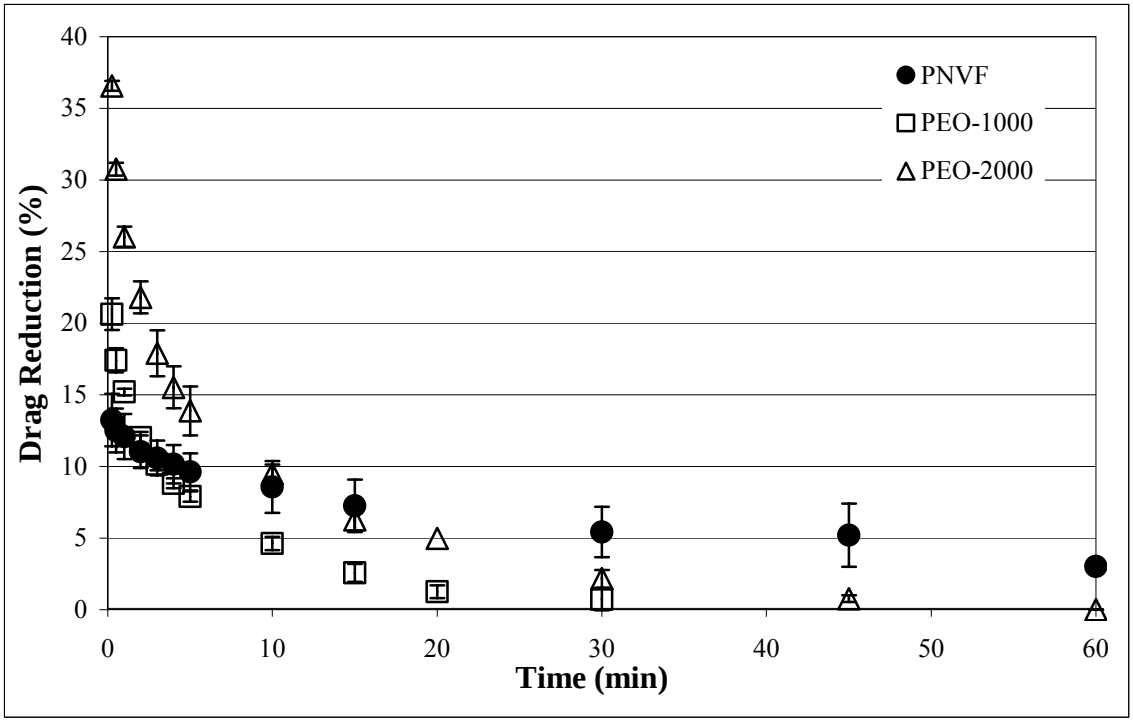

Figure 5-14. Drag reducing ability of PNVF maintained after exposure to flow compared to that of several PEOs

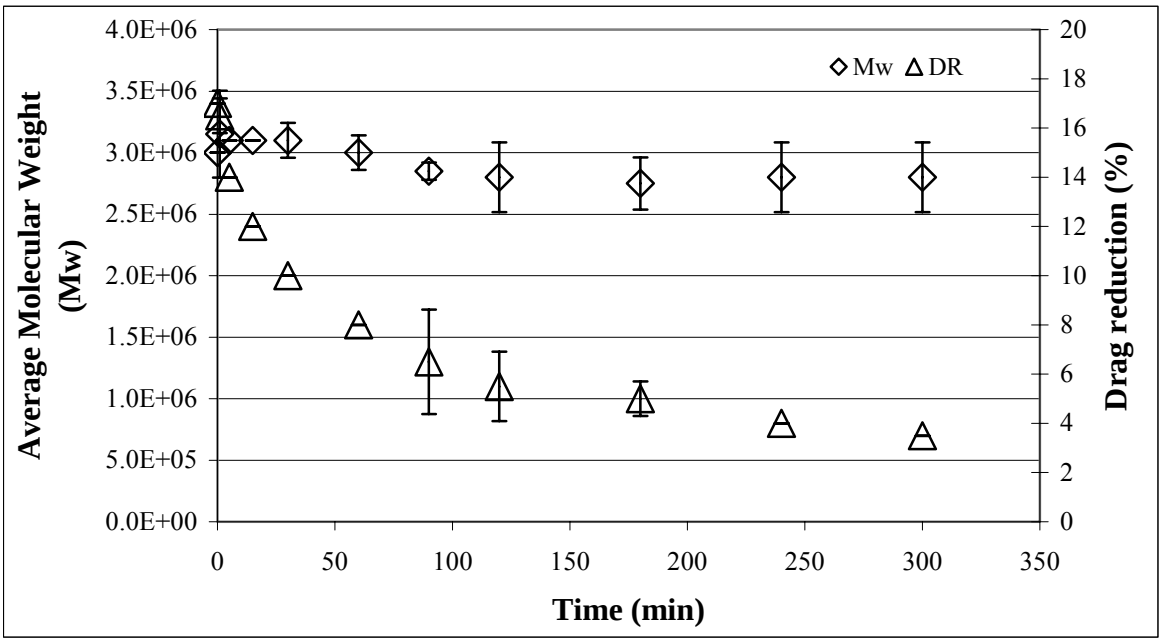

Figure 5-15. Weight average molecular weight decreases slightly as the PNVF drag reducing ability degrades during exposure to turbulent flow

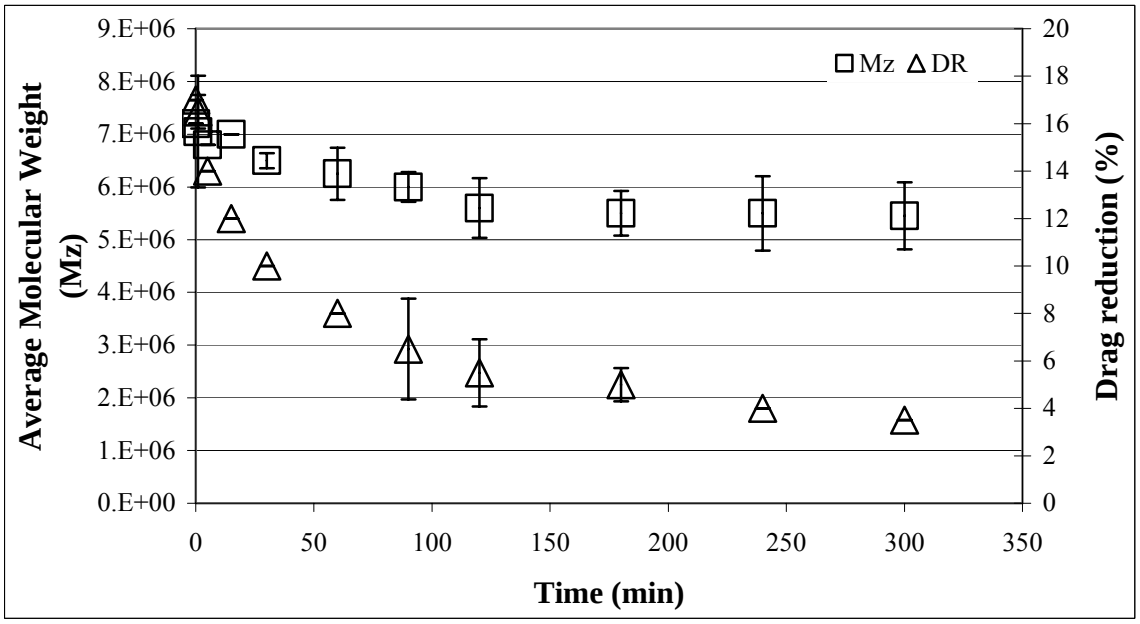

Figure 5-16. Z average molecular weight decreases slightly as the PNVF drag reducing ability degrades during exposure to turbulent flow

5.2.3 Characterization of high molecular weight hyaluronic acid for use as a DRP for potential use *in vivo*

HA has long been known to have drag reducing ability [72] and currently has FDA approval for some biomedical applications (unrelated to its drag reducing properties) [73], making it an desirable candidate to be applied for enhancement of blood circulation. Therefore, several HA preparations, provided by Lifecore Biomedical, were characterized and evaluated for potential use in such applications.

5.2.3.1 GPC

M_w, IV, Rg, and PDI were measured for a series of HA samples. Table 5-1 shows the measured characteristics for each tested HA.

Table 5-1. Comparison of molecular parameters of several HA samples obtained from Lifecore Biomedical

Sample	M_w	IV	R_g	PDI
	(Da)	(dL/g)	(nm)	
002941	1.28×10^5	4.2	26	1.5
P9411-1	4.74×10^5	15	62	1.2
P0207-1	1.11×10^6	20.4	80	1.9
P9711-9	1.30×10^6	27.2	106	1.1

5.2.3.2 *In vitro* test of drag reducing ability

The addition of HA (with the exception of that with MW ~130 kDa) to turbulent flow produced a significant reduction in resistance to flow. Drag reducing effectiveness of the tested HAs increased with increase in concentration and with increase in M_w. Drag reduction produced by

the tested HA samples at various concentrations is shown in Table 5-2. The DR of the highest MW HA could not be tested in the flow system at 500 μg/ml since, due to its high viscosity, turbulent flow could not be achieved in the recirculating flow system. A dimensionless friction factor vs. Reynolds number curve for these experiments performed at 0.1 mg/ml is shown in Figure 5-17. The two HAs with MW above 10^6 Da produced a statistically significant reduction in friction compared to saline (control) over the entire range of studied Reynolds numbers ($p < 0.01$), while the lower molecular weight polymers produced no significant change in friction factor.

Table 5-2. Comparison of maximum DR produced by various HAs at several concentrations in the turbulent flow system.

Sample	Actual M_w (Da)	Max. DR (%) 10 μg/ml	Max. DR (%) 100 μg/ml	Max. DR (%) 250 μg/ml	Max. DR (%) 500 μg/ml
002941	1.28×10^5	0	0	0	0
P9411-1	4.74×10^5	3	8	16	20
P0207-1	1.11×10^6	6	17	26	37
P9711-9	1.30×10^6	10	35	43	N/A

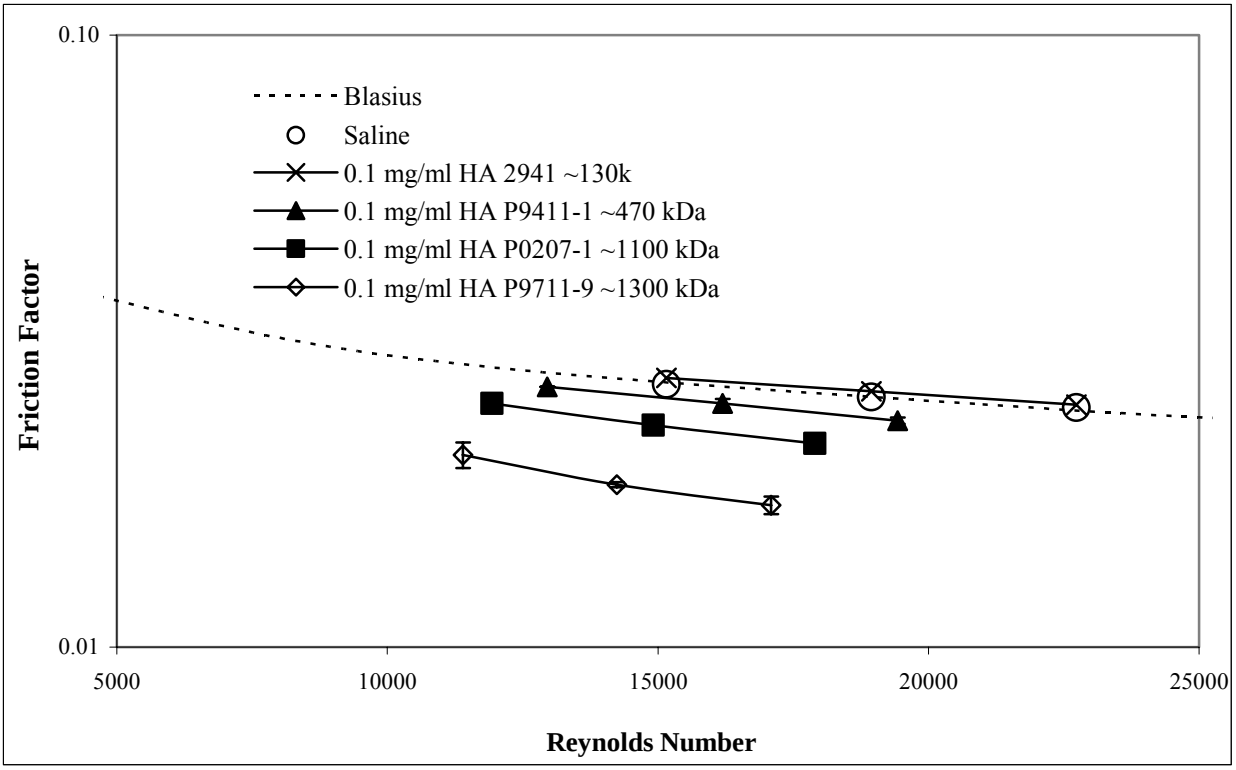

Figure 5-17. Friction factor vs. Reynolds number obtained for several HAs at 0.1 mg/ml

5.2.3.3 Viscoelasticity

Concentrated HA solutions with MW ~ 500 kDa and above exhibited non-Newtonian behavior, a well-known property of DRPs. The viscosity vs. shear rate curves for these solutions at a concentration of 2.5 mg/ml, determined using a cone and plate viscometer, are shown in Figure 5-18. Due to the very high solution viscosity of HA with MW of 1100 kDa and 1300 kDa, it was not possible to obtain viscosity at higher shear rates. The viscosity, elasticity, and relaxation time vs. shear rate curves for the 2.5 mg/ml HA solutions, measured using the Vilastic 3 viscoelastometer, are shown in Figures 5-19, 5-20, and 5-21. Elasticity and relaxation time are negligible for the lower MW polymers and are therefore shown only for the two highest MW

HAs. Viscosities at a concentration of 0.1 mg/ml were measured using capillary viscometers and are shown in Table 5-3.

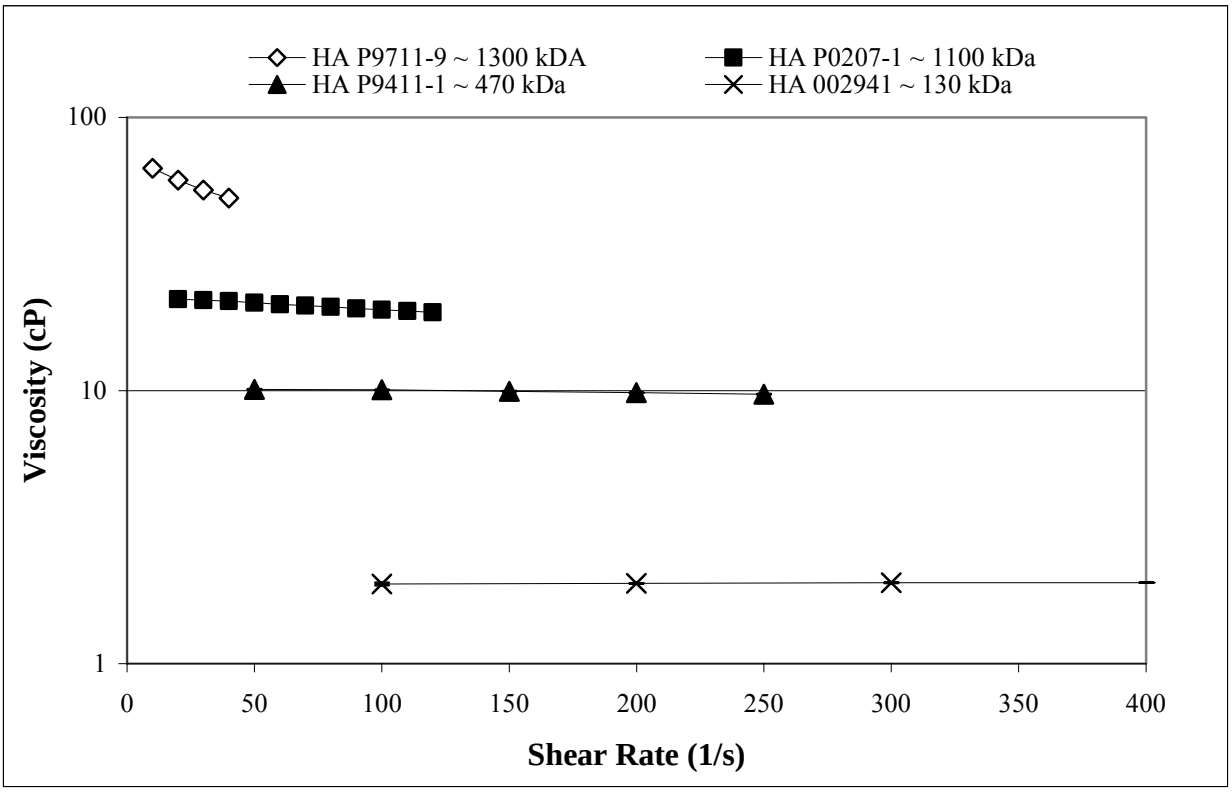

Figure 5-18. Viscosity of HA solutions at a concentration of 2.5 mg/ml

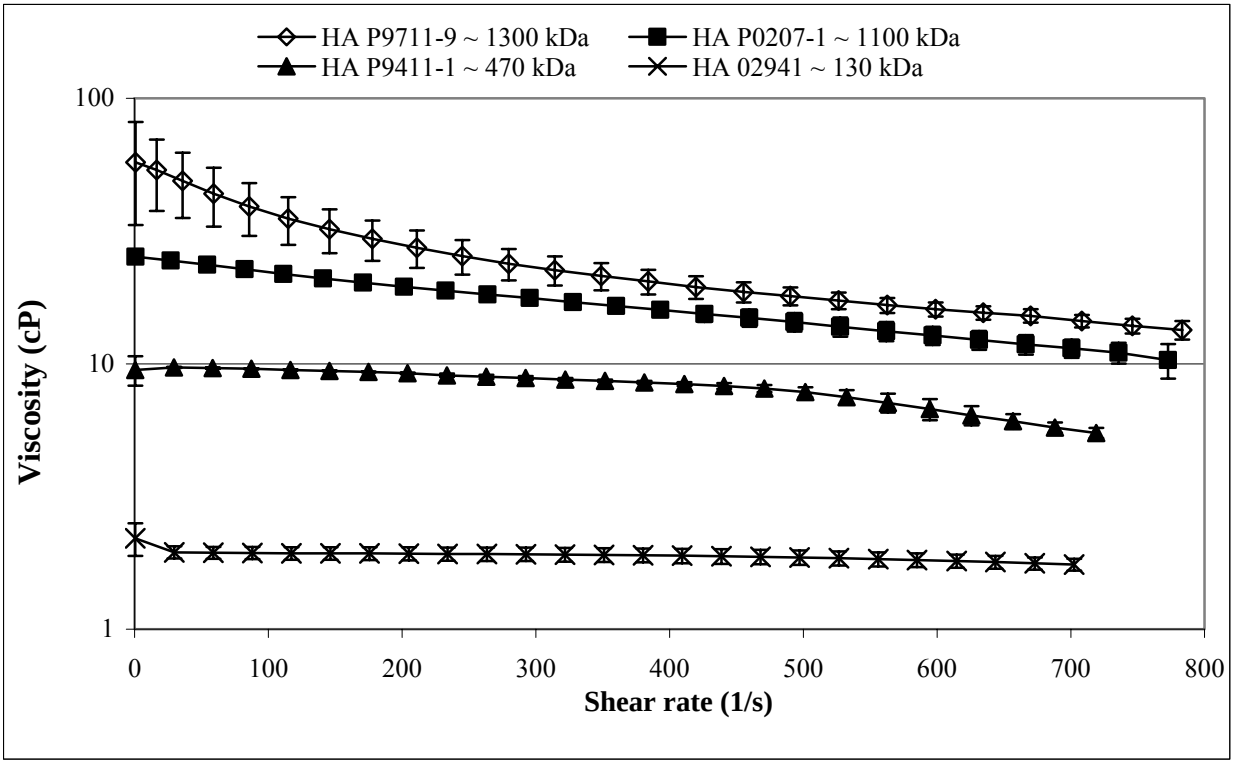

Figure 5-19. Viscosity of HA solutions measured in viscoelastometer at a concentration of 2.5 mg/ml

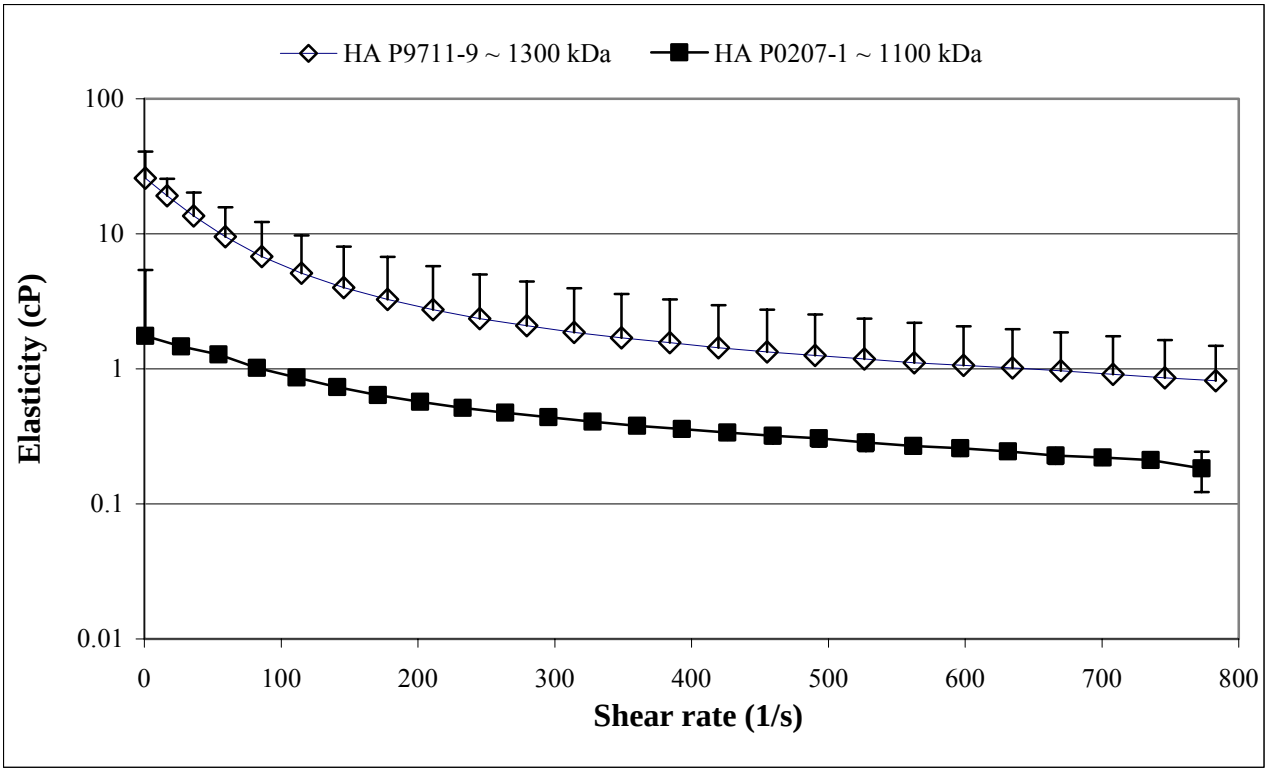

Figure 5-20. Elasticity of HA solutions measured in viscoelastometer at a concentration of 2.5 mg/ml

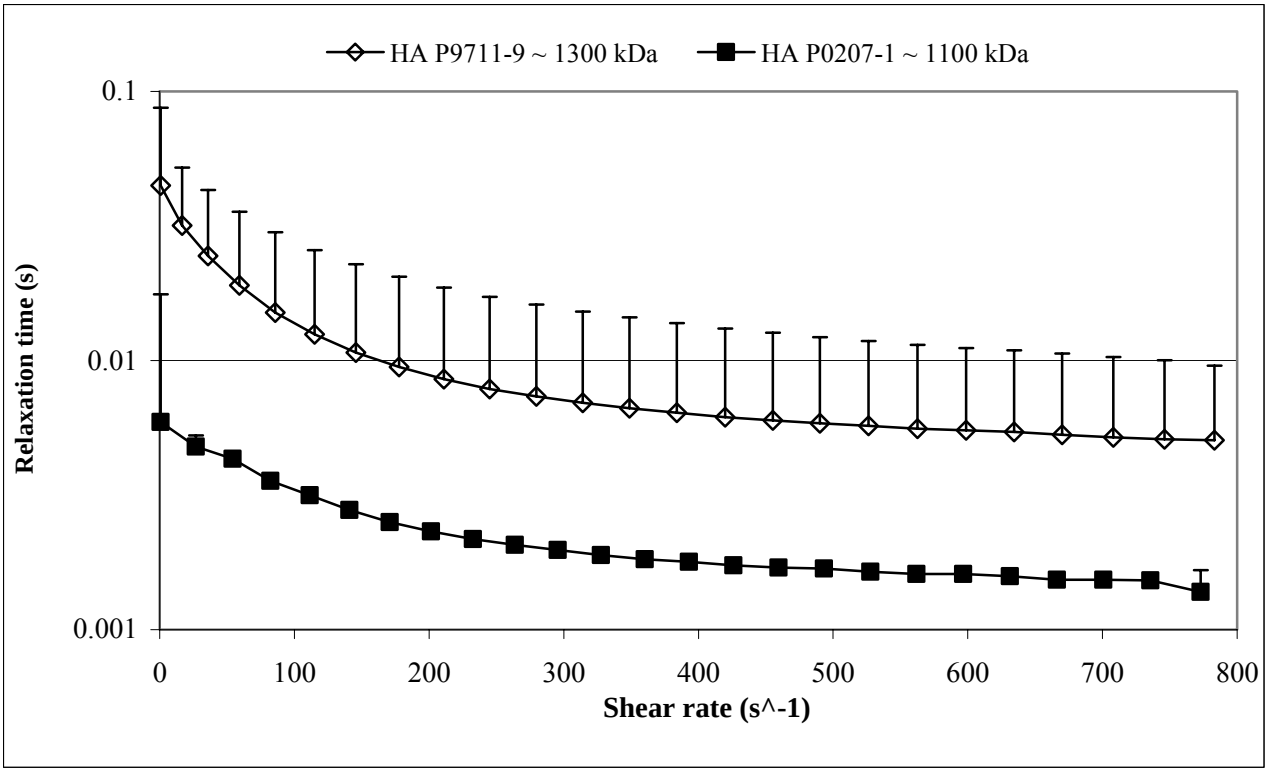

Figure 5-21. Relaxation time of HA solutions measured in viscoelastometer at a concentration of 2.5 mg/ml

Table 5-3. Viscosities of HAs measured using a capillary viscometer at a concentration of 0.1 mg/ml at 22 °C ± 1°C.

Sample	Actual M_w (Da)	Capillary viscosity at 0.1 mg/ml (cP)
002941	1.28×10^5	1.09
P9411-1	4.74×10^5	1.17
P0207-1	1.11×10^6	1.27
P9711-9	1.30×10^6	1.33

5.2.3.4 Mechanical degradation studies of HA

The HA with MW ~ 1300 kDa initially reduced resistance to flow by 20% when added into the flow system at a concentration of 0.1 mg/ml and a Reynolds number of 15,000. The HA maintained its drag reducing efficiency well with continuing exposure to flow. The degradation of HA was compared to that of PEO-1000 and PEO-2000. Figure 5-22 shows the drag reducing ability of these DRPs following exposure to flow induced shear stresses. HA maintained over 90% of its original drag reducing ability throughout the entire five hours of exposure to turbulent flow. The PEO-1000 lost its drag reducing ability completely within 30 minutes and PEO-2000 within one hour.

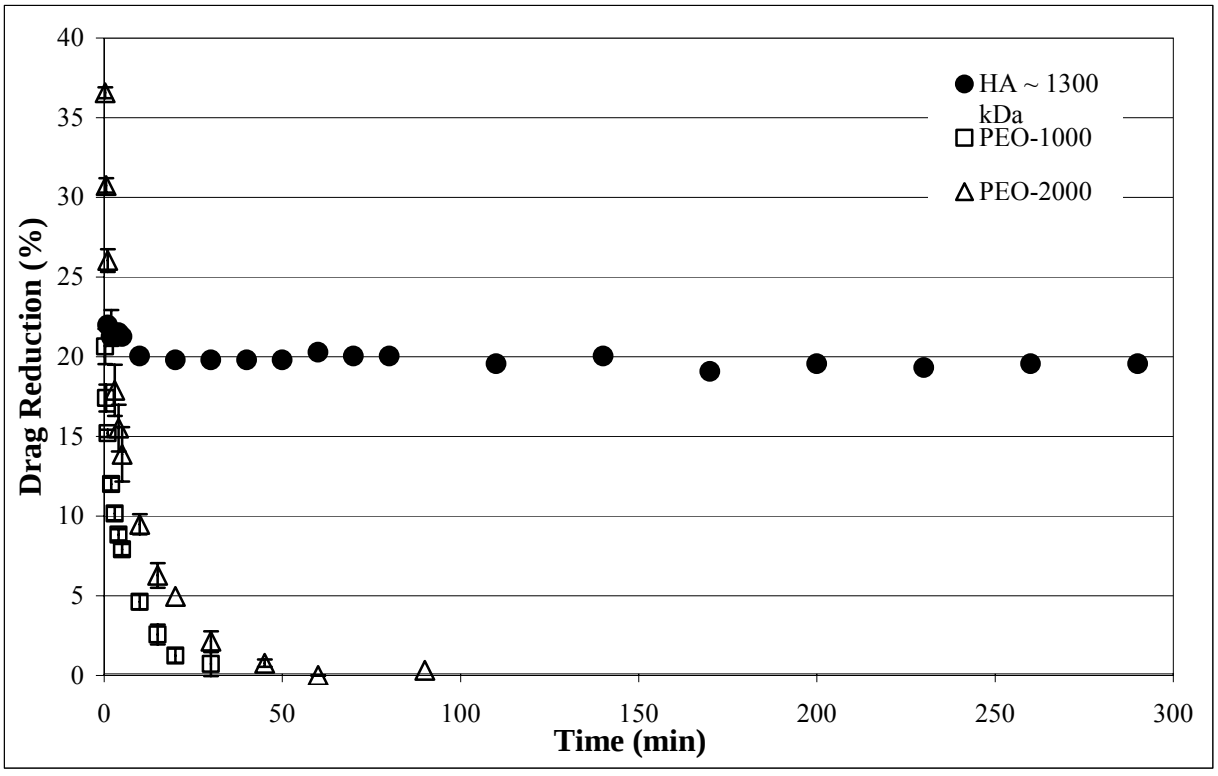

Figure 5-22. Percentage of original drag reducing ability maintained after exposure to flow

5.2.4 Comparison and correlation the DRP physicochemical and rheological properties with their drag reducing activity

In order to help identify the best candidates for a DRP to be used for biomedical applications, as well as the properties which would best define drag reducing effectiveness, the molecular and rheological properties, drag reducing ability, and mechanical degradation of several DRPs, including well-known DRPs such as PAM and PEO as well as novel DRPs such as AVP, HA, and PNVF, were compared.

5.2.4.1 Correlations between DRP physicochemical and rheological properties and their drag reducing effectiveness

Correlations were investigated between drag reducing efficiency and polymer properties including MW, R_g, IV, concentrated solution viscosity, elasticity, and relaxation time for PEO-4500, PAM (Praestol 2510, Stockhausen, Inc.), AVP, PNVF, HA (P9711-9, Mw ~ 1300 kDa), and dextran. Drag reducing ability was found to best correlate with relaxation time measured in concentrated solutions ($r^2 = 0.85$ at a shear rate of 50 s^{-1} and $r^2 = 0.82$ at 500 s^{-1}) and radius of gyration ($r^2 = 0.85$). Elasticity in concentrated solutions ($r^2 = 0.64$ at a shear rate of 50 s^{-1} and $r^2 = 0.60$ at 500 s^{-1}) and IV ($r^2 = 0.63$) also correlated fairly well with drag reducing effectiveness. Solution viscosity did not correlate with drag reducing ability as well as the other tested parameters did ($r^2 = 0.50$ at a shear rate of 50 s^{-1} and $r^2 = 0.34$ at 500 s^{-1}). Molecular weight was found to be a good predictor of polymer drag reducing ability within the class of DRPs ($r^2 = 0.90$). However, no correlation was found between drag reducing ability and M_w for polymers in general. For example, the tested dextran had the highest M_w of all the tested polymers, but it had no drag reducing ability.

5.2.4.2 Correlations between DRP physicochemical and rheological properties and their effects in microflow of RBCs

Correlations were determined between the effects of DRPs on flow of RBCs in microchannels and their physical properties including MW, R_g, IV, concentrated solution viscosity, elasticity, and relaxation time for PEO-4500, PAM (Praestol 2510), AVP, and HA (Hyvisc, Boehringer Ingelheim Vetmedica).

Observed near wall plasma layer size was determined to best correlate with relaxation time measured at high shear rate in solutions with a concentration of 2.5 mg/ml (r^2 = 0.92 at a shear rate of 500 s^{-1}) and with radius of gyration (r^2 = 0.98). Since polymers with larger gyration radii and relaxation times led to lower reduction in near wall plasma layers, it can be concluded that DRPs which have lower R_g and relaxation time were more effective in altering flow of RBCs in microchannels. It should be noted that this is true only within the class of DRPs. Polymers such as PEO-200 and high molecular weight dextran, which had no drag reducing properties, had no effect on flow of RBC suspension in microchannels even though their R_g and relaxation time were the lowest of the studied polymers. Intrinsic viscosity (r^2 = 0.64) and elasticity measured at high shear rate in concentrated solutions (r^2 = 0.64 at a shear rate of 500 s^{-1}) also predicted the effect of DRPs on plasma layer size fairly well.

5.2.4.3 Comparison of mechanical degradation behavior among the class of DRPs

Comparison of the mechanical degradation rates of different DRPs was important since it is necessary for the DRPs to be able to withstand shear forces in the body for some length of time, especially for use in treating chronic circulatory disorders. AVP was found to be the most effective drag reducer of the tested polymers at the starting point of the hydrodynamic tests, reducing resistance to flow by 50% at 0.1 mg/ml and a Reynolds number of ~ 20,000. PAM

(Praestol 2510) was also very effective, reducing resistance by 45% under the same conditions, followed by PEO-4500 (40%), HA (P9711-9, M_w ~ 1500 kDa) (22%), and PNVF (13%) tested at the same concentration. Following 15 minutes of exposure to stresses in the turbulent flow recirculating system, AVP was still the most effective DRP (50 % DR or 100% of its original DR) followed by PAM (30% or 67% of its original DR), HA (20% or 91% of its original DR PEO (8% or 20% of its original DR), and PNVF (7% or 54% of its original DR). AVP remained the most effective DRP after one hour (40% or 80% of its original DR) followed by HA (20% or 91% of its original DR), PAM (15% or 33% of its original DR), PNVF (3% or 23% of its original DR), and PEO (2% or 5% of its original DR). After five hours of exposure to flow, AVP continued to be the most effective DRP (30% DR, 60% of original DR) followed by HA (20%, 91% of the original DR), and PAM (5% or 11% of original DR). Both PEO and PNVF completely degraded within five hours of exposure. Figure 5-23 shows the percentage of original drag reducing effectiveness maintained after one hour of exposure to flow. The polysaccharides, HA and AVP, were found to be the most resistant to mechanical degradation of the tested polymers.

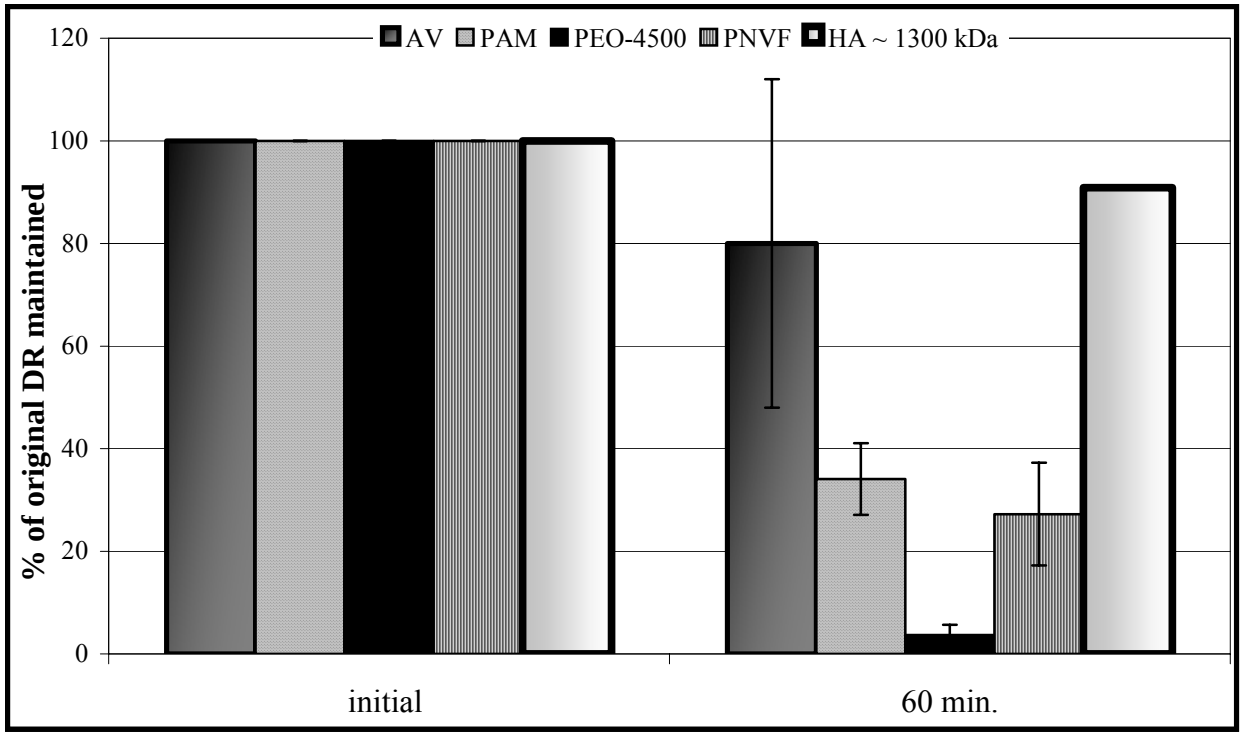

Figure 5-23. Percentage of original drag reducing effectiveness maintained after one hour of exposure to flow

5.3 DISCUSSION

DRPs have been shown to improve impaired blood circulation caused by numerous pathologies in animal models [1-4, 6, 9, 12, 16]. Although commonly used DRPs such as PEOs, PAMs, and plant derived polysaccharides are very effective in these models, they are not optimal for potential clinical applications. PEO is degraded quickly by high stresses [45], PAM presents toxicity issues [9, 12, 93], and natural polymers are often difficult to manufacture consistently in the necessary quantities. Therefore, the search continues for better synthetic or easily produced natural DRPs, which are resistant to mechanical degradation, biocompatible, well reproducible,

and easy to manufacture, for potential clinical use. The three polymers discussed in this section, an aloe derived polysaccharide, poly(N-vinylformamide), and hyaluronic acid, all proved to be effective DRPs, and have physicochemical characteristics attractive for use in clinical applications.

AVP was found to be the most effective drag reducer of the tested polymers, reducing resistance to turbulent pipe flow by up to 50% at the accessible range of Reynolds numbers in the turbulent flow system used for these studies. The active drag reducing component was determined to be a polysaccharide consisting of β-1,4 linked mannose residues, but additional studies are needed to elucidate the exact chemical structure of this polymer. Molecular and rheological properties of AVP are typical for an effective drag reducer. High standard deviations in molecular and rheological properties are likely the result of variations between aloe preparations caused by variations between plants, or slight variance in the extraction procedure. The fact that standard deviations in viscoelastic parameters are highest at low shear rates may also indicate the presence of some molecular aggregation which varied between samples. This aggregation was also likely to be responsible for the higher viscosities measured using the cone and plate rheometer compared to those measured using the Vilastic viscoelastometer. The oscillatory flow in the viscoelastometer could break up these aggregates significantly reducing the observed viscosity, especially at low shear rates.

AVP was much more resistant to mechanical degradation than PEO in both saline and in the presence of RBCs making it a promising candidate for potential use in treatment of chronic circulatory disorders. It has been previously hypothesized that certain polysaccharides may have increased resistance to degradation due to their strong bonds between monomer units as well as intra- and intermolecular interactions lessening the stresses on those bonds [22]. It has also been

suggested that branches on a polymer molecule increase its mechanical stability [23]. Although the exact structure of the DRP component of aloe is not yet known, a structure proposed for the main component of the aloe polysaccharide may contain some branches [60] while PEO does not. Finally, since polysaccharides, such as the aloe-based polysaccharide, are comprised of numerous six-carbon rings linked together, the molecules are more rigid, and therefore degradation is not entropically favored [21]. The presence of rings could also allow for some bonds to be broken without breaking up the polymer backbone. Therefore, unlike PEO, the aloe polymer could likely withstand some bond breakage without compromising its drag reducing activity. The degradation of AVP caused by biologic mechanisms *in vivo*, however, has not been studied, but must be evaluated before AVP could be used clinically.

Unlike the natural AVP, the synthetic nature of PNVF makes production in large quantities and consistent batches more feasible. Therefore, high molecular weight PNVF ($4.5x10^6$ Da) was synthesized and tested as a DRP for possible biomedical applications. The synthesized PNVF had molecular properties characteristic of DRPs, including high molecular weight and relatively large intrinsic viscosity and radius of gyration, and was effective in reducing resistance to turbulent flow. While the PNVF was shown to be an effective drag-reducer, reducing resistance to turbulent flow by over 30% at a concentration of 0.5 mg/ml at turbulent flow conditions produced in the recirculating system, it was not as effective as PEO of the same molecular weight ($4.5x10^6$ Da). One possible explanation for this is that, since NVF polymerization is known to exhibit some chain transfer [66], the PNVF is likely not entirely linear. This hypothesis is supported by the fact that its intrinsic viscosity (4 dl/g) is significantly lower than the 13 dl/g intrinsic viscosity of PEO-4500. Another factor that may contribute to this difference in drag reducing efficiency is that the molecular weight of the NVF monomer is much

higher that the molecular weight of the ethylene oxide monomer. It is well known that, at the same polymer molecular weight, the polymer with the lower monomer molecular weight and therefore a higher degree of polymerization is a better drag-reducer [26]. The drag reducing ability of the PNVF is close to that of PEO-1000 and PEO-2000 (at least in the applied range of Reynolds numbers). In addition, viscoelastic properties of the PNVF correspond well to these two PEOs, indicating that the viscosity, elasticity, and relaxation time are important parameters in determining a polymer's drag reducing activity.

Although PNVF was susceptible to mechanical degradation, losing all of its drag reducing ability after 90 minutes of circulation in the turbulent flow system, its degradation rate was significantly lower than that of PEO-1000 and PEO-2000, which lost their drag reducing ability after circulation for 20 and 45 minutes respectively at the same concentration and identical flow conditions. While there was a significant loss of drag reducing ability over time for both PNVF and PEO, the molecular weight of PNVF decreased only slightly. These results are consistent with previously published studies of mechanical degradation of drag reducing polymers [49, 51]. Two theories have been proposed to explain this phenomenon, which is also seen in polyacrylamide degradation. The first of these theories is the molecules at the high end of the molecular weight distribution are most influential in a determining a DRP's efficiency [98] and scission of those molecules would account for loss in drag reducing ability. This is supported by the decrease in M_z, which defines the high end of the molecular weight distribution. The second hypothesis proposes that shear induced structure formation and molecular aggregation are partially responsible for the DRP effects, and therefore, the irreversible breakup of these structures is responsible for the declining drag reducing effect produced by polymers [49, 51]. The drag reducing ability of the PNVF was not restored after stopping the flow for one hour.

This is consistent with the experiments of Liberatore et al, suggesting that that polymer aggregates contribute to the drag reducing ability and irreversibly break up as the solution degrades [49]. The loss of the high molecular weight fraction of the PNVF during exposure to high mechanical stresses might also be responsible for the loss of the polymer's ability to form molecular aggregates since flow-induced structure formation is highly dependent on molecular weight [49, 99]. Sellin et al. suggested a similar theory for PEO degradation, proposing that both chain scission and disentangling of molecular agglomerates could contribute to DRP degradation [52]. Although there is evidence that either of these theories or a combination of them could explain the loss of drag reducing ability, the mechanisms behind the degradation of DRPs and the drag reducing phenomenon itself are still not completely understood, and therefore, it is likely that a combination of these theories and other factors may contribute to the degradation of PNVF. Due to its higher stability against mechanical stress than PEO, PNVF might be a more favorable polymer for chronic medical uses.

In vitro and *in vivo* studies showed that the PNVF seemed to be biocompatible with blood [39]. Preliminary *in vivo* studies showed that PNVF was efficient in reducing vascular resistance without producing adverse effects, at least in acute experiments [39]. However, further *in vivo* studies are necessary to prove beneficial effects of PNVF on normal and especially on pathological blood circulation. Nevertheless, due to its obvious drag reducing effectiveness at both *in vitro* and *in vivo* flow conditions, relatively slow mechanical degradation, and its very low toxicity, PNVF can be considered as a DRP for potential biomedical applications.

HA, at MW above 10^6 Da, possessed molecular and rheological characteristics indicative of DRPs. This natural polymer is available commercially and has been used in some medical applications [70, 71, 100], making it more attractive for the potential translation to clinical use as

DRP than AVP. In this study, HA was proven to be an effective drag reducer which was more resistant to mechanical degradation than any of the tested polymers. As with AVP, this increased resistance to mechanical degradation is likely due to the strong bonds between monomer units, characteristic of polysaccharides, and intra- and intermolecular interactions reducing stresses on those bonds [22] as well as the ring-like structure of the monomer units providing stability. A concern with HA, however, is degradation caused by biological mechanisms *in vivo*. HA was found to degrade quickly in the blood stream, and the main method of HA removal from the blood is by endothelial cells of liver sinusoids [100]. This is an issue that would need to be addressed before HA can be used clinically for treating circulatory diseases as a DRP.

Various water-soluble DRPs have been shown to enhance blood flow in animal models of several pathologies including diabetes hemorrhagic shock and myocardial ischemia [1-4, 6, 8-10, 12, 14, 16, 17, 53]. It was shown that the effective biological half life of one DRP, PAM (Separan AP-30), was about 35 hours in rats [53]. Mechanical degradation could be at least partially responsible for this observed loss of effectiveness. PEO was shown to be one of the most effective drag reducers among well known DRPs and was used in many *in vitro* and *in vivo* studies. Mechanical degradation, however, is a serious concern when considering using DRPs for potential chronic treatment of patients. The stresses produced by cell motion in blood flow, as evidenced in the current studies, cause even more rapid degradation of PEO. AVP, PNVF, and HA, as well as PAM, were shown to degrade more slowly than PEO when exposed to mechanical stresses.

The possibility that the decreased drag reducing ability may be a result of the polymer adhering to the tube and pump walls and, thus, reduction of its concentration in the flowing solution was considered in this study. The concentration of polymer in solution during five hours

of turbulent flow, determined using a refractive index detector, remained constant throughout the experiment, and therefore the loss in drag reducing activity was not caused by polymer adherence to the wall. More studies need to be done to further understand the DRP degradation mechanisms. For potential biomedical use, it would be beneficial to have a DRP that degrades relatively slowly since it can last for a significant amount of time after intravascular injection. Considering that the blood flow in the cardiovascular system is not turbulent and that the shear stresses in the *in vitro* turbulent flow systems are significantly higher than physiological shear stresses, one can expect much a longer time of DRP circulation *in vivo* without degradation than that in the *in vitro* turbulent flow system used in these studies.

A surprising result found in these studies was that, within the class of DRPs, polymers which have lower R_g and IV and exhibit shorter relaxation times and lower elasticity in concentrated solutions are more effective in redistributing RBCs in microchannels. The mechanism by which the DRPs alter RBC distribution in microchannels remains unknown, and, therefore, the properties necessary for this phenomenon have yet to be identified. One possible explanation is that the effectiveness of DRPs on microflow is based on flexibility of the polymer molecules. It was shown that, of the tested DRPs, those which have the lower monomer weight, and are thus more flexible, are more effective in altering microchannel blood flow. This is supported by the fact that DRPs which have lower elasticity, gyration radii, and intrinsic viscosities, and therefore higher flexibility, performed best in RBC microflow experiments.

6.0 SUMMARY

6.1 CONCLUSIONS

A series of tests was developed to effectively evaluate and characterize water soluble DRPs for possible clinical use in treating circulatory disorders and to further elucidate mechanisms of their beneficial effects on blood circulation *in vivo*.

The mechanism responsible for the DRP beneficial effects in the microcirculation was explained, at least in part, by the redistribution of RBCs flowing in the microcirculation, leading to a reduction of near wall plasma layer size and thus attenuation of plasma skimming at microvessel bifurcations. This, in turn, can improve gas transport between RBCs and the tissue by significantly reducing the diffusion distance of gas molecules, as well as increase shear stress on microvessel walls which would promote the release of shear stress dependent vasodilators, leading to local vasodilation and a decrease in overall vascular resistance.

Additionally, this study provided a better understanding of mechanical degradation behavior of DRPs exposed to flow induced shear stresses, especially in the presence of particles such as RBCs in a flowing solution. It was found that an increase in particle concentration led to an increase in degradation rate, and that presence of rigid particles led to an even larger degradation rate increase than deformable RBCs.

Finally, three blood soluble DRPs with great potential for clinical use were characterized and evaluated. These DRPs offer advantages of biocompatibility and resistance to stress induced degradation over several of the commonly used DRPs. An aloe derived polysaccharide was found to produce the largest drag reducing effect of any of the tested polymers. It proved to be relatively resistant to mechanical degradation, and is likely non-toxic since some studies have shown that the injection of aloe inner gel derived products produced little systemic toxicity [24]. Poly(N-vinyl formamide) was synthesized from a non-toxic isomer of acrylamide and found to be an effective drag reducer which, given its synthetic nature, could be easily manufactured. Finally, high molecular weight hyaluronic acid, a natural DRP which is currently used in certain medical applications, was found to be a good drag reducer and was most mechanically stable of any of the tested DRPs.

This study also lead to a better understanding of the characteristics that best predict a DRP's effectiveness, both in turbulent pipe flow and on blood flow in microchannels. Two parameters, relaxation time in relatively concentrated solution (2.5 mg/ml) and gyration radius of the polymer molecules, were found to be the physicochemical properties which are most indicative of a polymer's effectiveness in both cases. However, while larger radius of gyration and intrinsic viscosity, longer relaxation time, and higher elasticity are characteristic of better turbulent flow drag reducers, polymers within the class of DRPs which exhibit smaller gyration radii, lower solution relaxation times and elasticity, and lower intrinsic viscosities, were actually more effective in altering the microflow of blood, and would therefore be most likely to have the largest effect in microcirculation *in vivo*.

The combination of these studies provided a significant step in the development of this novel therapy, aimed at treating impaired circulation caused by a number of pathologies, toward clinical use.

6.2 STUDY LIMITATIONS

While the performed DRP degradation study provided an effective, comparative assessment of the relative ability of polymers to resist stress induced degradation, there were several limitations in this study. The flow conditions necessary to quantify mechanical degradation using turbulent flow drag reduction, as well as to compare degradation over relatively short exposure times, produced shear stresses significantly higher than those found in the normal vascular system. Therefore, only relative resistance to degradation, and not actual lifetime of DRPs in circulation, could be determined from this study. Another limitation is that this study quantifies only mechanical degradation and not degradation that would be produced by biological mechanisms such as enzymatic degradation. It would be advantageous to investigate biological degradation in the future since the polymers will be exposed to various enzymes in the vascular system. Finally, the shear stresses encountered inside the pump head were not considered in this study. Since all polymers were exposed to similar flow conditions in the pump, the comparative study is valid. However, the magnitude of this stress and exposure time must be determined in order to accurately quantify the magnitude of shear stress which caused the observed degradation.

Another major limitation of this study is that, although the work represents significant progress toward the elucidation of the mechanisms of the intravascular DRP phenomenon, the exact mechanism remains unknown. One of the potential mechanisms of the intravascular DRP

effect was found to involve redistribution of RBCs across vessels in the microcirculation, reducing the size of the near wall plasma layer and delivering more RBCs to the smaller vessels and thus capillaries. *In vivo*, this would likely lead to improved oxygen transport as well as local vasodilatation which could account for the decrease in vascular resistance observed in animal models. Although the current work has provided a much better understanding of the action of the DRPs in the vascular system, the exact mechanisms of the intravascular DRP effect, including the mechanism by which DRPs are preventing relocation of RBCs toward the center of the microtube/microvessel, still remain unknown. One hypothesis for the DRP effect on distribution of RBCs is that the polymers align along the flow paths and diminish RBC rotation, which is important factor in the development of a near-wall plasma layer in microvessels [1]. Additionally, the increase in blood viscoelasticity caused by DRPs may strengthen non-Newtonian patterns of the axial velocity profile, blunting the velocity profile and shifting mean RBC velocity closer to that of the blood [1]. Examination of these hypotheses would help to further elucidate mechanism by which DRPs act *in vivo*.

There were several other limitations in the *in vitro* microflow studies that should be addressed in order to further understand the actions of DRPs in blood flow. One such limitation was that the *in vitro* experiments to determine the effects of DRPs on blood flow in microchannels were performed in steady flow in rigid tubes, while, *in vivo*, blood flow is pulsatile and vessels are distensible. Steady flow was applied in these studies in order to allow for quantification and simpler modeling, as well as due to the known fact that the pulsatility is diminished in the microcirculation [59, 86]. However, physiological blood flow, even on the microcirculatory level, does exhibit some pulsatility. It was discovered that the Fåhraeus effect also occurred in pulsatile blood flow [101]. Therefore, studies of the DRP effects on pulsatile

blood flow in microchannels would help to determine whether DRPs had the same effect on reduction of near wall plasma layer in unsteady flow as in steady flow. Additionally, although blood vessels *in vivo* are distensible, the microflow studies in this project were performed in tubes with rigid walls. This allowed for the quantification of DRP effects on wall shear stresses via measurements of pressure gradients across a microchannel. If an increase in pressure gradient was seen with the addition of DRP to blood, it could be assumed that in an *in vivo* situation this would cause vasodilation. A study of DRP effects on blood flowing in distensible vessels would provide further understanding of the effects of DRPs on the microcirculation.

Finally, some limitations are presented in the imaging and image analysis methods. It was difficult to obtain images with no flow due to RBC sedimentation as well as due to the fact that even with the pump stopped some residual flow still existed, and delay of imaging would change the near wall RBC concentration due to their sedimentation. Therefore, due to this slow flow, some slight RBC elongation was observed in some images taken when the pump was stopped. Additionally, in order to quantify the plasma layer size, the near wall area which did not contain cells had to be selected manually. Therefore, this determination of the exact edge of the cell free layer is a possible source of error in measurement of plasma layer size.

In general, the limitations of the study relate to the fact that the experiments were performed *in vitro*, and that the real vascular system is much more complex than the models that were developed and applied in this work. Biological factors as well as the complex environments that the polymers would encounter *vivo* have not yet been sufficiently addressed. While additional *in vitro* experiments could help to provide more insight on the polymers action in the vascular system, ultimately, the complete behavior of DRPs in the vascular system will be able to be determined only through *in vivo* studies.

6.3 FUTURE STUDIES

The mechanism of the intravascular DRP effect was found to involve redistribution of RBCs across vessels in the microcirculation, reducing the near wall cell-free plasma layer size and leading to improved oxygen transport and, potentially, local vasodilatation. Although the current work has provided a much better understanding of the action of the DRPs in the vascular system, an important future study would involve elucidation of the mechanism by which DRPs are causing relocation of RBCs. It was hypothesized that alignment and stretch of the polymers along flow paths may diminish RBC rotation, which is an important factor in the formation of a near-wall plasma layer in microvessels [1]. However, this hypothesis has not been confirmed experimentally yet. An increase in blood viscoelasticity caused by DRPs may also strengthen non-Newtonian patterns of the axial velocity profile, blunting the velocity profile and shifting mean RBC velocity closer to the mean velocity of blood [1]. Evaluation of these hypotheses would lead to a better understanding of the mechanism by which DRPs facilitate blood flow *in vivo*.

While the DRPs developed and characterized for biomedical applications show promise, much more work is still needed before these polymers can be used clinically. The candidate polymers were all shown to be effective drag reducers that are at least somewhat resistant to mechanical degradation. In the case of AVP [1] and PNVF [39], preliminary *in vitro* and *in vivo* studies have shown biocompatibility and efficacy. However, in order for these polymers to be used clinically, additional animal studies, including a formal toxicity investigation, must be

completed. Biological degradation must be considered along with mechanical degradation in order to determine the length of time that DRPs, in particular the polysaccharides (AVP and HA) will be effective in improving blood flow in the body. In the case of AVP, additional work to standardize the extraction process and further characterization of the DRP composition are also needed before clinical use can be considered. These additional studies would continue the progress of this novel therapy for impaired microcirculation toward clinical use.

Finally, while this project provided a comparative study of DRP mechanical degradation which could be used to determine which polymers were most mechanically stable, shear stresses inside the pump incorporated in the turbulent flow system need to be determined in order to quantify their effects on DRP degradation. Using computational fluid dynamics to evaluate stresses experienced in the pump would allow for a better understanding of the mechanical degradation of DRPs which could ultimately be used to predict degradation caused by shear stress experienced *in vivo*. Investigation of the degradation of DRPs at different concentrations would also be a useful study in evaluating the mechanical stability of DRPs.

APPENDIX A

PROPAGATION OF ERROR

Propagation of error is based on Equation 22 [102, 103].

$$\sigma_\lambda^2 = \left(\frac{d\lambda}{d\alpha}\right)^2_{\beta,\gamma} \sigma_\alpha^2 + \left(\frac{d\lambda}{d\beta}\right)^2_{\alpha,\gamma} \sigma_\beta^2 + \left(\frac{d\lambda}{d\gamma}\right)^2_{\alpha,\beta} \sigma_\gamma^2 \tag{22}$$

where λ is a computed quantity calculated from α, β, and γ, which are measured or previously calculated quantities with known uncertainty, σ. The differentials in Equation 22 represent the change in λ with change in any of the measured or previously calculated quantities.

In the case of addition, given by Equation 23

$$\lambda = \alpha + \beta + \gamma \tag{23}$$

the differentials in Equation 22 are determined to be

$$\frac{d\lambda}{d\alpha} = \frac{d\lambda}{d\beta} = \frac{d\lambda}{d\gamma} = 1 \tag{24}$$

Substitution of Equation 24 into Equation 22 gives the following equation for propagation of error in the case of addition.

$$\sigma_\lambda^2 = \sigma_\alpha^2 + \sigma_\beta^2 + \sigma_\gamma^2 \tag{25}$$

In the case of multiplication,

$$\lambda = \alpha\beta\gamma \quad , \tag{26}$$

the differentials in Equation 22 are evaluated as follows.

$$\frac{d\lambda}{d\alpha} = \beta\gamma \tag{27}$$

$$\frac{d\lambda}{d\beta} = \alpha\gamma \tag{28}$$

$$\frac{d\lambda}{d\gamma} = \alpha\beta \tag{29}$$

Substituting Equations 27, 28, and 29 into Equation 22, the following Equation for propagation of error in the case of multiplication can be derived.

$$\sigma_\lambda^2 = (\beta\gamma)^2 \sigma_\alpha^2 + (\alpha\gamma)\sigma_\beta^2 + (\alpha\beta)\sigma_\gamma^2 \tag{30}$$

Equation 30 can be simplified by dividing through by

$$\lambda^2 = \alpha^2\beta^2\gamma^2 \tag{31}$$

to give

$$\%\sigma_\lambda^2 = \%\sigma_\alpha^2 + \%\sigma_\beta^2 + \%\sigma_\gamma^2 \tag{32}$$

where $\%\sigma_i$ is defined as

$$\%\sigma_i = \frac{\sigma_i}{i} * 100\% \tag{33}$$

In the case of multiplication of the quantities raised to some power,

$$\gamma = \alpha^a \beta^b \gamma^c \tag{34}$$

the differentials in Equation 22 can be evaluated as follows.

$$\frac{d\lambda}{d\alpha} = a\alpha^{a-1}\beta^b\gamma^c \tag{35}$$

$$\frac{d\lambda}{d\beta} = b\beta^{b-1}\alpha^a\gamma^c \tag{36}$$

$$\frac{d\lambda}{d\gamma} = c\gamma^{c-1}\beta^{b}\alpha^{a} \tag{37}$$

Substituting Equations 35, 36, and 37 into Equation 22, the following equation for propagation of error can be derived.

$$\sigma_{\lambda}^{2} = \left(a\alpha^{a-1}\beta^{b}\gamma^{c}\right)^{2}\sigma_{\alpha}^{2} + \left(b\beta^{b-1}\alpha^{a}\gamma^{c}\right)^{2}\sigma_{\beta}^{2} + \left(c\gamma^{c-1}\beta^{b}\alpha^{a}\right)^{2}\sigma_{\gamma}^{2} \tag{38}$$

The expression can be simplified by dividing through by Equation 39 to obtain Equation 40.

$$\lambda^{2} = \alpha^{2a}\beta^{2b}\gamma^{2c} \tag{39}$$

$$\%\sigma_{\lambda}^{2} = a^{2}\%\sigma_{\alpha}^{2} + b^{2}\%\sigma_{\beta}^{2} + c^{2}\%\sigma_{\gamma}^{2} \tag{40}$$

APPENDIX B

FRICTION FACTOR ERROR ANALYSIS

Friction factor can be calculated using Equation 4.

$$\lambda = \frac{d^5 \cdot \pi^2 \cdot P}{8 \cdot l \cdot \rho \cdot Q^2} \tag{4}$$

Since λ is calculated through multiplication of variables raised to some exponent, percent error can be calculated using Equation 40.

$$\%\sigma_\lambda^2 = a^2 \%\sigma_\alpha^2 + b^2 \%\sigma_\beta^2 + c^2 \%\sigma_\gamma^2 \tag{40}$$

For a given flow system, the quantity $\frac{d^5 \cdot \pi^2}{8 \cdot l \cdot \rho}$ is a constant based on geometry and fluid properties. Therefore, the percent error for friction factor can be calculated by

$$\%\sigma_\lambda^2 = \%\sigma_P^2 + (-2)^2 \%\sigma_Q^2$$

For the turbulent flow system, the flow probe accuracy is ± 2% [104]. Pressure transducer accuracy is ± 0.25% [105]. Therefore, $\%\sigma_\lambda^2 =$ 4% for the turbulent flow studies.

Equation 40 can also be used to determine error for the friction factor in laminar flow studies. Flow rate accuracy for the syringe pump (σ_Q) is ± 0.35% [106], and pressure transducer accuracy (σ_P) is ± 0.25% [105]. Therefore σ_λ is calculated to be 0.74%.

BIBLIOGRAPHY

1. Kameneva, M.V., et al., *Blood soluble drag-reducing polymers prevent lethality from hemorrhagic shock in acute animal experiments.* Biorheology, 2004. **41**: p. 53-64.

2. Faruqui, F.I., M.D. Otten, and P.I. Polimeni, *Protection against atherogenesis with the polymer drag-reducing agent Separan AP-30.* Circulation, 1987. **75**(3): p. 627-35.

3. Golub, A.S., et al., *Influence of polyethylene oxide on the capillary blood flow of diabetic rats.* Soviet Physics -- Doklady, 1987. **32**: p. 620-621.

4. Greene, H.L., R.A. Mostardi, and R.F. Nokes, *Effect of drag reducing polymers on initiation of atherosclerosis.* Polymer Engineering Science, 1980. **20**: p. 499-504.

5. Grigorian, S.S., I.A. Sokolova, and A.A. Shakhnazarov, *[The action of high-molecular linear polymers on the circulatory system].* Usp Fiziol Nauk, 1995. **26**(2): p. 31-43.

6. Macias, C.A., et al., *Survival in a rat model of lethal hemorrhagic shock is prolonged following resuscitation with a small volume of a solution containing a drag-reducing polymer derived from aloe vera.* Shock, 2004. **22**(2): p. 151-156.

7. McCloskey, C.A., et al., *Tissue hypoxia activates JNK in the liver during hemorrhagic shock.* Shock, 2004. **22**(4): p. 380-6.

8. Mostardi, R.A., et al., *The effect of drag reducing agents on stenotic flow disturbances in dogs.* Biorheology, 1976. **13**(2): p. 137-41.

9. Mostardi, R.A., et al., *Suppression of atherosclerosis in rabbits using drag reducing polymers.* Biorheology, 1978. **15**(1): p. 1-14.

10. Pacella, J.J., et al., *Effect of drag reducing polymers on myocardial perfusion during coronary stenosis.* European Heart Journal, 2006. **19**: p. 2362-2369.

11. Polimeni, P.I., B. Ottenbreit, and P. Coleman, *Enhancement of aortic blood flow with a linear anionic macropolymer of extraordinary molecular length.* J Mol Cell Cardiol, 1985. **17**(7): p. 721-4.

12. Polimeni, P.I. and B.T. Ottenbreit, *Hemodynamic effects of a poly(ethylene oxide) drag-reducing polymer, Polyox WSR N-60K, in the open-chest rat.* J Cardiovasc Pharmacol, 1989. **14**(3): p. 374-80.

13. Gannushkina, I.V., A.L. Antelava, and M.V. Baranchikova, *Diminished experimental alimentary atherogenesis under the influence of polymers that decrease the hydrodynamic resistance of the blood.* Bull. Exp. Biol. Med., 1993. **116**: p. 367–370.

14. Gannushkina, I.V., et al., *The possibility that after circulatory ischemia of the brain the blood circulation can be restored by introducing special polymers to the blood.* Soviet Physics -- Doklady, 1981. **26**(4): p. 376.

15. Toms, B.A. *Some observations on the flow of linear polymer solution through straight tubes at large Reynolds numbers*. in *1st Int. Congr. Rheology*. 1948. Amsterdam.

16. Grigorian, S.S., M.V. Kameneva, and A.A. Shakhnazarov, *Effect of high molecular weight compounds dissolved in blood on hemodynamics.* Soviet Physics -- Doklady, 1976. **21**(12): p. 702-703.

17. Polimeni, P.I., J. Al-Sadir, and A.F. Cutilletta, *Polysaccharide for enhancement of cardiac output*. 1979: United States.

18. Hoyt, J.W., *Blood transfusion fluids having reduced turbulent friction properties*. 1971: United States.

19. Kameneva, M.V., M.S. Polyakova, and E.V. Fedoseeva, *Effect of drag-reducing polymers on the structure of the stagnant zones and eddies in models of constricted and branching blood vessels.* Fluid Dyn., 1990. **25**: p. 956-959.

20. Kameneva, M.V., M.S. Polyakova, and I.A. Gvozdkova, *Nature of the influence of polymers that lower hydrodynamic resistance on blood circulation.* Proc. Acad. Sci. USSR. Biophysics Section., 1988: p. 22-24.

21. D'Almeida, A.R. and M.L. Dias, *Comparative study of shear degradation of carboxymethylcellulose and poly(ethylene oxide) in aqueous solution.* Polymer Degradation and Stability, 1997. **56**: p. 331-337.

22. Kenis, P.R., *Turbulent Flow Friction Reduction Effectiveness and Hydrodynamic Degradation of Polysaccharides and Synthetic Polymers.* Journal of Applied Polymer Science, 1971. **15**: p. 607-618.

23. Kim, C.A., et al., *Characterization of drag reducing guar gum in a rotating disk flow.* Journal of Applied Polymer Science, 2002. **83**(13): p. 2938-2944.

24. Talmadge, J., et al., *Fractionation of Aloe vera L. inner gel, purification and molecular profiling of activity.* International Immunopharmacology, 2004. **4**: p. 1757-1773.

25. Williams, D.L., et al., *Pre-clinical safety evaluation of soluble glucan.* Int. J. Immunopharmacol, 1988. **10**(4): p. 405-414.

26. Kulicke, W.M., M. Kotter, and H. Grager, *Drag reduction phenomenon with special emphasis on homogeneous polymer solutions*, in *Advances in Polymer Science*. 1989. p. 1-68.

27. Virk, P.S., *Drag reducing fundamentals.* AIChE Journal, 1975. **21**(4): p. 625-654.

28. Kinnier, J.W., *A correlation between friction reduction and molecular size for the flow of dilute aqueous polyethyleneoxide solutions in pipes*. 1970, U.S. Naval Postgraduate School.

29. Keller, A., G. Kiss, and M.R. Mackley, *Polymer drag reduction in Taylor vortices.* Nature, 1975. **257**: p. 304-305.

30. Driels, M.R. and S. Ayyash, *Drag reduction in laminar flow.* Nature, 1976. **259**: p. 389-390.

31. Kenis, P.R., *Drag Reduction by Bacterial Metabolites.* Nature, 1968. **217**: p. 940-942.

32. Shenoy, A.V., *A reveiw on drag reduction with special reference to micellar systems.* Colloid Polym. Sci., 1984. **262**: p. 319-337.

33. Rosen, M. and N. Cornford, *Fluid Friction of Fish Slimes.* Nature, 1971. **234**: p. 49-51.

34. Kameneva, M.V., et al., *Artificial blood fluids and microflow drag reducing factors for enhanced blood circulation* 2002: United States.

35. Fabula, A.G., J.L. Lumley, and W.D. Taylor, *Some interpretations of the Toms effect*, in *Mechanics of Continua*, S. Eskanaiz, Editor. 1966, Academic Press: New York. p. 100-120.

36. Hoyt, J.W., *The effect of additives on fluid friction.* Trans ASME, J Basic Eng, 1972. **94**: p. 258-285.

37. Burger, E.D., L.G. Chorn, and T.K. Perkins, *Studies of drag reduction conducted over a broad range of pipeline conditions when flowing Prudhoe Bay crude oil.* J Rheol, 1980. **24**: p. 603.

38. Grigorian, S.S. and M.V. Kameneva, *Resistance-reducing polymers in the blood circulation*, in *Contemporary Problems of Biomechanics*, G.G. Chernyi and S.A. Regirer, Editors. 1990, Mir Publ., CRC Press: Moscow, Boca Raton, FL. p. 99-110.

39. Marhefka, J.N., et al., *Poly(N-vinylformamide)-A drag-reducing polymer for biomedical applications.* Biomacromolecules, 2006. **7**(5): p. 1597-603.

40. *National Vital Statistics Reports*, in *National Vital Statistics Reports*. 2002, Department of Health and Human Services: Hyattsville, MD.

41. Fahraeus, R. and T. Lindquist, *The viscosity of blood in narrow capillary tubes.* Am. J. Physiol, 1931. **96**: p. 562-568.

42. Tsai, A.G. and M. Intaglietta, *High viscosity plasma expanders: Volume resuscitation fluids for lowering the transfusion trigger.* Biorheology, 2001. **2001**(38): p. 229-237.

43. Brostow, W., *Drag reduction and mechanical degradation in polymer solutions in flow.* Polymer, 1983. **24**: p. 631-638.

44. Choi, H.J., et al., *An exponential decay function for polymer degradation in turbulent drag reduction.* Polymer Degradation and Stability, 2000. **69**: p. 341-346.

45. Fisher, D.H. and F. Rodriguez, *Degradation of Drag Reducing Polymers.* Journal of Applied Polymer Science, 1971. **15**: p. 2975-2985.

46. Hunston, D.L. and J.L. Zakin, *Flow-assisted degradation in dilute polystyrene solutions.* Polymer Engineering and Science, 1980. **20**(7): p. 517-523.

47. Kim, C.A., et al., *Drag reduction and mechanical degradation of poly(ethylene oxide) in seawater.* Journal of Chemical Engineering of Japan, 1999. **32**(6): p. 803-811.

48. Lee, K., et al., *Mechanical degradation of polyisobutylene under turbulent flow.* Colloid Polym. Sci., 2002. **280**: p. 779-782.

49. Liberatore, M.W., et al., *Turbulent drag reduction of polyacrylamide solutions: Effect of degradation on molecular weight distribution.* J Non-Newtonian Fluids, 2004. **123**: p. 175-183.

50. Sung, J.H., et al., *Turbulent drag reduction efficiency and mechanical degradation of poly(acrylamide).* Journal of Macromolecular Science, 2004. **B43**(2): p. 507-518.

51. Vlachogiannis, M., et al., *Effectiveness of a drag reducing polymer: Relation to molecular weight distribution.* Physics of Fluids, 2003. **15**(12): p. 3786-3794.

52. Sellin, R.H.J., J.W. Hoyt, and O. Scrivener, *The effect of drag-reducing additives on fluid flows and their industrial applications part 1: Basic aspects.* Journal of Hydraulic Research, 1982. **20**(1): p. 29-68.

53. Nokes, R.F., et al. *Biological fate of friction reducing agents*. in *ACEMB*. 1972.

54. Groisman, A.S., V., *Efficient mixing at low Reynolds numbers using polymer additives.* Nature, 2001. **410**(6831): p. 905-908.

55. Fahraeus, R., *The suspension stability of the blood.* Physiol. Rev., 1929. **IX**: p. 241-275.

56. Goldsmith, H.L., G.R. Cokelet, and P. Gaehtgens, *Robin Fahraeus: Evolution of his concepts in cardiovascular physiology.* Am. J. Physiol, 1989. **257**: p. H1005-H1015.

57. Fenton, B.M., R.H. Carr, and G.R. Cokelet, *Non-uniform red cell distribution in 20 - 100 μm bifurcations.* Microvascular Research, 1985. **29**: p. 103-126.

58. Wu, Z.J., et al., *Modification of flow behavior of red blood cells by blood soluble drag-reducing polymers*, in *International Congress on Biological and Medical Engineering*. 2002: Mandarin, Singapore.

59. Guyton, A.C. and J.E. Hall, *Textbook of medical physiology*. 9th ed. 1996, Philadelphia: W.B. Saunders. xliii, 1148.

60. Chow, J.T., et al., *Chemical characterization of the immunomodulating polysaccharide of Aloe vera L.*, in *The International Aloe Science Council, Inc., 23rd Annual Scientific Seminar* 2004: Seoul, Korea.

61. Gowda, D.C., B. Neelisiddaiah, and Y.V. Anijaneyalu, *Structural Studies of Polysaccharides from Aloe Vera.* Carbohydrate Research, 1979. **72**: p. 201-205.

62. Marhefka, J.N., et al., *Further development of a drag-reducing component for artificial blood.* ASAIO Journal, 2004. **50**(2): p. 170.

63. Ni, Y., et al., *Isolation and characterization of structural components of Aloe vera L. leaf pulp.* International Immunopharmacology, 2004. **4**: p. 1745-1755.

64. Eshun, K. and Q. He, *Aloe vera: A valuable ingredient for the food, pharmaceutical, and cosmetic industries -- A review.* Critical Reviews in Food Science and Nutrition, 2004. **44**(2): p. 91-96.

65. Pinschmidt, R.K., et al., *N-vinylformamide -- Building block for novel polymer structures.* J.M.S. -- Pure Appl. Chem., 1997. **A34**(10): p. 1885-1905.

66. Gu, L., et al., *Kinetics and modeling of free radical polymerization of N-vinylformamide.* Polymer, 2001. **42**: p. 3077-3086.

67. Badesso, R.J., R.K. Pinschmidt, and D.J. Sagi, *Synthesis of amine functional homopolymers with n-ethenylformamide.* Proc Am Chem Soc, Div Polymer Mat Sci Eng, 1993. **69**: p. 251-252.

68. Badesso, R.J., et al., *High and Medium Molecuar Weight Poly(Vinylamine).* Polymer Preprints, 1991. **32**: p. 110-111.

69. McAndrew, T.P., *Drag reduction with amine functional polymers*. 1993, Air Products and Chemicals, Inc.: United States.

70. Kakehi, K., M. Kinoshita, and S. Yasueda, *Hyaluronic acid: separation and biological implications.* Journal of Chromatography B: Analytical Technologies in the Biomedical & Life Sciences, 2003. **797**(1-2): p. 347-55.

71. *Hyaluronan...Utilizing nature to improve life*. 2004 [cited 2005; Available from: http://www.lifecore.com/Products/Resource_Files/Pdf/Hyaluronan.pdf.

72. Hoyt, J.W., *Symposium on Rheology*, in *ASME*. 1965: New York.

73. Hamburger, M.I., et al., *Intra-articular hyaluronans: A review of product-specific safety profiles.* Seminars in Arthritis and Rheumatism, 2003. **32**(5): p. 296-309.

74. White, F.M., *Fluid mechanics*. 4th ed. McGraw-Hill series in mechanical engineering. 1999, Boston, Mass.: WCB/McGraw-Hill. xiv, 826.

75. Stevens, M.P., *Polymer chemistry : an introduction*. 2nd ed. 1990, New York: Oxford University Press. xviii, 633.

76. Riande, E., et al., *Polymer Viscoelasticity*. 200, New York: Marcel Dekker, Inc.

77. Caro, C., et al., *The mechanics of the circulation*. 1978: Oxford University Press.

78. Klaus, S., et al., *Investigation of flow and material induced hemolysis with a Couette type high shear system.* Mat.-wiss. u. Werkstofftech, 2001. **32**: p. 922-925.

79. Marhefka, J.N., P.J. Marascalco, and M.V. Kameneva, *Studies on the mechanism of the intravascular effect of drag-reducing polymers*, in *BMES*. 2004: Philadelphia, PA.

80. Stein, P.D. and H.N. Sabbah, *Hemorheology of turbulence.* Biorheology, 1980. **17**(4): p. 301-319.

81. Pohl, M., et al., *Mechanical degradation of polyacrylamide solutions as a model for flow induced blood damage in artificial organs.* Biorheology, 2000. **37**(4): p. 313-324.

82. Kameneva, M.V., et al., *Effects of turbulent stresses upon mechanical hemolysis: experimental and computational analysis.* ASAIO Journal, 2004. **50**(5): p. 418-23.

83. McDonald, J.C., et al., *Fabrication of microfluidic systems in poly(dimethylsiloxane).* Elecrophoresis, 2000. **21**: p. 27-40.

84. Boyle, J., *Microcirculatory hematocrit and blood flow.* J. Theor Biol. , 1988. **131**(2): p. 223-229.

85. Whitmore, R.L., *Rheology of the circulation*. 1st ed. 1968, Oxford, New York,: Pergamon Press. xii, 196.

86. Popel, A.S. and P.C. Johnson, *Microcirculation and Hemorheology.* Annual Review of Fluid Mechanics, 2005. **37**: p. 43-69.

87. Bonn, D., et al., *Turbulent drag reduction by polymers.* Journal of Physics: Condensed Matter, 2005. **17**: p. S1195-S1202.

88. Carr, R.H. and L.L. Wickham, *Influence of Vessel Diameter on Red Cell Distribution at Microvascular Bifurcations.* Microvascular Research, 1991. **41**(41): p. 184-196.

89. Haynes, R.H., *Physical basis of the dependence of blood viscosity on tube radius.* Am. J. Physiol, 1960. **198**: p. 1193-1200.

90. Jordan, A., et al., *The effects of margination and red cell augmented platelet diffusivity on platelet adhesion in complex flow.* Biorheology, 2004. **41**(5): p. 641-53.

91. Karino, T. and H.L. Goldsmith, *Aggregation of Human Platelets in an Annular Vortex.* Microvascular Research, 1979. **17**: p. 217-237.

92. Karino, T. and H.L. Goldsmith, *Adhesion of human platelets to collagen on the walls distal to a tubular expansion.* Microvascular Research, 1979. **17**(3 Pt 1): p. 238-62.

93. McCollister, D.D., F. Oyen, and V.K. Rowe, *Toxicology of acrylamide.* Toxicology and Applied Pharmacology 1963. **6**(2): p. 172-181.

94. Dourembos, N.J., et al., *Cultivation, extraction and analysis of Cannabis sativa L.* Ann NY Acad of Sci, 1971: p. 3-14.

95. Turner, C.E., et al., *Evaluation and comparison of commercially available Aloe vera L. products using size exclusion chromatograpy with refractive index and multi-angle laser light scattering detection.* International Immunopharmacology, 2004. **4**: p. 1727-1737.

96. Ebling, W., et al., *Proteinase K from Tritirachium album Limber.* Eur. J. Biochem, 1974. **47**: p. 91-97.

97. Voet, D., J.G. Voet, and C.W. Pratt, *Fundamentals of biochemistry*. 1999, New York: Wiley. xxiii, 931.

98. Paterson, R.W. and F.H. Abernathy, *Turbulent flow drag reduction and degradation with dilute polymer solutions.* Journal of Fluid Mechanics, 1970. **43**: p. 698-710.

99. Kishbaugh, A.J. and A.J. Mchugh, *A Note on the Sensitivity of Birefringence to Polymer-Solution Degradation.* Journal of Rheology, 1992. **36**(6): p. 1213-1222.

100. Fraser, J.R.E., T.C. Laurent, and U.B.G. Laurent, *Hyaluronan: its nature, distribution, functions, and turnover.* Journal of Internal Medicine, 1997. **242**(1): p. 27-33.

101. Cokelet, G.R., *Rheology and hemodynamics.* Annual Review of Physiology, 1980. **42**: p. 311-24.

102. Taylor, J.R., *An introduction to error analysis : the study of uncertainties in physical measurements*. 1982, Mill Valley, Calif.: University Science Books. x, 270.

103. Brant, A.M., *Hemodynamics and mass transfer aspects of arterial disease*. 1986. p. xix, 247 leaves.

104. *Transonic Systems, Inc.* [cited 2007 2/5]; Available from: http://www.transonic.com/Research_Home/Products__Laboratory_Research/p._16-17_probe_specs.pdf.

105. *Model 1502B01EZ5V20GPSI Thin Film Pressure Transducer / Transmitter Installation and Operating Manual*. PCB Piezotronics [cited 2007 2/5]; Available from: http://www.pcb.com/contentstore/docs/PCB_Corporate/Pressure/products/Manuals/1502B01EZ5V20GPSI.pdf.

106. *Harvard Apparatus*. [cited 2007 2/5]; Available from: http://www.harvardapparatus.com/webapp/wcs/stores/servlet/product_11051_10001_44006_-1_HAI_ProductDetail_37314____.